ABSTRACT

Title of dissertation: A Multivariate Stochastic Lévy Correlation Model
with Integrated Wishart Time Change and
Its Application in Option Pricing

Peng Gao, Doctor of Philosophy, 2012

Dissertation directed by: Professor Dilip B. Madan
Department of Finance

We develop a new multivariate Lévy correlation model which is formulated by evaluating Lévy processes subordinate to the integral of a Wishart process. This new model captures not only stochastic mean, stochastic volatility, and stochastic skewness, but also stochastic correlation of cross-sectional asset returns while still being analytical tractable. It is a multivariate extension of the time changed Lévy process introduced by Carr, Geman, Madan and Yor, which can capture the individual dynamics as well as the interdependencies among several assets.

In this dissertation, two different methods are employed to simulate paths of the instantaneous rate of time change matrix $A(t)$, followed by a Wishart process. The simulation paths successfully display desirable clustering and persistence features. In addition, we analyze the behavior of the joint log return distribution generated in this new model and show that the model provides a rich dependence structure. The option pricing problem involves computing the closed form of the characteristic functions, which are usually not easily obtained in the multivariate

correlated case. In this thesis, we derive explicit forms of both marginal and joint conditional characteristic functions by applying the 'Matrix Riccati Linearization' technique creatively. Our work is distinguished from existing multivariate stochastic volatility models, with the advantage that it can deal with stochastic skewness effects introduced by Carr and Wu. Finally, we derive pricing methods for multi-asset options as well as single asset options by using both simulation and Fast Fourier transform methods. More important, this model can be well calibrated to the real market. We chose options on two major FX currencies to perform the calibration and remarkable consistency has been observed.

A Multivariate Stochastic Lévy Correlation Model
with Integrated Wishart Time Change and
Its Application in Option Pricing

by

Peng Gao

Dissertation submitted to the Faculty of the Graduate School of the
University of Maryland, College Park in partial fulfillment
of the requirements for the degree of
Doctor of Philosophy
2012

Advisory Committee:
Professor Dilip B. Madan, Chair/Advisor
Professor Tobias von Petersdorff
Professor Paul J. Smith
Professor Leonid Koralov
Professor Victor M. Yakovenko

Dedication

To my Parents and Hua.

Acknowledgments

Earning a Ph.D degree is about learning and the pursuit of knowledge. However, for myself, it is much more than that. It is a process of learning knowledge, a process of developing my ability to analyze and solve complex problems independently, a process of annealing my willpower that keeps pursuing hope even in despair, a process of building my characteristics of honesty, precision and maturity. During the past five years at the University of Maryland, many, many people helped and supported me, without whose help I would never have finished this thesis. I feel that I am extremely fortunate to have been learning and working in such an intellectually rich, stimulating and friendly environment.

First of all, I would like to express my deepest appreciation to my advisor, Professor Dilip B. Madan, for guiding me through all the time of my research at the University of Maryland. I appreciate having an advisor who always shares his brilliant ideas and who is extremely experienced with almost every aspect of mathematical finance and also deep theoretical knowledge. In addition, I really appreciate being allowed to freely develop my own independent ideas and to work on them. I always consider myself extremely lucky having him as my advisor and having a chance to learn from him.

I would like to thank Professor Tobias von Petersdorff, Professor Paul J. Smith, Professor Leonid Koralov and Professor Victor M. Yakovenko for agreeing to serve on my dissertation committee and spending time reviewing my manuscript.

I also wanted to thank all the participants of the Mathematical Finance re-

search interaction team (RIT) for interesting and helpful discussions in the past years.

I would like to make special thanks to my parents and my husband who always stand on my side and support me.

Finally, I would like to thank all my friends. Your care, your help, your suggestions and your encouragement and much more, all of these are all really important for my pursuing this Ph.D. I could not have accomplished it without my friends. In the future, I will keep moving forward and never let down anyone who cares me.

Table of Contents

List of Tables

List of Figures

List of Abbreviations

α	alpha
β	beta
i.i.d.	independent and identically distributed
$\mathbb{R}^d$	Euclidean space
M_n	the sets of $n \times n$ square matrix
$M_n(\mathbb{R})$	the sets of $n \times n$ real square matrix
$S_n(\mathbb{R})$	the sets of $n \times n$ real symmetric square matrix
$GL_n(\mathbb{R})$	the sets of $n \times n$ real invertible matrix
VG	variance gamma
NIG	normal inverse Gaussian
FFT	fast Fourier transform
WAR	Wishart Autoregressive process
OU	Ornstein-Uhlenbeck
CIR	Cox-Ingersoll-Ross
RMSE	root mean squared error
APE	absolute percent error
FX	Foreign Exchange
OTC	over the counter
ATM	at the money
ITM	in the money
OTM	out of the money

Chapter 1

Introduction

1.1 Background and Motivation

Correlation structure plays a crucial role in pricing multi-asset derivatives and managing risks exposed to multiple financial assets. Appropriate correlation forecasts are important parameters in pricing models of structured financial instruments. While there is a wide variety of literature on pricing of single-asset options in equity market, (e.g. Black-Scholes [8], Merton [51], Madan and Seneta [48], Kou [45], Madan et al. [49], Prause [53], Hull, and White [41], Schoutens [56] , Cont and Tankov [17]), the amount of literature considering the multi-asset case is rather limited. It is most likely due to the fact that the large numbers of state variables and parameters used in the multivariate setting increase the complexity of a model. On the other hand, since not only the individual assets but also their joint behavior has to be taken into account, the model under consideration should be able to be calibrated by real market prices without sacrificing flexibility and tractability. However, this becomes challenging when dealing with multiple underlying cases.

In the financial market, it has become quite common that the payoff functions of several structured products are determined by more than one asset or underlying factor. In addition, due to the fact that most multi-asset options are traded over the counter (OTC), it is much more difficult to obtain real price quotes com-

pared to pricing a single asset options. The classical approach to model dependence structures among multiple underlying is through constructing multivariate correlated Brownian motion based processes. Although this may seem to be the natural way to build the dependence, it has been questioned by the well-documented heavy tail phenomena of stock returns and the volatility skew effects observed in the options market. Therefore, many researchers have shown increasing interest in more sophisticated models such as stochastic volatility models, (e.g. Heston [38], Hull and White [41], Bates [5] [6] etc.) and infinite activity jump models (e.g. Lévy models including the NIG model of Barndorff-Nielsen [2], the VG model of Madan and Seneta [48], and the CGMY model of Carr, Geman, Madan and Yor [13]). Besides these well developed models which successfully explain the dynamics of a single price process, multivariate stochastic volatility modeling and multivariate Lévy process modeling has also attracted considerable interest in option pricing over the last few years. (See Gourieroux [34], Da Fonseca, Grasselli and Tebaldi [22], Con, and Tankov [17], Luciano, Schoutens [47], Dimitroff, Lorenz and Szimayer [24], Hubalek and Nicolato [40]).

There is lots of empirical evidence suggesting that both stochastic volatility and jumps are needed in modeling. As asset prices jump, leading to non-Gaussian daily return distributions, stochastic volatility models driven by Brownian motion are not quite appropriate. In addition, return volatilities vary stochastically over time and are clustered, which has not been captured in general Lévy processes. Moreover, the correlation between assets' returns and their volatilities (or leverage effect) turns out to be stochastic. While many stochastic volatility models have well

explained the phenomena of volatility clustering and volatility persistence, they lack the flexibility of considering the stochastic skewness effect introduced by Carr and Wu [14]. Therefore, stochastic volatility is naturally extended to Lévy processes.

In a recent work, Carr, Geman, Madan and Yor [12] proposed an approach to modeling stochastic volatility with Lévy processes by evaluating Lévy processes subordinate to the integral of a mean reverting process, for example, the Cox-Ingersoll-Ross (CIR) process. This stochastic time-changed Lévy process is able to capture the jumps, stochastic volatility, and leverage effect mentioned above simultaneously. However, the framework considered in [12] is not able to capture the joint behavior among several assets since its construction is under a single asset.

Furthermore, a vast literature focuses on modeling stochastic volatility effects by evaluating return innovation driven by Brownian motions and volatility innovation following a Wishart process, e.g., Gourieroux and Sufana [33], Da Fonseca, Grasselli and Tebald [22] [23], Gourieroux, Jasiak and Sufana, [35], Gourieroux [34], Benabid, Bensusan, and El Karoui [7], Buraschi, Porchia, and Trojani, [10]. Although these models are multifactor or multivariate stochastic volatility extensions of Heston's [38] model, unfortunately none of them have been successfully calibrated to the real market.

This dissertation presents a new multivariate Lévy correlation model formulated by evaluating Lévy processes subordinate to the integral of a Wishart process. As the Wishart process is considered to be a multivariate extension of the Cox Ingersoll Ross (CIR) process, my work extends the time-changed Lévy process [12] to a multi-asset version and is able to recapture the individual dynamics as well as the

interdependencies among several assets. Our new model captures not only stochastic mean, stochastic volatility, stochastic skewness, but also stochastic correlation of cross-sectional of asset returns while still be highly analytical tractable. And more importantly, it could be successfully calibrated to the market option prices varying across both the strike and maturity dimensions.

1.2 Lévy Processes

Lévy processes, named in honor of Paul Lévy, have been used in mathematical finance for many years. The well known Brownian motion is a purely continuous Lévy process. The classic Black-Scholes model assumes the underlying asset price follows a geometric Brownian motion with constant drift and volatility. Although the Black-Scholes model is quite successful in explaining stock prices, it does have known shortcomings. One of the main problems with the Black-Scholes model is that the log returns of most financial assets do not follow a normal distribution. In addition, the well-documented heavy tail phenomena of stock returns and the volatility skew effect observed in real market also raises doubts about the traditional Black-Scholes model. Therefore, non-normal Lévy processes have become increasingly popular because they can describe features observed in financial markets more accurately than diffusion models based on Brownian motion. Mandelbrot first studied the non-normal exponential Lévy process in his paper [50] published in 1963. After that, many models based on pure jump Lévy processes have been developed (e.g., variance gamma (VG) model, normal inverse gaussian (NIG) model and CGMY model, etc.)

These Lévy models incorporate jumps observed in stock prices and depict features of stock prices such as heavy tails, skewness, and high kurtosis.

1.2.1 Definition and Properties

Definition 1.1. (***Lévy process***) *A càdlàg[1] stochastic process* $(X_t)_{t \geq 0}$ *with* $X_0 = 0$ *almost surely, defined on a probability space* $(\Omega, \mathcal{F}, \mathbb{P})$, *is called a Lévy process if the following properties are satisfied:*

- *X has independent increments:* $\forall\ 0 \leq t_0 < t_1 < ... < t_n$, *the random variables* $X_{t_0}, X_{t_1} - X_{t_0}, ..., X_{t_n} - X_{t_{n-1}}$ *are independent.*

- *X has stationary increments: the distribution of* $X_{t+h} - X_t$ *does not depend on t for any $t, h \geq 0$.*

- *X is stochastically continuous:* $\forall \epsilon > 0, \quad lim_{h \to 0} P(|X_{t+h} - X_t| \geq \epsilon) = 0.$

We usually study the Lévy process through its characteristic functions instead of its distributions. The Lévy-Khintchine formula provides the characterization of infinitely divisible random variables through their characteristic functions. Before we move on to the Lévy-Khintchine formula, we are going to explore the relationship between Lévy process and infinite divisibility.

1.2.1.1 Infinitely Divisible Distribution

Definition 1.2. (***Infinite divisibility***) *The law of a random variable X is infinitely divisible if for all $n \in \mathbb{N}$ there exist i.i.d. random variables* $X_1^{(1/n)}, ..., X_n^{(1/n)}$

---

[1]Càdlàg process is a stochastic process for which the paths are right continuous with left limits.

such that

$$X \stackrel{d}{=} X_1^{(1/n)} + ... + X_n^{(1/n)}. \tag{1.1}$$

Proposition 1.3. *The law of a random variable X is infinitely divisible if and only if for each $n \in \mathbb{N}$, there exists $X^{(1/n)}$ such that*

$$\phi_X(u) = (\phi_{X^{(1/n)}}(u))^n. \tag{1.2}$$

Proposition 1.4. *If X is a Lévy process, then X_t is infinitely divisible for each $t \geq 0$.*

By Proposition 1.4, we can easily express the characteristic function $\Phi_X(u)$ of Lévy process X_t in a simple form.

Theorem 1.5. *If X is a Lévy process, then*

$$\phi_{X_t}(u) = E(e^{iuX_t}) = e^{t\psi_{X_1}(u)} \tag{1.3}$$

for each $u \in \mathbb{R}^d$, $t \geq 0$, where $\psi_{X_1}(u)$ is the characteristic exponent of the Lévy process at unit time.

1.2.1.2   The Lévy-Khintchine formula

The connection between infinitely divisible distributions and the Lévy processes leads to the famous Lévy-Khintchine formula. This formula provides a complete characterization of random variables with infinitely divisible distribution via their characteristic functions and enables us to study Lévy processes through studying infinite divisible distributions.

6

Theorem 1.6. (*Lévy-Khintchine formula*) *Let* $(X_t)_{t \geq 0}$ *be a Lévy process on* $\mathbb{R}$. *Then the characteristic exponent* $\psi_{X_1}(u)$ *is given by*

$$\psi_{X_1}(u) = i\gamma u - \frac{1}{2}\sigma^2 u^2 + \int_{\mathbb{R}\backslash\{0\}} \left(e^{iux} - 1 - iux\mathbf{1}_{|x|\leq 1}\right) \nu(dx) \tag{1.4}$$

with

$$\int_{\mathbb{R}\backslash\{0\}} (1 \wedge x^2)\nu(dx) < \infty \tag{1.5}$$

where $\gamma \in \mathbb{R}$, $\sigma^2 \geq 0$ *and* ν *is a measure on* $\mathbb{R}\backslash\{0\}$.

The triplet (γ, σ^2, ν) is called the *Lévy triplet*. From equation (1.4), we can observe that a Lévy process can be decomposed into three independent components: a deterministic drift, a continuous Brownian motion, and a pure jump process. We call $k(x)$ the Lévy density, if the Lévy measure is of the form $\nu(dx) = k(x)dx$. Moreover, $\gamma \in \mathbb{R}$ is called the *drift term*, $\sigma^2 \in \mathbb{R}_+$ the *Gaussian* or *diffusion coefficient* and ν the *Lévy measure*.

Now, we consider the path properties of Lévy processes. The Levy triplet (γ, σ^2, ν) determines the path property of Lévy processes. For example, the Lévy process is a pure jump process if $\sigma^2 = 0$ (no diffusion part). If $\sigma^2 = 0$, and $\int_{|x|\leq 1} \nu(dx) < \infty$, there are infinitely many jumps in any finite interval, and we call the Lévy process is of finite activity. When $\int_{|x|\leq 1} \nu(dx) = \lambda = \infty$ instead, the mean arrival rate of jumps λ is infinity, and then the Lévy process is said to have infinite activity. A Lévy process is a pure jump process with finite variation if it satisfies $\sigma^2 = 0$ and $\int_{|x|\leq 1} |x|\nu(dx) < \infty$. In that case the characteristic exponent can be re-expressed as

$$\psi_{X_1}(u) = i\gamma' u + \int_{\mathbb{R}\backslash\{0\}} (e^{iux} - 1)\nu(dx) \tag{1.6}$$

where γ' is a new drift coefficient. On the other hand, a pure jump Lévy is of infinite variation when $\sigma^2 = 0$ and $\int_{|x| \leq 1} |x| \nu\,(dx) = \infty$.

To see how the Lévy-Khintchine formula disintegrates into Brownian motion and Poisson distribution terms, we introduce the Lévy-Itô decomposition theorem.

1.2.1.3 The Lévy-Itô Decomposition

Theorem 1.7. (*Lévy-Itô decomposition*) *Let X_t be a Lévy process with triplet (γ, σ^2, ν), where $\gamma \in \mathbb{R}$, $\sigma \in \mathbb{R}_+$ and let ν be a measure satisfying $\int_{\mathbb{R}\setminus\{0\}}(1 \wedge x^2)\nu\,(dx) < \infty$. Then there exists a probability space $(\Omega, \mathcal{F}, \mathbb{P})$ on which the Lévy process can be decomposed into four independent components as $X_t = \gamma t + B_t + N_t + M_t$, where γt is a constant drift, B_t is a Brownian motion, N_t is a compound Poisson process with $N_t = \int_0^t \int_{|x| \geq 1} x \mu^L(ds, dx)$, and M_t is a pure jump martingale with $M_t = \int_0^t \int_{|x| < 1} x \mu^L\,(ds, dx) - t \int_{|x| < 1} x \nu\,(dx)$. ($\mu^L$ denotes the random measure counting the jumps of M_t)*

It is easy to see that N_t counts the 'large jumps' and M_t counts the small jumps within the finite time interval $[0, t]$. Considering characteristic exponents and the Lévy-Itô decomposition, we can split the Lévy exponent into three parts:

$$\psi(u) = \psi^1(u) + \psi^2(u) + \psi^3(u) \tag{1.7}$$

where

- $\psi^1(u) = i\gamma u$, linear or constant drift with parameter γ.

- $\psi^2(u) = \frac{1}{2}\sigma^2 u^2$, Brownian motion with coefficient σ.

- $\psi^3(u) = \int_{\mathbb{R}\setminus\{0\}}(e^{iux} - 1 - iux\mathbf{1}_{|x|\leq 1})\nu(dx)$, compensated Poisson process.

Therefore, Brownian motion and Poisson based models are special cases of a general Lévy process model.

1.2.2 Measure Change for Lévy Processes

Measure change is an crucial tool in connecting the physical measure with the risk-neutral measure in financial mathematics. The well-known theorem is Girsanov theorem, which shows how stochastic processes change under changes in measure.

Theorem 1.8. *(**Girsanov theorem**) Let W_t be a standard Brownian motion on $(\Omega, \mathcal{F}, \mathbb{P}, \mathcal{F}_t)$. Let $Z_t = e^{Y_t}$ be an exponential martingale under $\mathbb{P}$ with Y_t being of the form:*

$$Y_t = \int_0^t X_s\, dW_s - \frac{1}{2}\int_0^t X_s^2\, ds. \tag{1.8}$$

Then, a new process $\tilde{W}_t$ defined by

$$\tilde{W}_t = W_t - \int_0^t X_s\, ds \tag{1.9}$$

is a Brownian motion under new measure $\mathbb{Q}$, which is equivalent to measure $\mathbb{P}$. Moreover measure $\mathbb{Q}$ can be defined by the Radon-Nikodym derivative:

$$\frac{d\mathbb{Q}}{d\mathbb{P}}\bigg|_{\mathcal{F}_t} = Z_t \tag{1.10}$$

To change measures between two general Lévy processes, we have the similar results which need to find equivalent martingale measures (for details refer to [55] [17] [42]). We now state the partial extension of Girsanov's theorem:

Proposition 1.9. *(**Extension of Girsanovs theorem**) If the Levy-type stochastic integral Y_t is given by*

$$dY_t = G_t dt + F_t dW_t + H_{t,x}\tilde{N}_{dt,dx} + K_{t,x}N_{dt,dx}, \tag{1.11}$$

then $Z_t = e^{Y_t}$ is a local martingale if and only if for $t \geq 0$,

$$
\begin{aligned}
Z_t &= 1 + \int_0^t e^{Y_{s-}} F_s dW_s + \int_0^t \int_{|x|<1} e^{Y_{s-}}(e^{H_{s,x}} - 1)\tilde{N}_{ds,dx} \\
&\quad + \int_0^t \int_{|x|\geq 1} e^{Y_{s-}}(e^{K_{s,x}} - 1)\tilde{N}_{ds,dx}.
\end{aligned} \tag{1.12}
$$

The probability measure we use in pricing a contingent claim traded in the real market is usually different from the statistical measure of the observed process. In addition, by non-arbitrage pricing theory, all option pricing problems should be treated under the risk-neutral measure. Therefore, Girsanov's theorem is especially important in the theory of financial mathematics as it tells how to convert from the physical measure to risk-neutral measure.

1.2.3 The Lévy Market Model

The Lévy process has been used in financial modeling for a long time of period due to its nice features and more flexible distribution, compared to Brownian motion. Instead of modeling the log returns with a normal distribution, we replace it with a Lévy process. The Lévy market model assumes the market consists of one riskless asset (the bond) and one risky asset (the stock or index). The price process for the riskless asset is given by $B_t = e^{rt}$, and the risky asset model is

$$S_t = S_0 e^{X_t} \tag{1.13}$$

where X_t can be any Lévy process, for example, a VG Lévy process, NIG process and CGMY process. Except when X_t is a Brownian motion or a Poisson process, the Lévy model in equation (1.13) leads to incomplete markets. Therefore, there exist many different equivalent martingale measures in the Lévy market and one needs to choose the risk-neutral one from these measures in order to price an option under Lévy processes.

There are many ways to find an equivalent martingale measures, for instance, the Esscher transform, the mean-correcting martingale measure, and indifference pricing. We now introduce *the mean-correcting martingale measure* as one of the most convenient choices. It is can be done by changing the parameter in an appropriate way such that the discounted stock-price process becomes a martingale. Assuming no dividend ($q = 0$), interest rate is r,and X_t is a Lévy process, S_t is a martingale defined as

$$S_t = S_0 e^{(r-q)t} \frac{e^{X_t}}{E(e^{X_t})}. \tag{1.14}$$

In equation (1.14), we can see that X_t is mean corrected by $X_t + r - ln\phi(-i)$.

1.2.4   Subordinated Lévy Process

The subordinated stochastic process was proposed by Clark in 1973 [16] as a model to account for non-normality of returns. The return process $X(t)$ was written as a subordinated process $X(t) = Z(T(t))$, where $T(t)$ is an increasing Lévy process with independent and stationary increments, and $T(t)$ is called a *subordinator*.

Theorem 1.10. *(**Subordinator**) A subordinator is an increasing (in t) Lévy pro-*

cess. Equivalently, if $T(t)$ is a subordinator then its Lévy triplet (γ, σ^2, ν) must satisfy $\nu(-\infty, 0) = 0$, $\sigma = 0$, $\int_{(0,\infty)} (x \wedge 1)\nu(dx) < \infty$ and $\gamma = b + \int_{(0,1)} x\nu(dx) > 0$, where $b \geq 0$.

The pair (b, ν) is called the *characteristics* of the subordinator $T(t)$.

Proposition 1.11. *For each $t \geq 0$, the Laplace transform of the subordinator $T(t)$ is:*

$$E(e^{-uT(t)}) = e^{-t\psi(u)}, \tag{1.15}$$

where $\psi(u) = bu + \int_{(0,\infty)} (1 - e^{-ux})\nu(dx)$, and the function $\psi(u)$ is usually called the Laplace exponent of the subordinator.

Subordinators play an important role in the construction of some Lévy processes. Subordination enables us to construct a new Lévy processes through random time change by an increasing Lévy process.[2] For example, the VG process [48] is a Brownian motion subordinated by a Gamma time change, the NIG process [2] is a Brownian motion subordinated by a Inverse Gaussian process, and the stochastic volatility Lévy process [12] is a Lévy process subordinated by the integration of a CIR process.[3]

Now we discuss one of the popular Lévy processes, the VG process, which is an important building block for this dissertation.

---

[2] The stochastic time changed Lévy process is discussed in Chapter 2.

[3] Lévy models with stochastic volatility is discussed in Chapter 2.

1.3 The Variance Gamma Process

The VG process was introduced and developed by Madan and Seneta [48] in 1990, and is one of the most popular Lévy models. As we discussed in previous section, the VG process is a Brownian motion subordinated by a Gamma time change, or a gamma time-changed Brownian motion. It is a pure jump process with infinite activity.

1.3.1 Definition and Properties

1.3.1.1 The VG Process as Subordinated Brownian Motion

The VG process is a process with infinite activity and finite variation, and can be considered as drifted Brownian motion evaluated at a random time given by a Gamma process. It is defined as

$$X_t = \theta G_t + \sigma W_{G_t} \tag{1.16}$$

where $W = (W_t; t \geq 0)$ is a Brownian motion with constant drift θ and volatility σ. The independent subordinator G_t is a gamma process with unit mean rate and variance rate ν.

The characteristic function of the $VG(\theta, \sigma, \nu)$ law is obtained by conditioning on the gamma time, and then applying the Laplace transform to get the unconditional characteristic function of simple form:

$$\phi_{VG}(u; \theta, \sigma, \nu) = (1 - iu\theta\nu + \frac{1}{2}\sigma^2\nu u^2)^{-1/\nu}. \tag{1.17}$$

This distribution is infinitely divisible and we can define the VG process $X^{(VG)} = \{X_t^{(VG)}, t \geq 0\}$ as the process which starts at zero, has independent and stationary increments and for which the increment $X_{s+t}^{(VG)} - X_x^{(VG)}$ follows a $VG(t\theta, \sigma\sqrt{t}, \nu/t)$ law over the time interval $[s, t + s]$ [56].

The class of VG distributions is flexible to control both skewness and kurtosis. Generally speaking, the parameter θ controls the skewness of the distribution: If $\theta = 0$, the Lévy density distribution is symmetric with no skewness; negative skewness is generated by negative values of θ. The parameter ν determines the kurtosis of the distribution. And σ provides the control of volatility as in the Black-Scholes model.

1.3.1.2 The VG Process as Difference of Gamma Processes

Madan [49] showed that the VG process can be written as the difference of two independent Gamma processes. The VG model with (C, G, M) as an alternative parametrization is a special case of the CGMY model with $Y = 0$. With this characterization, the Lévy density $k_{VG}(x)$ of a VG process is determined by:

$$k_{VG}(x) = \begin{cases} C\exp(Gx)/|x|, & x < 0 \\ \\ C\exp(-Mx)/x, & x > 0 \end{cases} \tag{1.18}$$

where

$$C = 1/\nu > 0$$

$$G = \left(\sqrt{\frac{1}{4}\theta^2\nu^2 + \frac{1}{2}\sigma^2\nu} - \frac{1}{2}\theta\nu\right)^{-1} > 0$$

$$M = \left(\sqrt{\frac{1}{4}\theta^2\nu^2 + \frac{1}{2}\sigma^2\nu} + \frac{1}{2}\theta\nu\right)^{-1} > 0.$$

With these parameters, the VG process $X_t^{(VG)}(C, G, M)$ can be written as the difference of two Gamma processes:

$$X_t^{(VG)}(C, G, M) = G_t^+(tC, 1/M) - G_t^-(tC, 1/G) \tag{1.19}$$

Moreover, the characteristic function of $X_t^{(VG)}$ can be written in terms of C, G, M as follows:

$$\phi_{VG}(u; C, G, M) = \left(\frac{GM}{GM + (M - G)iu + u^2}\right)^C. \tag{1.20}$$

1.3.2   The VG Stock Price Model

By replacing the Brownian motion in the Black-Scholes model with a VG process, the risk neutral VG stock price model is written as:

$$S_t = S_0 \exp[(r - q)t + X_t(\theta, \nu, \sigma) + wt], \tag{1.21}$$

where r is the continuously compound interest rate, q is the dividend, X_t is a VG process, and w is a correction factor which helps to make the discounted stock price a martingale. By choosing a mean-correcting measure as the risk-neutral measure, we have

$$w = -\ln \phi_{X_{VG}}(-i) = \frac{1}{\nu} \ln(1 - \theta\nu - \frac{1}{2}\sigma^2\nu), \tag{1.22}$$

and the characteristic function for the log return as:

$$\phi_{\ln S_t}(u) = E(e^{iu(\ln S_0 + (r-q)t)} \frac{\phi_{X_{VG}}(u)}{[\phi_{X_{VG}}(-i)]^{iu}} \tag{1.23}$$

This equation (1.23) is used to calculate the VG option prices by the Fast Fourier Transform (FFT) method.[4]

---

[4]FFT is introduced in the next section 1.4

The density function of log stock price can be obtained and expressed in terms of the modified Bessel functions of the second type [49].

Theorem 1.12. *The density for the log return* $z_t = \ln(S_t/S_0)$*, when prices follows the risk neutral VG stock process* (1.14)*, is given as follows:*

$$f(z) = \frac{2\exp(\theta x/\sigma^2)}{\nu^{1/\nu}\sigma\sqrt{2\pi}\Gamma(t/\nu)} \left(\frac{x^2}{2\sigma^2/\nu + \theta^2}\right)^{t/2\nu - 1/4} K_{t/\nu - 1/2}\left(\frac{1}{\sigma^2}\sqrt{x^2\left(2\sigma^2/\nu + \theta^2\right)}\right)$$

(1.24)

where $K_{t/\nu - 1/2}$ *is the modified Bessel function of the second type and*

$$x = z - rt - \frac{t}{\nu}\ln(1 - \theta\nu - \sigma^2\nu/2).$$

(1.25)

While the closed-form expression for pricing an European call option with strike K is derived by Madan et al [49] (see Theorem 1.13), this expression involves computing the Bessel function of the second type.

Theorem 1.13. *The European call option price with strike price* K *on a stock under the risk-neutral price process is given by*

$$c(S_0; K, t) = S_0 \Psi\left(d\sqrt{\frac{1 - c_1}{\nu}}, (a + s)\sqrt{\frac{\nu}{1 - c_1}}, \frac{t}{\nu}\right)$$
$$- Ke^{-rt}\Psi\left(d\sqrt{\frac{1 - c_2}{\nu}}, (as)\sqrt{\frac{\nu}{1 - c_2}}, \frac{t}{\nu}\right),$$

(1.26)

where

$$d = \frac{1}{s}[\ln\left(\frac{S_0}{K}\right) + rt + \frac{t}{\nu}\ln\left(\frac{1 - c_1}{1 - c_2}\right)],$$

$$a = -\frac{\theta}{\sigma\sqrt{1 + (\theta/\sigma)^2\nu/2}},$$

$$c_1 = \frac{\nu(a + s)^2}{2},$$

$$c_2 = \frac{\nu a^2}{2},$$

and the function Ψ is defined in terms of the modified Bessel function of the second kind and the degenerate hypergeometric function of two variables.

Instead of computing the Bessel function, Carr and Madan provided a more efficient way to compute the option pricing using the Fast Fourier Transform (FFT) [11]. The FFT has been widely used in pricing options under Lévy process.

1.4   The FFT Method and Option Pricing

As an efficient approach of pricing European options, the Carr-Madan FFT method has become a popular pricing tool. This method evaluates the value of an option by applying the inverse Fourier transform to the characteristic function of the log price. Given any characteristic function, the option value can be expressed in a simple analytic form via the FFT approach. In other words, the only thing required for using FFT is the closed form of the characteristic function. In the previous section, we can see that the analytic formula of call option price involves computing a numerical integration of the modified Bessel function of the second type. This FFT method is much faster and become widely used for most of Lévy and stochastic volatility models. We sketch the method as follows:

Let $k = \ln K$ (the log of the strike price), and let $C_T(k)$ be the value of a call option with maturity T. The characteristic function of the risk neutral measure of $\ln S_T$(the log stock price) is denoted as $\phi_T(u)$. Then the Fourier transform considered in [11] is:

$$\psi_T(\nu) = \exp(-\alpha k) \int_{-\infty}^{\infty} e^{i\nu k} C_T(k) \, dk. \tag{1.27}$$

where $\exp(-\alpha k)$ is the damping factor needed to obtain a square integrable call pricing function. By using the inverse transform, call prices can be obtained numerically as

$$C_T(k) = \frac{\exp(-\alpha k)}{\pi} \int_0^\infty e^{-i\nu k} \psi_T(\nu) \, d\nu \qquad (1.28)$$

and where an analytical expression for $\psi_T(\nu)$ is available in terms of $\phi_T(u)$:

$$\psi_T(\nu) = \frac{e^{-rT} \phi_T(\nu - (\alpha + 1)i)}{\alpha^2 + \alpha - \nu^2 + i\nu(2\alpha + 1)}. \qquad (1.29)$$

We can approximate the integral in (1.28) using the trapezoidal rule, and write:

$$C_T(k) \approx \frac{\exp(-\alpha k)}{\pi} \sum_{j=1}^N e^{-i\nu_j k} \psi_T(\nu_j)\eta. \qquad (1.30)$$

In order to take the full advantage of fast Fourier transform, N is usually chosen to be a power of 2, and η is the step size for the grid of the characteristic function, $\nu_j = (j-1)\eta$, $j = 1, ..., N$. Let a be the upper limit of the integration. Then $\eta = a/N$. If λ is chosen to be the step size of the log strike k, then the log strikes vary from $-b$ to b on the grid of $k_u = -b + \lambda(u-1)$, $u = 1, ..., N$. Then C_T can be written approximately:

$$C_T(k_u) \approx \frac{\exp(-\alpha k)}{\pi} \sum_{j=1}^N e^{-i\lambda\eta(j-1)(k_u-1)} e^{ib\nu_j} \psi_T(\nu_j)\eta. \qquad (1.31)$$

In addition, if $\lambda\eta = 2\pi/N$, the call price is of the following form through applying Simpson's rule:

$$C_T(K_u) = \frac{\exp(-\alpha k)}{\pi} \sum_{j=1}^N \exp\left(-i\frac{2\pi}{N}(j-1)(u-1) + ib\nu_j\right) \psi_T(\nu_j)\frac{\nu}{3}(3+(-1)^j-\delta_{j-1}),$$
$$(1.32)$$

where δ_n is the Kronecker delta function,

$$
\delta_n = \begin{cases} 1 & n = 0, \\ \\ 0 & n \neq 0. \end{cases}
$$

We now recall the FFT, which is an algorithm for computing the following

sum

$$
w(k) = \sum_{j=1}^{N} e^{-i\frac{2\pi}{N}(j-1)(u-1)} x(j). \quad k = 1, ..., N \tag{1.33}
$$

If we take $x(j) = e^{ib\nu_j} \psi_T(\nu_j) \frac{\nu}{3}(3+(-1)^j - \delta_{j-1})$ in equation (1.33), the equation (1.32)

can be written as:

$$
C_T(K_u) = \frac{\exp(-\alpha k)}{\pi} \sum_{j=1}^{N} e^{-i\frac{2\pi}{N}(j-1)(u-1)} x(j). \tag{1.34}
$$

Consequently, we may apply FFT to equation (1.34) to compute the call option

price efficiently. The option prices across all the strikes can be calculated via the

FFT method for only one single run, which makes the calibration of the model to

the real market data very fast.

Chapter 2

Lévy Models with Stochastic Volatility

2.1 Overview

The Black-Scholes model has been widely used in pricing European-style options. It assumes the underlying asset price follows a geometric Brownian motion with constant drift and volatility under risk neutral measure:

$$dS_t = rS_t dt + \sigma S_t dB_t, \tag{2.1}$$

where r is the interest rate, B_t is the standard Brownian motion and σ denotes the constant volatility over time t. However, the constant volatility assumption contradicts the options data from the market. On the other hand, the well-documented heavy tail phenomena of the stock returns and the volatility skew effect observed in the option market also raises doubts traditional Black-Scholes model. Therefore, more sophisticated models such as stochastic volatility models have attracted considerable interest in option pricing.

There are at least two approaches of incorporating a volatility effect. The first method is replacing the constant volatility parameter of Black-Scholes model with stochastic volatility, and the volatility process is driven by a Brownian motion.(e.g. Hull and White [41], and Heston [38]). Unlike from a constant volatility geometric Brownian motion model, the general stochastic volatility model deals with the

volatility as another stochastic process:

$$dS_t = \mu S_t dt + \sqrt{\nu_t} S_t \, dW_t \tag{2.2a}$$

$$d\nu_t = \alpha_t dt + \beta_t \, dB_t \tag{2.2b}$$

where μ represents the mean rate return of the stock, ν_t is the volatility, W_t and B_t are Brownian motions, and α_t, β_t are functions of ν_t. By assuming the volatility of the underlying price is a stochastic process rather than a constant, this approach can resolve the shortcoming of Black-Scholes model.

There exists lots of empirical evidence implying that not only stochastic volatility but also the jump effect should be taken into account in modeling. The main feature missing from general Lévy processes introduced in Chapter One is the fact that volatility varies stochastically and is clustered over time. Thus, stochastic volatility is naturally extended to Lévy processes. Carr, Geman, Madan and Yor [12] construct a stochastic volatility Lévy process by evaluating a Lévy process subordinated to the integral of a CIR process. Their approach is considered as another way of incorporating the stochastic volatility effect. In this chapter, we are mainly focus on the second method–Carr, Geman, Madan, and Yor's approach.

2.2 The Stochastic Time Changed Process

One approach to build in stochastic volatility effects is to make time stochastic. The mathematical concept of time changed stochastic processes can be regarded as one of the standard tools for building financial models.

Definition 2.1. (***The Time-Changed Process***) *Given a stochastic process* $X = (X_t)_{t \geq 0}$, *sometimes referred to as the 'base process', the time-changed process* Y_t *is defined by:*

$$Y_t \equiv X_{\mathcal{T}_t}, \quad t \geq 0, \tag{2.3}$$

where $\mathcal{T} = (\mathcal{T}_t)_{t \geq 0}$ *is a non-negative, non-decreasing stochastic process not necessarily independent of* X.

The process $\mathcal{T}_t$ is referred to as time change, stochastic clock, or business time. It reflects the varying speed of Y_t.

The application of stochastic time change to asset pricing goes back to Clark [16]. In Clark's model, the asset price is modeled as a geometric Brownian motion subordinated by an independent Lévy subordinator. He investigated the time-changed process as $Y_t = B_{\mathcal{T}_t}$, where $X_t = (B_t)_{t \geq 0}$ is standard Brownian motion in (2.3) and $\mathcal{T}_t$ is an independent continuous time change.

2.2.1 Choice of Time Change

As we see in Definition 2.1, a time change $\mathcal{T}_t$ is a non-negative, non-decreasing stochastic process. There are two popular classes of such processes chosen as a time change in financial models: *subordinators* and *absolutely continuous time changes.* In the finance literature, the terms subordinator and time change are sometimes used synonymously. However, in probability theory, the term subordinator does not include all time changes. Instead it describes a particular class of stochastic

processes.[5]

Definition 2.2. *(**Absolutely Continuous Time Changes**) The absolutely continuous time change is of the form:*

$$\mathcal{T}_t = \int_0^t y_s\, ds, \tag{2.4}$$

where $y = (y_s)_{s \geq 0}$ is a positive and integrable process, and is often called 'instantaneous (business) activity rate'.

We note that $\mathcal{T}_t$ is always continuous, but y_s can exhibit jumps.

A variety of possible stochastic processes can serve for the rate of time change. Since time must increase, all processes modeling the rate of time change need to be positive. Popular candidates for the instantaneous activity rate are the non-Gaussian OU process [4] and the classical mean-reverting CIR process [20].

2.2.2 Mean-Reverting Process

Mean reversion is a mathematical concept sometimes used for stock investing, but it can be applied to other assets. It can be thought of as a modification of the random walk, where price changes are not completely independent as in random walk, but rather related. In general terms, the essence of the concept is the assumption that both a stock's high and low prices are temporary and that a stock's price will tend toward its average price over time. In other words, the process which tends to drift towards its long-term mean over time is called a mean-reverting process.

---

[5]Refer to the theorem in 1.10 for subordinator.

Mean reverting processes have also been widely used in modeling stochastic volatility. As has been observed by several authors such as Engle [28], Bates [5] [6], Heston [38], and Barndroff-Nielsen and Shephard [4], volatilities estimated from time series are usually clustered. The phenomenon is referred to as volatility persistence. This persistence suggests that volatilities eventually move back towards the mean or average.

2.2.2.1 The OU Process

The most basic mean-reversion model is the **Ornstein-Uhlenbeck (OU)** process. The well known Vasicek [58] process is a model in which an instantaneous interest rate follows an OU process. The OU process is widely used for modeling a mean-reverting process. It is defined as follows:

Definition 2.3. *(**OU Process**) The Ornstein-Uhlenbeck process x_t is given by the following stochastic differential equation:*

$$dx_t = \theta(\mu - x_t)dt + \sigma\, dW_t \tag{2.5}$$

where W_t is a standard Brownian motion on $t \in [0, \infty)$, $\theta > 0$ is the rate of mean reversion, μ represents the equilibrium value or the long-term mean of the process, and $\sigma > 0$ is the volatility, and $x_0 > 0$.

2.2.2.2 The CIR Process

The **Cox-Ingersoll-Ross(CIR)** process is a mean-reverting process. It was introduced in 1985 by John C. Cox, Jonathan E. Ingersoll and Stephen A. Ross [19]

as an extension of the OU process. In mathematical finance, the CIR process can describe the evolution of interest rates, return volatilities, stochastic discount factors, the difference between ask and bid prices, or latent risk factors. We now introduce the dynamics and the distributional properties of this process.

Definition 2.4. (**CIR Process**) *The Cox-Ingersoll-Ross process y_t is defined by the following stochastic differential equation(SDE):*

$$dy_t = \theta(\mu - y_t)dt + \sigma\sqrt{y_t}\,dW_t \tag{2.6}$$

where W_t is a Brownian motion, and the parameters satisfy: $\theta\mu > 0$, $\sigma > 0$.

This process is also called *square root process* due to the expression $\sigma\sqrt{y_t}$ for the process volatility. The drift factor $\theta(\mu - y_t)$ is exactly the same as in the OU process. It ensures mean reversion of y_t towards the long-term value μ, with speed of adjustment governed by the strictly positive parameter θ. The standard deviation factor, $\sigma\sqrt{y_t}$, avoids the possibility of negative y_t for all nonnegative values of θ and μ. If $2\theta\mu > \sigma^2$, the process is strictly positive.

The CIR process belongs to the class of *affine process*, and exhibits the *affine property*, which makes major contributions in deriving the closed form expression of conditional Laplace transform of the CIR process. Before moving onto the explicit form of conditional Laplace transform of CIR process, we introduce the affine property.

Definition 2.5. (**Affine Function**) *Affine functions are vector-valued functions of the form*

$$f(x_1, ..., x_n) = A_1 x_1 + ... + A_n x_n + b \tag{2.7}$$

The coefficients can be scalars or matrices. The constant term is a scalar or a column vector.

In equation (2.6), we note that the drift $\theta(\mu - y_t)$, and the volatility $V_t(dy_t) = \sigma^2 y_t \, dt$ are both affine functions of the process y_t. Therefore, the CIR process is a so-called *affine process* introduced by Duffie,and Kan [25].

Definition 2.6. *(**Affine Process**) The Markov process X is called affine if*

(i) it is stochastically continuous, with the state space $D = \mathbb{R}_+^m \times \mathbb{R}^n$, and

(ii) its Laplace transform has exponential-affine dependence on the initial state, or in other words,it has the 'affine property': There exist functions ϕ and ψ, taking values in $\mathbb{C}$ and $\mathbb{C}^{m+n}$ respectively, such that

$$E^x[e^{\langle X_t, u \rangle}] = exp(\underbrace{\phi(t, u) + \langle x, \psi(t, u) \rangle}_{affine\ in\ x}) \tag{2.8}$$

for all $x \in D$ and for all $(t, u) \in \mathbb{R}_+ \times \mathcal{U}$, where $\mathcal{U} = \{u \in \mathbb{C} : Re\langle x, u \rangle \leq 0$ for all $x \in D\}$

In other words, an affine process is a stochastically continuous, time-homogeneous Markov process X_t, with state space $D = \mathbb{R}_+^m \times \mathbb{R}^n$, whose characteristic function is an exponentially-affine function of the state vector.

Affine processes have attracted much interest, due to their wide applications in mathematical finance. A variety of models fall into the class of affine models. The classical Black-Scholes model [8], Heston model [38], Bates model [5] [6], Vasicek [58] model, Barndorff-Nielsen and Shephard model [4], as well as many time-change models for stochastic volatility such as Carr and Wu [12] are all affine. Moreover,

all Lévy processes, the Lévy driven OU-processes [56], the CIR process [19], the Wishart process [9][6] are based on affine processes.

Affine processes exhibit a high degree of analytic tractability. As the CIR process is an affine, its Laplace transform is *exponentially affine* as in equation (2.8), which can be derived in closed form.

Proposition 2.7. *(Conditional Laplace Transform of the CIR Process)*

If y_t is a positive CIR process, its conditional Laplace transform is:

$$\psi_{t,h}(u) = E[\exp(-uy_{t+h})|\mathcal{F}_t] = \exp[-a(h,u)y_t - b(h,u)], \qquad (2.9)$$

where $h \geq 0$, and the functions a, b satisfy the differential equations:

$$\begin{cases} \dfrac{\partial a(h,u)}{\partial h} = -ka(h,u) - \dfrac{\eta^2}{2}a(h,u)^2, \\[3mm] \dfrac{\partial b(h,u)}{\partial h} = k\theta a(h,u), \end{cases} \qquad (2.10)$$

with initial conditions: $a(0,u) = u$, $b(0,u) = 0$.

The explicit solutions of the system in equation (2.10) are:

$$\begin{cases} a(h,u) = \dfrac{u\,e^{-kh}}{1 + 2k^{-1}\eta^2 u[1 - e^{-kh}]}, \\[4mm] b(h,u) = \dfrac{2k\theta}{\eta^2} \log\left[1 + u\dfrac{\eta^2}{2k}(1 - e^{-kh})\right]. \end{cases} \qquad (2.11)$$

Proof: See Appendix. □

From equation (2.9), we see that the conditional Laplace transform of the CIR process y_t is an exponential affine function.

The CIR process can also be defined as a sum of squared Ornstein-Uhlenbeck processes.

---

[6]The Wishart process is introduced in chapter 3.

2.2.2.3 Link the CIR Process with the OU Process

Proposition 2.8. *The sum of squares of J independent OU processes with identical parameters a, w^2 is a CIR process as in Equation (2.6) with parameters: $\theta = -2a$, $\sigma = 2w$, $\theta\mu = Jw^2$. That is,*

$$dy_t = (2ay_t + Jw^2)dt + 2wy_t^{1/2}\, dW_t. \tag{2.12}$$

If we consider an OU process x_t defined by: $dx_t = ax_t dt + w\, dW_t$, the square of this process $y_t = x_t^2$ can be obtained by applying Ito's formula. Then we get

$$dy_t = (2ay_t + w^2)dt + 2wy_t^{1/2}\, dW_t.$$

More generally, if there are J independent OU processes with identical parameters: $dx_{jt} = ax_{jt}dt + w\, dW_{jt}$, $j = 1, ..., J$, where $W_{jt}, j = 1, ..., J$, are independent Brownian motions. The sum of these OU processes, $y_t = x_{1t}^2 + ... + x_{Jt}^2$, is such that

$$dy_t = \sum_{j=1}^{J} d(x_{jt}^2) = \sum_{j=1}^{J}(2ax_{jt}^2 + w^2)\, dt + \sum_{j=1}^{J} 2wx_{jt}\, dW_{jt},$$

or equivalently by aggregating the Brownian motions,

$$dy_t = (2ay_t + Jw^2)dt + 2wy_t^{1/2}\, dW_t.$$

From the above equation, we can see that y_t is a CIR process with parameters $\theta = -2a$, $\sigma = 2w$, $\theta\mu = Jw^2$.

2.2.2.4 The Integrated CIR Time Change

Proposition 2.9. (*The Integrated CIR Process*) *Let y_s be a CIR process as in definition 2.4. The integrated CIR process $Y = \{Y_t,\ t \geq 0\}$ is given as*

$$Y_t = \int_0^t y_s\, ds. \tag{2.13}$$

Since y_t is a positive process, Y_t is an increasing process.

Proposition 2.10. (*The Characteristic Function of the Integrated CIR Process*) *The characteristic function of Y_t (given y_0) is explicitly given by*

$$E[\exp(iuY_t)|y_0] = \phi(u, t; \theta, \mu, \sigma, y_0) = A(t, u) \exp(B(t, u)y_0), \tag{2.14}$$

where

$$A(t, u) = \frac{\exp\left(\theta^2 \mu t / \sigma^2\right)}{(\cosh(\gamma t/2) + \gamma^{-1}\theta \sinh(\gamma t/2))^{2\theta\mu/\sigma^2}}$$

$$B(t, u) = \frac{2iu}{\theta + \gamma \coth(\gamma t/2)}$$

with $\quad \gamma = \sqrt{\theta^2 - 2\sigma^2 iu}.$

2.3 The Lévy Stochastic Volatility Market Model

A stochastic time changed Lévy process, where the time-change process is given by a subordinator or an absolutely continuous time change, can be considered as a Lévy process running on a new random clock. One can regard this new stochastic clock as business time, and the original clock as calendar time. A more active business day implies a faster business clock. Randomness in business activity generates randomness in volatility [15].

2.3.1 The Stochastic Volatility Lévy Process

A Lévy process subordinated to the integral of a mean reverting CIR process was proposed by Carr, Geman, Madan and Yor [12] as a model to generate desired volatility features. The basic intuition of their approach to stochastic volatility arises from the *Brownian scaling property*. By virtue of this property, random changes in volatility can be scaled to random changes in time, and thus random changes in volatility can alternatively be captured by random changes in time.

2.3.1.1 Brownian Scaling Property

There is a well-known set of transformations of Brownian motion which produce another Brownian motion. One of these is the *scaling property*:

Proposition 2.11. *(Scaling Property)*

If $W = \{W_t, t \geq 0\}$ is a Brownian, then, for every $c \neq 0$, $\tilde{W} = \{\tilde{W}_t = cW_{t/c^2}, t \geq 0\}$ is also a Brownian motion.

From this property, one can see that Brownian scaling property relates changes in scale to changes in time. Therefore, random changes in volatility can be represented by a random clock in time.

2.3.1.2 The Generic Stochastic Volatility Lévy Process

As defined in Chapter One, a Lévy process X_t has stationary independent increments and its characteristic function is of the form:

$$E[e^{iuX_t}] = e^{t\psi_X(u)} \tag{2.15}$$

where $\psi_X(u)$ is the Lévy exponent. The class of stochastic volatility Lévy processes is defined as

$$Z_t = X_{Y_t}. \tag{2.16}$$

where Y is independent of X. We can obtain a simple form of the characteristic functions for these processes as follows:

$$E[e^{iuZ_t}] = E[e^{(Y_t)\psi_X(u)}] = \phi(-i\psi_X(u), t, y_0; \theta, \mu, \sigma). \tag{2.17}$$

where ϕ is defined as in Equation (2.14) and has a closed form.

2.3.2   The Stock Price Process

The risk-neutral stock price process is $S = \{S_t, t \geq 0\}$, r is the constant continuously compounded interest rate and the dividend yield is q. Let X_{Y_t} be a stochastic volatility Lévy process as described in Equation (2.16). Then the stock price S_t at time t by mean-correcting argument is modeled as follows,

$$S_t = S_0 \frac{e^{(r-q)t + X_{Y_t}}}{E[e^{X_{Y_t}}]}. \tag{2.18}$$

Note that

$$E[e^{X_{Y_t}}] = \phi(-i\psi_X(-i), t, y_0; \theta, \mu, \sigma).$$

Then the characteristic function for the log of the stock price at time t is given by:

$$E[e^{iu \ln(S_t)}] = e^{(iu \ln(S_0 + (r-q)t))} \frac{\phi(-i\psi_X(u), t, y_0; \theta, \mu, \sigma)}{\phi(-i\psi_X(-i), t, y_0; \theta, \mu, \sigma)^{iu}}. \tag{2.19}$$

Chapter 3

The New Multivariate Stochastic Lévy Correlation Model

3.1   An Overview

Correlation structure plays a vital role in multivariate modeling, since not only the individual assets but also their joint behavior should be taken into account. The natural way to build the dependence structures among multiple underlying assets is to construct multivariate Brownian motion based processes. However, the well known shortcomings questioned this classical approach, and prevents it pricing consistently. Therefore, more complex models, such as multivariate Lévy process modeling and multivariate stochastic volatility modeling have been introduced to financial modeling over the last few years. There are a vast literature on developing multivariate Lévy processes (e.g. Con, and Tankov [17], Luciano and Schoutens [47], and Barndorff-Nielsen [3]). Although the dependence structures have been successfully described in these multivariate models, resulting the return volatilities are nearly constant. As real world volatilities vary stochastically over time and are clustered, stochastic volatility has been extended to Lévy processes by Carr, Geman, Madan and Yor [12] as mentioned in Chapter Two.

On the other hand, much literature focuses on modeling stochastic volatility effects by evaluating return innovation driven by Brownian motion and volatility innovation following a Wishart process. (See Gourieroux and Sufana [33], Da Fonseca,

Grasselli and Tebald [22] [23], Gourieroux, Jasiak and Sufana [35], Gourieroux [34], Benabid, Bensusan, and El Karoui [7], Buraschi, Porchia, and Trojani [10].) Although these models are multifactor or multivariate stochastic volatility extensions of Heston's [38] model, unfortunately none of them have been successfully calibrated to the real market.

In Chapter Two we discussed the stochastic volatility for a Lévy process [12] , in which the Lévy process is subordinated to the integral of a CIR process. However, this framework does not taken correlations into account. Thus it is not able to capture the joint behavior of several assets. In this dissertation we build a new multivariate stochastic Lévy correlation model which extends the time-changed Lévy process [12] to a multi-asset version and which may able to recapture the individual dynamics as well as the interdependencies between several assets.

We design a new Lévy correlation model, which can be considered as multivariate extension of the existing time-changed Lévy model [12]. To construct such a complex model, the following questions need to be taken into account, which do not have to be studied in single asset setting (Time-changed Lévy model [12]):

- How to allow flexible correlation dynamics with independent variation?

- How to allow each asset–economic shock–has its own business clock.

- How to model the co-movements of business clocks of multiple assets–economic sources?

In this dissertation, the Wishart process has been applied as a base process for modeling the instantaneous time change rate. Since the Wishart process is a

multivariate extension of the Cox Ingersoll Ross (CIR) process, it may deal with all questions listed above. Therefore, evaluating Lévy processes subordinate to the integral of a Wishart process can be considered as a multivariate extension of the stochastic volatility Lévy process proposed by Carr, Geman, Madan and Yor in [12].

Before discussing the construction of our new model, we now introduce the Wishart process.

3.2   Wishart processes

Wishart processes were developed mathematically by Bru [9] in 1991, and have recently been applied to finance by Gourieroux and Sufana [33] in 2004. Since then, a large amount of literature has shown increasing interest in describing multivariate models with Wishart stochastic volatility matrices, in which the volatility-covolatility matrices are driven by Wishart random processes. (See Da Fonseca, Grasselli and Tebald [22] [23], Gourieroux, Jasiak and Sufana [35], Gourieroux [34], Benabid, Bensusan, and El Karoui [7], Buraschi, Porchia, and Trojani [10].)

The Wishart process addresses the limitations of the CIR process and increases the dimensionality of the risk by replacing a scalar volatility in CIR process with a volatility-covolatility matrix. It is also a multivariate extension of the CIR process, and allows us to model not only the dynamics of volatilities, but also the evolution of covolatilities. Wishart processes are flexible enough to incorporate the volatility-covolatility dynamics and enable a dynamic analysis of multivariate risk.

3.2.1 Wishart Process and its properties

The standard Wishart distribution is a multidimensional generalization of the χ^2 distibution and is very useful for the estimation of the covariance matrices in multivariate statistics [54].

Proposition 3.1. *(**Wishart Distribution**) Let $X_1, ... X_n \in \mathbb{R}^p$ be n independent identically distributed Gaussian vectors with $X_i \sim \mathcal{N}(0, \Sigma)$, $i = 1, ..., n$. The law of the random matrix: $S = \sum_{i=1}^{n} X_i X_i^T$ is called the Wishart distribution, and is denoted $S \sim W(\Sigma, p, n)$, S is a $p \times p$ random matrix. For more general case, when $X_i \sim \mathcal{N}(\mu_i, \Sigma)$, $i = 1, ..., n$, the law of $S = \sum_{i=1}^{n} X_i X_i^T$ is called 'non central Wishart distribution'.*

In modeling the dynamics of covariance matrices, we need to focus on processes taking values in the set of nonnegative definite matrices. Therefore, the trace of these nonnegative definite matrices may be considered for modeling positive stochastic volatility process. Now let us see how to construct the Wishart process.

The simplest way to derive the distribution of a Wishart process is to start from multivariate OU processes with identical dynamics.

Proposition 3.2. *(**Construction of the Wishart Process**) Let $\beta \in \mathbb{N}$, and $\{X_{k,t}^{OU}, t \geq 0\}_{1 \leq k \leq \beta}$ be independent vectorial OU processes in $\mathbb{R}^n$ with dynamics:*

$$dX_{k,t}^{OU} = M X_{k,t}^{OU} dt + Q^T dW_{k,t}, \tag{3.1}$$

where $\{W_{k,t}, t \geq 0, 1 \leq k \leq \beta\}$ are independent vectorial Brownian motions, M, Q

are $n \times n$ matrices and Q is invertible. Then let us consider the matrix process:

$$V_t = \sum_{k=1}^{\beta} X_{k,t}^{OU}(X_{k,t}^{OU})^T. \tag{3.2}$$

which has dynamics:

$$dV_t = (\beta Q^T Q + MV_t + V_t M^T)dt + \sqrt{V_t}\,dW_t Q + Q^T dW_t^T \sqrt{V_t}. \tag{3.3}$$

Proof: Thanks to the Itô calculus, we easily get:

$$dV_t = (\beta Q^T Q + MV_t + V_t M^T)dt + \sum_{k=1}^{\beta} X_{k,t}dW_{k,t}^T Q + Q^T dW_{k,t}X_{k,t}^T.$$

Then, by using the Lévy criterion for Brownian motion, we can define a matrix-valued Brownian motion W so that:

$$\sqrt{V_t}dW_t = \sum_{k=1}^{\beta} X_{k,t}dW_{k,t}^T$$

. $\qquad\qquad\qquad\qquad\qquad\qquad\qquad\qquad\qquad\qquad\qquad\qquad\qquad\qquad\qquad\qquad$ $\square$

Definition 3.3. (***The Wishart Process***) *The dynamics in* (3.3) *is called the Wishart process, and it is an affine process. The parameter β in* (3.3) *is not restricted to an integer, and it can be chosen as any positive real number:*

$$dV_t = (\Omega\Omega^T + V_t M^T + MV_t)\,dt + \sqrt{V_t}\,dW_t Q + Q^T\,dW_t \sqrt{V_t} \tag{3.4}$$

Equation (3.4) *characterizes the Wishart process introduced by Bru [9], where*

$$\Omega\Omega^T = \beta Q^T Q$$

Ω, M, $Q \in M_n$ *(the set of square matrices)*, $\beta \in \mathbb{R}$, Ω *is invertible and W_t is a Brownian motion matrix.*

The Wishart process is usually used to model the dynamics of volatility-covolatility matrices. It is a mean-reverting process with affine properties. In the framework of the Wishart process in Equation (3.4), the matrix M can be considered as the mean-reversion parameter and the matrix Q as the volatility parameter of V_t.[7] In order to guarantee the typical mean-reverting and strict positive definiteness features of the volatility, the matrix M is assumed to be negative semi-definite, and condition $\beta > n - 1$ is imposed to ensure existence and uniqueness of the solution V_t.

In addition, as the evolution dynamics of V_t is usually applied to modeling volatility-covolatlity matrices, the matrix Q can be considered as the volatility of volatility parameter, which takes into account the variance-covariance fluctuations. Moreover, the Wishart process is the multivariate extension of the CIR process introduced for scalar stochastic volatility, and this multi-variable Wishart process will provide some flexibility that can help explain some empirical observations that a collection of independent one variable CIR processes can not capture. Furthermore, the Wishart dynamics can describe the evolution of stochastic volatility-covolatility matrices and are very flexible. They are direct competitors of less structural multivariate ARCH models, multinomial trees [39], and dynamic conditional correlation GARCH models [29].

Proposition 3.4. (***The Wishart process is an affine process***) *Let V_t be a Wishart Process satisfying the matrix diffusion system in (3.4). Then the drift of V_t*

---

[7]There a vast literature chose V_t to be a volatility-covolatility matrices Σ_t. Thus in those cases, the matrix Q can be considered as the volatility of volatility parameter.

is

$$E(dV_t|\mathcal{F}_t) = (\beta QQ^T + V_t M^T + M^T V_t)dt, \qquad (3.5)$$

and the covariance of $\alpha^T dV_t \alpha$ (Since it is more difficult to represent the volatility matrix of dV_t, which has large dimension. Fortunately, it is equivalent to know the square of the norm associated with dV_t) for any $\alpha, \beta \in \mathbb{R}^n$ is:

$$Cov[(\alpha^T dV_t \alpha, \beta^T dV_t \beta)|\mathcal{F}_t] = (4\alpha^T dV_t \beta \alpha^T Q^T Q \beta)dt. \qquad (3.6)$$

The drift and volatility are both affine functions [8] of V_t, and therefore the Wishart process is an affine process.

Proof: See Appendix. □

Now, let us to see how to define the conditional Laplace transform of the Wishart process. For any symmetric matrix Γ

$$Tr(\Gamma V_t) = \sum_{i=1}^{n}(\Gamma V_t)_{ii} = \sum_{i=1}^{n}\sum_{j=1}^{n}\gamma_{ij}(V_t)_{ji} = \sum_{i=1}^{n}\gamma_{ii}(V_t)_{ii} + 2\sum_{i<j}\gamma_{ij}(V_t)_{ij},$$

where $\{\gamma_{ij}, \ i,j = 1,...,n\}$ are the entries of the matrix Γ. Thus, the conditional Laplace transform can be defined as

$$\psi_{t,h}(\Gamma) = E[e^{Tr(\Gamma V_{t+h})}|\mathcal{F}_t],$$

since any linear combination of the elements of V_t can be written as $Tr(\Gamma V_t)$. The explicit expression of $\psi_{t,h}(\Gamma)$ is given as follows:

---

[8]or equivalently the conditional Laplace transform is an exponential affine function of V_t

Proposition 3.5. *(The Conditional Laplace Transform of the Wishart Process) The Wishart process V_t has conditional Laplace transform*

$$\psi_{t,h}(\Gamma) = \frac{\exp Tr[\tilde{M}(h)^T \Gamma (Id - 2\Sigma(h)\Gamma)^{-1}\tilde{M}(h)V_t]}{(\det[Id - 2\Sigma(h)\Gamma])^{\beta/2}}. \tag{3.7}$$

where

$$\tilde{M}(h) = e^{Mh},$$

$$\Sigma(h) = \int_0^h e^{Ms} Q Q^T (e^{Ms})^T \, ds.$$

Proof: See Appendix. $\qquad\qquad\qquad\qquad\qquad\qquad\qquad\qquad\qquad\qquad$ □

This conditional Laplace transform can be recognized as the Laplace transform of a noncentral Wishart distribution. In particular, the transition probability density function at horizon h admits a closed form expression which involves a series expansion (See [1] and [52]).

Proposition 3.6. *(The transition pdf of the Wishart Process) The conditional density of the Wishart process V_{t+h}, given V_t is*

$$f(V_{t+h}|V_t) = \frac{1}{2^{\beta n/2}} \frac{1}{\Gamma_n(\beta/2)} (\det \Sigma(h))^{-\beta/2}$$

$$\times (\det V_{t+h})^{(\beta-n-1)/2} \exp -\frac{1}{2} Tr[\Sigma(h)^{-1}(V_{t+h} + \tilde{M}(h)V_t\tilde{M}(h)^T)] \tag{3.8}$$

$$\times {}_{\circ}F_1\left(\beta/2, \frac{1}{4}\tilde{M}(h)V_t\tilde{M}(h)^T V_{t+h}\right),$$

where

$$\Gamma_n(\beta/2) = \int_{M>>0} \exp[Tr(-M)](\det M)^{(\beta-n-1)/2}$$

is the multidimensional gamma function and ${}_{\circ}F_1$ is a hypergeometric function of matrix argument.

The hypergeometric function admits a series expansion which involves the so-called 'zonal polynomials'. These polynomials have no closed form expressions, but can be computed recursively [43], [52].

Proposition 3.7. *(**Infinitesimal Generator of the Wishart Process**) The infinitesimal generator associated with the Wishart process in (3.4) is:*

$$\mathcal{L}^V = Tr[(\beta Q^T Q + MV_t + V_t M^T)D + 2V_t D Q^T Q D], \tag{3.9}$$

where the operator D is defined by

$$D = \left(\frac{\partial}{\partial V_t^{ij}}\right)_{1 \leq i,j \leq n} \tag{3.10}$$

Proof: See Appendix. □

3.2.2 Integrated Wishart Process

Definition 3.8. *(**The Integrated Wishart Process**) If V_t follows the dynamics of Wishart processes as described in (3.4), the integrated Wishart process is defined by*

$$Y_t = \int_0^t Tr[V_s]\, ds.$$

Let us see the conditional Laplace transform (given by Gourieroux in [34]).

Proposition 3.9. *(**The Conditional Laplace Transform of the Integrated Wishart Process**) Given a symmetric matrix Γ, and a Wishart process V_t, the conditional Laplace transform of the integrated Wishart process defined in definition 3.8*

can be written as:

$$\psi_{t,h}^*(\Gamma) = E\left(\exp Tr\left[\Gamma\int_t^{t+h} V_\tau\, d\tau\right]|\mathcal{F}_t\right) \tag{3.11}$$

$$= \exp[Tr(M^*(h,\Gamma)V_t) + b^*(h,\Gamma)],$$

where

$$\begin{cases} \dfrac{\partial M^*}{\partial h}(h,\Gamma) = \Gamma + M^*(h,\Gamma)M + M^T M^*(h,\Gamma) + 2M^*(h,\Gamma)Q^T Q M^*(h,\Gamma), \\[2mm] \dfrac{\partial b^*}{\partial h}(h,\Gamma) = \beta Tr[M^*(h,\Gamma)QQ^T], \end{cases} \tag{3.12}$$

with initial conditions: $M^*(0,\Gamma) = 0$, $b^*(0,\Gamma) = 0$. The solution of this matrix Riccati differential system is:

$$M^*(h,\Gamma) = M^*(\Gamma) + \exp[(M + 2Q^T Q M^*(\Gamma))h]^T - (M^*(\Gamma))^{-1}$$

$$+ 2\int_0^h \exp[M + 2Q^T Q M^*(h,\Gamma)u]Q^T Q \exp[M + 2Q^T Q M^*(h,\Gamma)u]^T\, du$$

$$\times \exp[[M + 2Q^T Q M^*(\Gamma)]h], \tag{3.13}$$

where $M^*(\Gamma)$ satisfies:

$$M^T M^*(\Gamma) + M^*(\Gamma)M + 2M^*(\Gamma)Q^T Q M^*(\Gamma) + \Gamma = 0. \tag{3.14}$$

Proof: See Appendix. □

We note that the solution given in the above proposition is not a closed form solution. Therefore, it is not easy and may be impossible to get option prices when applying FFT. The closed form solution for the conditional Laplace transform of the integrated Wishart process will be derived later by using *Matrix Riccati Linearization* methods.

3.3 A New Multivariate Stochastic Lévy Correlation Model with Integrated Wishart Time Change

In this thesis, we introduce a new multivariate Lévy correlation model which can handle the following simultaneously:

1. stochastic stock price,

2. skewness, kurtosis, implied volatility smile/skew,

3. stochastic volatility,

4. stochastic skewness, and

5. stochastic correlation.

As we have discussed, there are some limitations to several existing models and not all five factors listed above can be captured at the same time. For instance, the classic Black-Scholes [8] model can only handle the first case, 'stochastic stock price'; general Lévy processes [48] [3] can handle 1 and 2; the Heston [38], Bates [5] or Merton [51] models can handle 1,2,and 3; and the Lévy models with stochastic volatility [12] can handle 1-4. Our new multivariate stochastic Lévy correlation model will be able to capture 1-5 and also has the following nice features:

- It is a multidimensional Lévy process with stochastic volatility, stochastic covolatility and flexible dependence structure.

- It allows flexible correlation dynamics with independent variation.

- It allows each asset has its own business clock as well as the co-movements of business clocks of multiple assets.

- It can be easily applied to other Lévy processes which are time-changed Brownian motions.

- The conditional marginal and joint characteristic functions can be derived in an explicit form.

- It can be calibrated to the real financial market and fit the option price surface across different maturities and strikes.

3.3.1 Model Design

While there are lots of literature dealing with multivariate Lévy process with dependence structures in recent few years, (e.g., Barndorff-Nielsen [3], Luciano and Schoutens [47], Cont and Tankov [17], Eberlein and Madan [27], Kallen and Tankov [44], Tankov [57] etc.), none of them have taken stochastic volatility into account and have limited capability to catch complex dependence structure. In addition, Carr, Geman, Madan and Yor [12] proposed an approach, which has been introduced in previous chapter, to model stochastic volatility with Lévy processes by evaluating Lévy processes subordinate to the integral of a Cox-Ingersoll-Ross (CIR) process. However, their framework is not able to capture the joint behavior among several assets and does not take stochastic correlation into account. Our aim is to build a new model with rich dependence structures and flexibilities to fill this gap.

As we discussed in Chapter Two, the random change in volatility can be captured by random change in time. Therefore stochastic volatility can be created via time change. We will construct a new multivariate model and capture the stochastic correlation feature by randomizing the calendar time t to business time $\mathcal{T}_t$.

We use Lévy processes to model return innovations and stochastic time changes to generate stochastic volatility and stochastic correlation. Each return i ($i = 1, ..., n$) is modeled as:

$$Return\ X_i \sim \sum_{j=1}^{n} L_{\mathcal{T}_t^{ij}}^{ij} \triangleq \sum_{j=1}^{n} L_{ij}(\mathcal{T}_{ij})$$

$$\sim \sum_{j=1}^{n} (Economic\ Shock\ From\ Source\ j)_{Stochastic\ impacts}$$

where L_{ij} is a independent Lévy process and $\mathcal{T}_{ij}$ is a stochastic time change (business time). In the above setting, we can think each Lévy process as capture one source of economic shock, and the stochastic time change on each Lévy process as captureing the random intensity of the impact of the economic shock on the financial security.

To model the stochastic correlation among multiple underlying assets, we design the stochastic time changes $\mathcal{T}_{ij}$ for return X_i ($i, j = 1, ..., n$) as new stochastic clocks given by

$$\mathcal{T}_{ij}(t, \tau) = \int_{t}^{t+\tau} a_{ij}^2(u)\, du,$$

where $a_{ij}, (i, j = 1, ..., n)$ are elements of the square root Wishart process $\sqrt{A(t)}$. They capture the intensity of business activity at time t. Then the stochastic Lévy

correlation model is constructed as follows:

$$X_i(t, \tau) = \sum_{j=1}^{n} L_{ij} \left(\int_t^{t+\tau} a_{ij}^2(u)\, du \right), \quad i = 1, ..., n. \tag{3.15}$$

We denote it as $X_t(\tau) \triangleq L_t \bullet \{A_t(\tau)\}$, where $X_t \in R^n$, $L_t, A_t \in R^{n \times n}$ and the element $L_{ij}(t)$ in matrix L_t is taken from a centered independent Lévy process family with unit variance

$$\sqrt{A(t)} = \begin{pmatrix} a_{11}(t) & ... & a_{1n}(t) \\ ... & ... & ... \\ a_{n1}(t) & ... & a_{nn}(t) \end{pmatrix}. \tag{3.16}$$

Here $\sqrt{A(t)}, A(t)$ are symmetric positive definite $n \times n$ matrices, and the process $A(t)$ is defined here as an instantaneous rate of time change matrix which follows the Wishart process law.

$$dA_t = (\beta Q^T Q + A_t M^T + M A_t)\, dt + \sqrt{A_t}\, dW_t Q + Q^T\, dW_t \sqrt{A_t}, \tag{3.17}$$

where $M, Q \in M_n(\mathbb{R})$, $\beta \in \mathbb{R}$, $\beta > n - 1$, Q is invertible and M is negative semi-definite.

The Wishart process is widely used in modeling the dynamics of volatility and co-volatility as a multivariate extension of the CIR process. In addition, the Wishart process is a mean-reverting process, and it belongs to the class of affine processes, in which the Laplace transform has affine property. Therefore, we choose the Wishart process to model the dynamics of instantaneous time change rates. The stochastic time change is modeled as in (3.15) based on the Wishart process, and the stochastic correlation structure can be captured by such construction. For simplicity, now let us examine the two dimensional case.

Definition 3.10. (*2D Stochastic Lévy Correlation Model*) *The two dimensional stochastic Lévy correlation model is defined as:*

$$X_1(0,t) = L_{11}\left(\int_0^t a_{11}^2(u)\,du\right) + L_{12}\left(\int_0^t a_{12}^2(u)\,du\right),$$
$$X_2(0,t) = L_{21}\left(\int_0^t a_{21}^2(u)\,du\right) + L_{22}\left(\int_0^t a_{22}^2(u)\,du\right) \tag{3.18}$$

or

$$X_1(t,\tau) = L_{11}(\int_t^{t+\tau} a_{11}^2(u)\,du) + L_{12}(\int_t^{t+\tau} a_{12}^2(u)\,du),$$
$$X_2(t,\tau) = L_{21}(\int_t^{t+\tau} a_{21}^2(u)\,du) + L_{22}(\int_t^{t+\tau} a_{22}^2(u)\,du) \tag{3.19}$$

where

$$\sqrt{A(t)} = \begin{pmatrix} a_{11}(t) & a_{12}(t) \\ a_{21}(t) & a_{22}(t) \end{pmatrix}. \tag{3.20}$$

In Equations (3.19), $L_{11}, L_{12}, L_{21}, L_{22}$ are centered independent Lévy processes with unit variance. The components L_{11}, L_{12} follow the the same Lévy process, which can be considered as the source of economic shock, and L_{21}, L_{22} are chosen from the same Lévy family, but different from L_{11}, L_{12}. For example, if we choose the variance gamma processes as independent Lévy processes in (3.19), $L_{11}, L_{12} \sim VG(\theta_1, \nu_1, \sigma_1)$ and $L_{21}, L_{22} \sim VG(\theta_2, \nu_2, \sigma_2)$, where $\{L_{ij}, ij = 1, 2\}$ are all independent. Since $\sqrt{A(t)}$ is a symmetric positive definite 2×2 matrix, then $\mathcal{T}_{12} = \int_t^{t+\tau} a_{12}^2(u)\,du = \int_t^{t+\tau} a_{21}^2(u)\,du = \mathcal{T}_{21}$ can be considered as the common business clock, which captures the random intensity of the common economic impacts and may model the co-movements of business clocks of multiple assets (economic sources). The processes $L_{11}(\int_t^{t+\tau} a_{11}^2(u)\,du)$ and $L_{22}(\int_t^{t+\tau} a_{22}^2(u)\,du)$ are two Lévy processes running under their own business clocks and can be considered as idiosyncratic factors for the two underlying assets separately.

3.3.2 Conditional Characteristic Function Derivation

It is well known that in order to solve the pricing problem, it is sufficient to compute the conditional characteristic function under the risk neutral measure of the underlying assets. Once the explicit characteristic function is obtained, one can easily perform the Fast Fourier transform to price options. In this section, we will derive the closed forms of the conditional marginal characteristic function as well as the joint characteristic function of our stochastic Lévy correlation model.

Proposition 3.11. *(**The Conditional Marginal Characteristic Function**) Let Lévy processes X_i be defined as:*

$$X_i(t, \tau) = \sum_{j=1}^{n} L_{ij} \left(\int_{t}^{t+\tau} a_{ij}^2(s) \, ds \right), \quad i = 1, ..., n.$$

Then the conditional marginal characteristic function for each X_i is

$$\phi_{X_i; t, \tau}(u_i) = E\left(\exp[iu_i X_i(t, \tau)] | \mathcal{F}_t\right) = E\left(\exp Tr[\Gamma \int_{t}^{t+\tau} A(s) \, ds] | \mathcal{F}_t\right), \quad (3.21)$$

with

$$\Gamma = \begin{pmatrix} 0 & 0 & ... & 0 \\ 0 & \psi_i(u_i) & ... & 0 \\ ... & ... & ... & ... \\ 0 & 0 & ... & 0 \end{pmatrix}$$

where $\psi_i(u_i)$ is the diagonal entries (in i_{th} row and i_{th} column) of matrix Γ, and represents a centered Lévy exponent. (e.g. if L_{ij} are VG processes, then $\psi_i(u_i) = -\frac{1}{\nu_i} \ln(1 - i\theta_i \nu_i u_i + \frac{\sigma_i^2 u_i^2 \nu_i}{2} - iu_i \theta_i))$

Proof: The conditional marginal characteristic function $\phi_{X_i;t,\tau}(u_i)$ is given by:

$$E(\exp[iu_i X_i(t,\tau)]|\mathcal{F}_t) = E\{\exp(iu_i[L_{i1}(\int_t^{t+\tau} a_{i1}^2(s)\,ds) + ... + L_{in}(\int_t^{t+\tau} a_{in}^2(s)\,ds)])|\mathcal{F}_t\}$$

$$= E\{\exp[\int_t^{t+\tau} a_{i1}^2(s)\,ds \cdot \psi_i(u_i) + ... + \int_t^{t+\tau} a_{in}^2(s)\,ds \cdot \psi_i(u_i)]|\mathcal{F}_t\}$$

$$= E(\exp[\sum_{j=1}^n \int_t^{t+\tau} a_{ij}^2(s)\,ds \cdot \psi_i(u_i)]|\mathcal{F}_t)$$

$$(3.22)$$

Since $\sqrt{A(t)}$ is constructed as in (3.16), then $A(t)$ is:

$$A(t) = \begin{pmatrix} a_{11}^2(t) + ... + a_{1n}^2(t) & * & ... & * \\ * & a_{21}^2(t) + ... + a_{2n}^2(t) & ... & * \\ * & * & ... & * \\ * & * & ... & a_{n1}^2(t) + ... + a_{nn}^2(t) \end{pmatrix}$$

where $\sqrt{A(t)}, A(t)$ are symmetric positive definite $n \times n$ matrices. If we define a

new symmetric matrix $A^\psi(t)$ as:

$$A^\psi(t) =$$

$$\begin{pmatrix} [a_{11}^2(t) + ... + a_{1n}^2(t)]\psi_1(u_1) & * & ... & * \\ * & [a_{21}^2(t) + ... + a_{2n}^2(t)]\psi_2(u_2) & ... & * \\ * & * & ... & * \\ * & * & ... & [a_{n1}^2(t) + ... + a_{nn}^2(t)]\psi_n(u_n) \end{pmatrix}$$

$$(3.23)$$

and chose Γ as:

$$\Gamma = \begin{pmatrix} 0 & 0 & ... & 0 \\ 0 & \psi_i(u_i) & ... & 0 \\ ... & ... & ... & ... \\ 0 & 0 & ... & 0 \end{pmatrix},$$

then

$$A_{ii}^{\psi}(s) = Tr[\Gamma A(s)] \tag{3.24}$$

where A_{ii}^{ψ} is the i-th diagonal element in A^{ψ}. Thus the conditional marginal characteristic function in (3.22) becomes:

$$E\left(\exp\left[iu_i X_i(t,\tau)\right]|\mathcal{F}_t\right) = E\left(\exp\left[\sum_{j=1}^{n}\int_{t}^{t+\tau} a_{ij}^2(s)\,ds \cdot \psi_i(u_i)\right]|\mathcal{F}_t\right)$$

$$= E\left(\exp\left[\int_{t}^{t+\tau} A_{ii}^{\psi}(s)\,ds\right]|\mathcal{F}_t\right) = E\left(\exp Tr\left[\Gamma\int_{t}^{t+\tau} A(s)\,ds\right]|\mathcal{F}_t\right).$$

where

$$\Gamma = \begin{pmatrix} 0 & 0 & ... & 0 \\ 0 & \psi_i(u_i) & ... & 0 \\ ... & ... & ... & ... \\ 0 & 0 & ... & 0 \end{pmatrix}.$$

$\square$

Proposition 3.12. (The Conditional Joint Characteristic Function)

Let Lévy processes X_i, $i = 1, ..., n$ are defined as:

$$X_i(t,\tau) = \sum_{j=1}^{n} L_{ij}\left(\int_{t}^{t+\tau} a_{ij}^2(s)\,ds\right), \quad i = 1, ..., n$$

then the conditional joint characteristic function for $X_1, ..., X_n$ is:

$$\phi_{X_1,...,X_n;t,\tau}(u_1, ..., u_n) = E\left[\exp\left(i\langle u, X(t,\tau)\rangle\right)|\mathcal{F}_t\right] = E\left(\exp Tr\left[\Gamma\int_{t}^{t+\tau} A(s)\,ds\right]|\mathcal{F}_t\right),$$

$$\tag{3.25}$$

where

$$\Gamma = \begin{pmatrix} \psi_1(u_1) & 0 & ... & 0 \\ 0 & \psi_2(u_2) & ... & 0 \\ ... & ... & ... & ... \\ 0 & 0 & ... & \psi_n(u_n) \end{pmatrix}$$

and where $\psi_i(u_i)$, $i = 1, ..., n$ *are centered Lévy exponents.*

Proof: The conditional joint characteristic function $\phi_{X_1,...,X_n;t,\tau}(u_1, ..., u_n)$ is

$$E\left[\exp\left(i\langle u, X(t, \tau)\rangle\right)|\mathcal{F}_t\right] = E\left[\exp\left(iu_1X_1 + ... + iu_nX_n\right)|\mathcal{F}_t\right]$$

$$= E\left[\exp\left(\sum_{i=1}^{n}\sum_{j=1}^{n}\int_t^{t+\tau} a_{ij}^2(s)\,ds \cdot \psi_i(u_i)\right)|\mathcal{F}_t\right] \quad (3.26)$$

$$= E\left[\exp\left(\sum_{i=1}^{n}\sum_{j=1}^{n}\int_t^{t+\tau} a_{ij}^2(s) \cdot \psi_i(u_i)\,ds\right)|\mathcal{F}_t\right].$$

As A^ψ is defined in (3.23), if Γ is chosen as:

$$\Gamma = \begin{pmatrix} \psi_1(u_1) & 0 & ... & 0 \\ 0 & \psi_2(u_2) & ... & 0 \\ ... & ... & ... & ... \\ 0 & 0 & ... & \psi_n(u_n) \end{pmatrix},$$

then we have

$$Tr[A^\psi(s)] = Tr[\Gamma A(s)] \quad (3.27)$$

Thus the conditional joint characteristic function in (3.26) becomes:

$$E\left[\exp(i\langle u, X(t, \tau)\rangle)|\mathcal{F}_t\right] = E\left[\exp\left(\sum_{i=1}^{n}\sum_{j=1}^{n}\int_t^{t+\tau} a_{ij}^2(s) \cdot \psi_i(u_i)\,ds\right)|\mathcal{F}_t\right]$$

$$= E\left(\exp\left[Tr\int_t^{t+\tau} A^\psi(s)\,ds\right]|\mathcal{F}_t\right) = E_t\left(\exp Tr\left[\Gamma\int_t^{t+\tau} A(s)\,ds\right]\right).$$
$$(3.28)$$

with Γ as:

$$\Gamma = \begin{pmatrix} \psi_1(u_1) & 0 & ... & 0 \\ 0 & \psi_2(u_2) & ... & 0 \\ ... & ... & ... & ... \\ 0 & 0 & ... & \psi_n(u_n) \end{pmatrix}.$$

$\square$

From Proposition 3.11 and Proposition 3.12, we note that the marginal and joint conditional characteristic functions become the Laplace transforms of the integrated Wishart process with different choices of Γ.

3.3.3 The Explicit Laplace Transform for the Integrated Wishart Process

It is well known that in order to solve the pricing problem of plain vanilla options, it is sufficient to compute the conditional characteristic function (or alternatively the conditional Laplace transform) under risk neutral measure of the underlying asset.(One can get option prices via the FFT approach discussed in Chapter One.) Therefore our essential task is to derive a closed form of the conditional Laplace transform, which is analytically tractable.

In the previous Section 3.2.2, we have introduced the integrated Wishart process. Its conditional Laplace transform is provided in the Proposition 3.9, derived by Gourieroux [34]. However, the expression given in this proposition is not an explicit form, and is very difficult to apply the FFT method to get option prices. In

general the Riccati differential systems in (3.34) do not admit closed form solution. Therefore, we need an explicit expression which makes pricing of derivative options possible. A different approach is introduced in this section to obtain a closed form solution for the conditional Laplace transform of the integrated Wishart process.

For any symmetric matrix Γ, let us denote the conditional Laplace transform of the integrated Wishart process as

$$\psi_{A_t,\tau}(\Gamma) = E\left(\exp Tr[\Gamma \int_t^{t+\tau} A(s)\,ds]|\mathcal{F}_t\right) = E_t(\exp Tr[\Gamma \int_t^{t+\tau} A(s)\,ds]).$$

As we have discussed before, the Wishart process is an affine process, which means the Laplace transform can be written as an exponential affine function, namely

$$\psi_{A_t,\tau}(\Gamma) = E_t(\exp Tr[\Gamma \int_t^{t+\tau} A(s)\,ds]) = \exp\left(Tr[C(\tau,\Gamma)A_t] + b(\tau,\Gamma)\right), \quad (3.29)$$

where $C(\tau,\Gamma) \in M_n(\mathbb{R}), C(0,\Gamma) = 0$, and $b(t) \in \mathbb{R}, b(0,\Gamma) = 0$. Thus, our goal is to look for two deterministic functions $C(\tau,\Gamma)$ and $b(\tau,\Gamma)$ that parametrize the Laplace transform in equation (3.29).

Unlike the integrated square-root process in Heston's model and Carr's time changed Lévy process, for which the Laplace transform have been extensively studied by Dufresne [26] and Cox [19], there are almost no references in the literature to the explicit form of the conditional Laplace transform of the integrated Wishart process in multi-dimension. Therefore, to our knowledge, the result we derive in this section are apparently new.

One way to derive the closed conditional Laplace transform form solution of this integrated Wishart process is to follow the method described by Da Fonseca, Grasselli, and Tebald in [23]. We borrow their idea and derive as follows:

Proposition 3.13. *(The Conditional Laplace Transform of the Integrated Wishart Process(explicit form))*

Given a symmetric positive definite $n \times n$ matrix $A(t)$ which follows the Wishart process, the conditional Laplace transform of the integrated Wishart process is given as:

$$\psi_{A_t,\tau}(\Gamma) = E_t(\exp Tr[\Gamma \int_t^{t+\tau} A(s)\,ds]) = \exp\left(Tr[C(\tau,\Gamma)A_t] + b(\tau,\Gamma)\right), \quad (3.30)$$

where

$$C(\tau,\Gamma) = C_{22}^{-1}(\tau,\Gamma)C_{21}(\tau,\Gamma)$$

$$b(\tau,\Gamma) = b(\tau) = -\frac{\beta}{2}[\tau\, Tr(M) + \ln(\det C_{22}(\tau,\Gamma)] \tag{3.31}$$

with

$$\begin{pmatrix} C_{11}(\tau,\Gamma) & C_{12}(\tau,\Gamma) \\ C_{21}(\tau,\Gamma) & C_{22}(\tau,\Gamma) \end{pmatrix} = exp\left[\tau\begin{pmatrix} M & -2Q^TQ \\ \Gamma & -M^T \end{pmatrix}\right].$$

With this proposition, the closed form of conditional characteristic functions in (3.22) and (3.26) can be obtained by choosing different Γ. Now let us see the derivation details.

Proof:

Because $\psi_{A_t,\tau}(\Gamma) = E_t(\exp Tr[\Gamma \int_t^{t+\tau} A(s)\,ds])$ where $A(t)$ is a Wishart process which is affine, then we can write

$$E_t(exp\, Tr[\Gamma \int_t^{t+\tau} A(s)\,ds]) = exp\left(Tr[C(\tau,\Gamma)A_t] + b(\tau,\Gamma)\right). \tag{3.32}$$

Thanks to Itô's lemma and the infinitesimal generator $\mathcal{L}^A$ of the Wishart process derived by Bru (1991) with

$$\mathcal{L}^A = Tr[(\beta Q^TQ + MA + AM^T)D + 2ADQ^TQD] \tag{3.33}$$

and

$$D = \left(\frac{\partial}{\partial A_{ij}} \right)_{1 \leq i,j \leq n}.$$

We obtain the following equation:

$$Tr[C'(\tau, \Gamma)A_t] + b'(\tau, \Gamma) = Tr[(C(\tau, \Gamma)M + M^T C(\tau, \Gamma) + 2C(\tau, \Gamma)Q^T QC(\tau, \Gamma) + \Gamma)A_t]$$

$$+ \beta Tr[C(\tau, \Gamma)QQ^T].$$

By identifying the coefficients of A_t, we get the following matrix Riccati ODE equation (see [30])

$$\frac{\partial C(\tau, \Gamma)}{\partial \tau} = C(\tau, \Gamma)M + M^T C(\tau, \Gamma) + 2C(\tau, \Gamma)Q^T QC(\tau, \Gamma) + \Gamma, \qquad (3.34)$$

with initial condition $C(0, \Gamma) = 0$.

The differential equation for $b(\tau, \Gamma)$ is

$$\frac{\partial b(\tau, \Gamma)}{\partial \tau} = \beta Tr[C(\tau, \Gamma)QQ^T],$$

$$b(0, \Gamma) = 0. \qquad (3.35)$$

The Equation (3.34) is a matrix Riccati equation which has several nice properties (see [30]). Riccati ODE is belong to a quotient manifold (see Grasselli and Tebaldi [36]), where their flow can be linearized by doubling the dimension of the problem. Thus, we can obtain the closed-form solution to (3.34), (3.35) with a linearization procedure, as presented by Da Fonseca et al. in [23].

By doubling the dimension of the problem, we put

$$C(\tau, \Gamma) = F(\tau, \Gamma)^{-1} G(\tau, \Gamma) \qquad (3.36)$$

with $F(\tau, \Gamma) \in GL_n(\mathbb{R})$, $G(\tau, \Gamma) \in M_n(\mathbb{R})$, $F(0, \Gamma) = I_n$, $G(0, \Gamma) = 0$.

Then, we have

$$\frac{\partial}{\partial \tau}\left[F(\tau,\Gamma)C(\tau,\Gamma)\right] - \frac{\partial F(\tau,\Gamma)}{\partial \tau}C(\tau,\Gamma) = F(\tau,\Gamma)\frac{\partial C(\tau,\Gamma)}{\partial \tau},$$

and by equations (3.36), (3.34), we obtain:

$$\frac{\partial G(\tau,\Gamma)}{\partial \tau} - \frac{\partial F(\tau,\Gamma)}{\partial \tau}C(\tau,\Gamma) = G(\tau,\Gamma)M + F(\tau,\Gamma)M^T C(\tau,\Gamma)$$

$$+ 2G(\tau,\Gamma)Q^T Q C(\tau,\Gamma) + \Gamma F(\tau,\Gamma).$$

The above ODE leads to a system of linear equations:

$$\begin{cases} \dfrac{\partial G(\tau,\Gamma)}{\partial \tau} = G(\tau,\Gamma)M + \Gamma F(\tau,\Gamma), \\[3mm] \dfrac{\partial F(\tau,\Gamma)}{\partial \tau} = -F(\tau,\Gamma)M^T - 2G(\tau,\Gamma)Q^T Q, \end{cases} \tag{3.37}$$

which can also be written as follows:

$$\frac{\partial}{\partial \tau}\begin{bmatrix} G(\tau,\Gamma) & F(\tau,\Gamma) \end{bmatrix} = \begin{bmatrix} G(\tau,\Gamma) & F(\tau,\Gamma) \end{bmatrix}\begin{pmatrix} M & -2Q^T Q \\ \Gamma & -M^T \end{pmatrix},$$

and can be easily solved by:

$$\begin{bmatrix} G(\tau,\Gamma) & F(\tau,\Gamma) \end{bmatrix} = \begin{bmatrix} G(0,\Gamma) & F(0,\Gamma) \end{bmatrix}\exp\left[\tau\begin{pmatrix} M & -2Q^T Q \\ \Gamma & -M^T \end{pmatrix}\right]$$

$$= \begin{bmatrix} C(0,\Gamma) & I_n \end{bmatrix}\exp\left[\tau\begin{pmatrix} M & -2Q^T Q \\ \Gamma & -M^T \end{pmatrix}\right]$$

$$= \begin{bmatrix} C(0,\Gamma)C_{11}(\tau,\Gamma) + C_{21}(\tau,\Gamma) & C(0,\Gamma)C_{12}(\tau,\Gamma) + C_{22}(\tau,\Gamma) \end{bmatrix}$$

$$= \begin{bmatrix} C_{21}(\tau,\Gamma) & C_{22}(\tau,\Gamma) \end{bmatrix},$$

where

$$\begin{pmatrix} C_{11}(\tau,\Gamma) & C_{12}(\tau,\Gamma) \\ C_{21}(\tau,\Gamma) & C_{22}(\tau,\Gamma) \end{pmatrix} = \exp\left[\tau\begin{pmatrix} M & -2Q^T Q \\ \Gamma & -M^T \end{pmatrix}\right]. \tag{3.38}$$

Therefore, we have

$$C(\tau,\Gamma) = F(\tau,\Gamma)^{-1}G(\tau,\Gamma) = C_{22}(\tau,\Gamma)^{-1}C_{21}(\tau,\Gamma). \tag{3.39}$$

which represents the closed form solution of the matrix Riccati ODE (3.34).

Now let us turn to solving the equation (3.35). We can use the following trick to improve the computation: From the second equation in (3.37) we obtain

$$G(\tau,\Gamma) = -\frac{1}{2}\left[\frac{\partial F(\tau,\Gamma)}{\partial \tau} + F(\tau,\Gamma)M^{T}\right](Q^{T}Q)^{-1},$$

and plugging it into equation (3.36) and using the properties of the trace we deduce

$$\frac{\partial b(\tau,\Gamma)}{\partial \tau} = -\frac{\beta}{2}Tr\left[F(\tau,\Gamma)^{-1}\frac{\partial F(\tau,\Gamma)}{\partial \tau} + M^{T}\right],$$

which can be easily integrated to get

$$b(\tau,\Gamma) = -\frac{\beta}{2}\left[Tr(M)\tau + Tr[\ln F(\tau,\Gamma)]\right].$$

By the matrix logarithm property we get

$$Tr[lnF(\tau,\Gamma)] = \ln[\det F(\tau,\Gamma)].$$

Therefore the expression of $b(\tau,\Gamma)$ is

$$b(\tau,\Gamma) = b(\tau) = -\frac{\beta}{2}\left[\tau\,Tr(M) + \ln\left(\det C_{22}(\tau,\Gamma)\right)\right]$$

$\square$

.

3.3.4   The Stochastic Lévy Correlation Market Model

As we have discussed in Section 2.3.2, the Lévy model as described in equation (1.13) leads to an incomplete market. Thus there exist infinitely many equiv-

alent martingale measures. In this dissertation, the mean-correcting martingale measure is chosen as a risk-neutral measure:

$$S_t = S_0 e^{(r-q)t} \frac{e^{X_{Y_t}}}{E(e^{X_{Y_t}})}. \tag{3.40}$$

Then we will easily get the conditional marginal characteristic function and joint characteristic function under the risk-neutral measure.

Proposition 3.14. (*The Marginal Characteristic Function*)

The marginal characteristic function for the log of stock price S_t with constant continuously compounded interest rate r and dividend yields q at time t is given by:

$$\phi_{\ln S_t}(u) = E[e^{iu \ln S_t}] = e^{(iu \ln(S_0 + (r-q)t))} \frac{\phi_{X;0,t}(u)}{[\phi_{X;0,t}(-i)]^{iu}}. \tag{3.41}$$

where $\phi_{X;0,t}(u)$ is defined as in proposition 3.11.

Proposition 3.15. (*The Joint Characteristic Function*)

The joint characteristic function for the log of stock prices $S_1(t), ..., S_n(t)$ with risk free rate r and dividend yield $q_1, ..., q_n$ at time t is given by:

$$\phi_{\ln S_1, ..., \ln S_n}(u_1, ..., u_n) = E[e^{i\langle u, \ln S_t \rangle}]$$
$$= \exp(\sum_{j=1}^{n} iu_j[\ln S_j(0) + (r - q_j)t]) \frac{\phi_{X_1, ..., X_n; 0, t}(u_1, ..., u_n)}{\prod_{j=1}^{n}[\phi_{X_j \, 0, t}(-i)]^{iu_j}}. \tag{3.42}$$

where $\phi_{X_1, ..., X_n; 0, t}(u_1, ..., u_n)$ is defined as in proposition 3.12

In this dissertation, we chose the VG processes as our base Lévy processes. However, one should notice that this correlation model can be applied to any Lévy process, for instance, the VG process, the NIG process, or the CGMY process. In

addition, we will discuss the performance and features in the rest of the paper in only two dimension for simplicity. But these results can be easily extended to higher dimensions.

3.4   Model Performance and Numerical Implementations

3.4.1   Path Simulation

In our multivariate Lévy correlation model setting, the instantaneous rate of time change matrix $A(t)$ follows the Wishart process

$$dA_t = (\beta Q^T Q + A_t M^T + M A_t)\, dt + \sqrt{A_t}\, dW_t Q + Q^T\, dW_t \sqrt{A_t},$$

which it captures all variation information of volatility-covolatility among multiple assets. In this section, Monte Carlo simulation is used to generate the simulated sample paths of the Wishart process. Monte Carlo simulation is widely used in financial engineering. It is a straightforward and easy implemented methodology in option pricing when an analytic solution is not available.

There is a problem with simulation of continuous Wishart processes when β is a real number. The problem is that one must ensure that the matrix $A(t)$ stays positive definite. The same problem occurs in the Heston model, and that is why the Euler-truncated scheme has been introduced (See Lord, Koekkoek, and Van Dijk [46] for details). For Wishart process simulation, in order to make the matrix $A(t)$ positive, the solution is to keep only positive eigenvalues and replace negative ones by zeros. This is very costly since this requires a matrix diagonalization at each

step of the diffusion. There exist some more efficient schemes such as the Discrete O-U scheme and Gaussian autoregressive scheme when β is an integer number. In addition, QE scheme to continuous Wishart process is introduced by Gauthier and Possamai in 2009 [32]. In this dissertation, we will introduce two efficient schemes to simulate the sample path of Wishart process with integer β. (See [32] for the general case.)

Discrete OU Scheme

In the particular case where β is an integer, we have already seen in Proposition 3.2 that a Wishart process can be expressed as a sum of vectorial OU processes:

$$dX_{k,t}^{OU} = M X_{k,t}^{OU} dt + Q^T dW_{k,t},$$

$$A_t = \sum_{k=1}^{\beta} X_{k,t}^{OU} (X_{k,t}^{OU})^T.$$

where $\{W_{k,t}, t \geq, 1 \leq k \leq \beta\}$ are independent vectorial Brownian motions. Then the discretization of these processes is as follows:

Algorithm: Discretization of the variance process:

$$X_{k,t+\Delta t}^{OU} = \Delta t \, M X_{k,t}^{OU} + \sqrt{\Delta t} Q^T \varepsilon_{k,t+\Delta t}, \qquad \varepsilon \sim N(0, I)$$

$$A_t = \sum_{k=1}^{\beta} X_{k,t}^{OU} (X_{k,t}^{OU})^T.$$

Input: matrices M, Q, integer β, time spacing $\Delta t_1, ..., \Delta t_n$ with $\sum_{i=1}^{N} \Delta t_i = T$.

Initialization: $A_0 = \sum_{k=1}^{\beta} X_{k,0} X_{k,0}^T$

for each $k = 1, ..., \beta$, X_k is n dimensional vector. (n assets)

Loop: from $i = 1$ to N:

    Loop: from $k = 1$ to β:

        Generate multivariate normal vector $\varepsilon_{k,t_{i+1}} \sim N(0, I)$

$$X_{k,t_{i+1}} = X_{k,t_i} + \Delta t_i \, M X_{k,t_i} + \sqrt{\Delta t} Q^T \varepsilon_{k,t_{i+1}}$$

Return: $A_t = \sum_{i=1}^{\beta} X_{k,t} X_{k,t}^T$.

Gaussian Autoregressive Vector Processes

The Wishart Autoregressive process (WAR) can be interpreted as an outer product of Guassian autoregressive vector processes, when the degree of freedom β is an integer. (See [35])

Algorithm: Guassian Autoregressive Vector Processes:

Discrete-time Wishart process: $A_t = \sum_{k=1}^{\beta} X_{k,t} X_{k,t}^T$

where $X_{k,t+h} = M_d X_{k,t} + \varepsilon_{k,t+h}$ $\varepsilon_{k,t+h} \sim N(0, \Sigma_d)$,

and $M_d = \exp(Mh), \quad \Sigma_d = \int_0^h \exp(Ms) Q Q^T [\exp(Ms)]^T \, ds$, h is the time step.

Input: matrices M, Q, integer β, time spacing $\Delta t_1, ..., \Delta t_n$ with $\sum_{i=1}^{N} \Delta t_i = T$

Initialization: $A_0 = \sum_{k=1}^{\beta} X_{k,0} X_{k,0}^T$

    for each $k = 1, ..., \beta$, X_k is n dimensional vector. (n assets)

Loop: from $i = 1$ to N:

    Loop: from $k = 1$ to β:

        Generate multivariate normal vector $\varepsilon_{k,t_{i+1}} \sim N(0, \Sigma_d)$

        where $\Sigma_d = \int_0^{\Delta t_i} \exp(Ms) QQ^T [\exp(Ms)]^T \, ds$

$$X_{k,t_{i+1}} = M_d X_{k,t_i} + \varepsilon_{k,t_{i+1}} \qquad M_d = exp(M \Delta t_i)$$

Return: $A_t = \sum_{i=1}^{\beta} X_{k,t} X_{k,t}^T$.

We now present simulation experiments to illustrate the dynamics of a bivariate Wishart process. The bivariate Wishart process has three components that can be interpreted as two volatility and one covolatility processes. In our model setting, the random change in volatility is captured by random change in time. Thus, the three components in our bivariate Wishart process represent the instantaneous time change rate. We examine the evolution of three following processes:

- $A_{11}(t), A_{22}(t)$, which capture the random change of two volatilities,

- $A_{12}(t)/\sqrt{A_{11}(t)A_{22}(t)}$ which captures the correlation, and

- the eigenvalues of the stochastic volatility matrix.

We simulate $T = 250$ observations in all experiments. Figures are provided.

Experiment 1 (Figure 3.1, 3.2, 3.3)

Simulation parameters for experiment 1:

$$M = \begin{pmatrix} -0.2 & -0.15 \\ -0.15 & -0.1 \end{pmatrix}, \quad Q = \begin{pmatrix} 0.5 & 0.4 \\ 0.3 & 0.2 \end{pmatrix}, \quad \beta = 4.$$
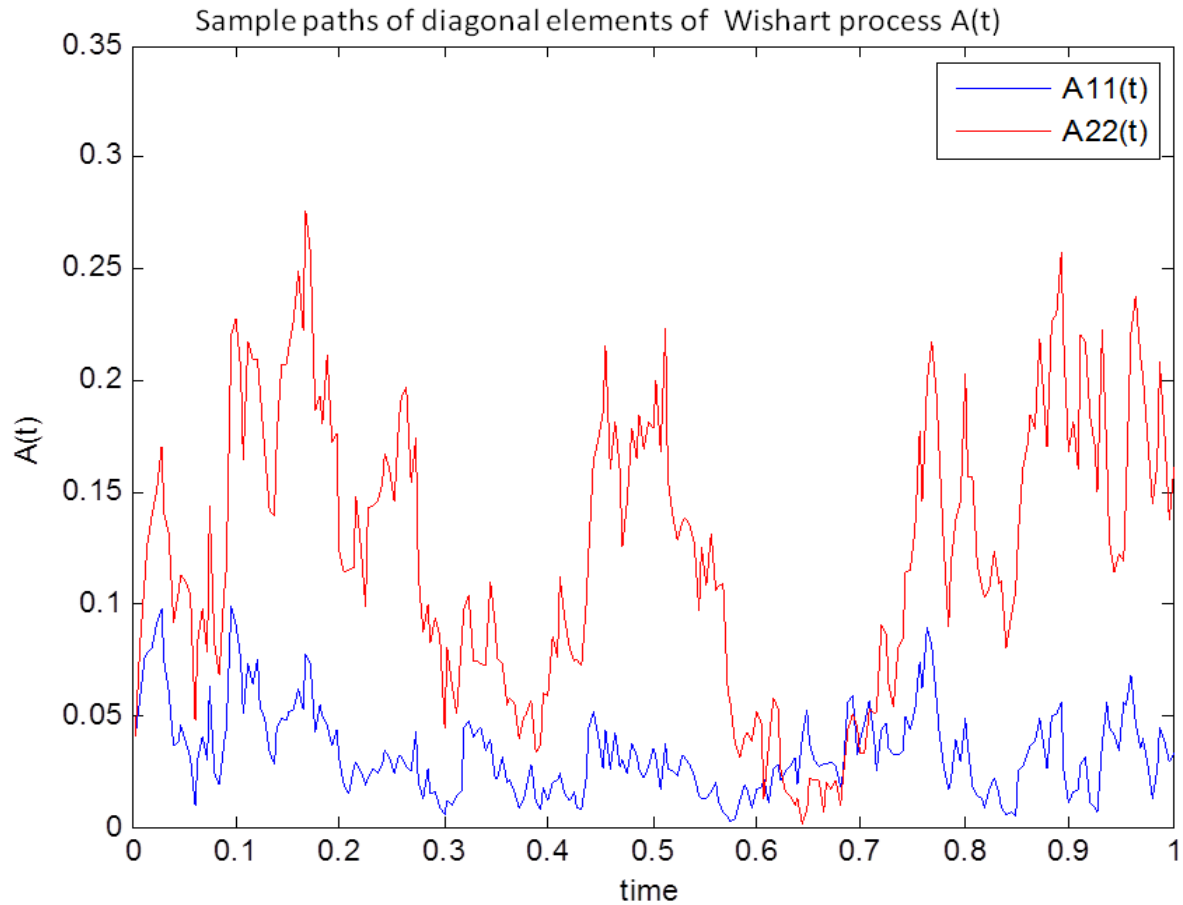

Figure 3.1: $A_{11}(t)$, $A_{22}(t)$ evolution (Volatilities)for experiment 1

Figure 3.1 displays the dynamics of the instantaneous time change rates $A_{11}(t)$ (Blue one) and $A_{22}(t)$ (Red one), which trace out the first and second diagonal components of the volatility series respectively. In all experiments, we observe that the bivariate Wishart process model is able to reproduce the volatility clustering. The higher
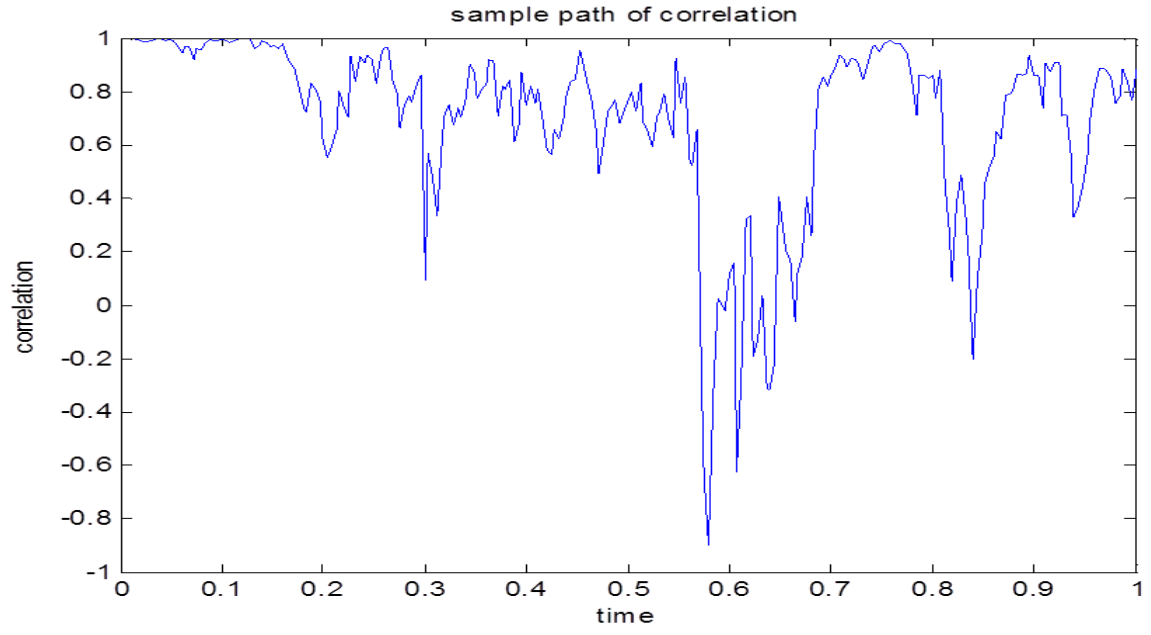
Figure 3.2: reflect covolatility evolution for experiment 1
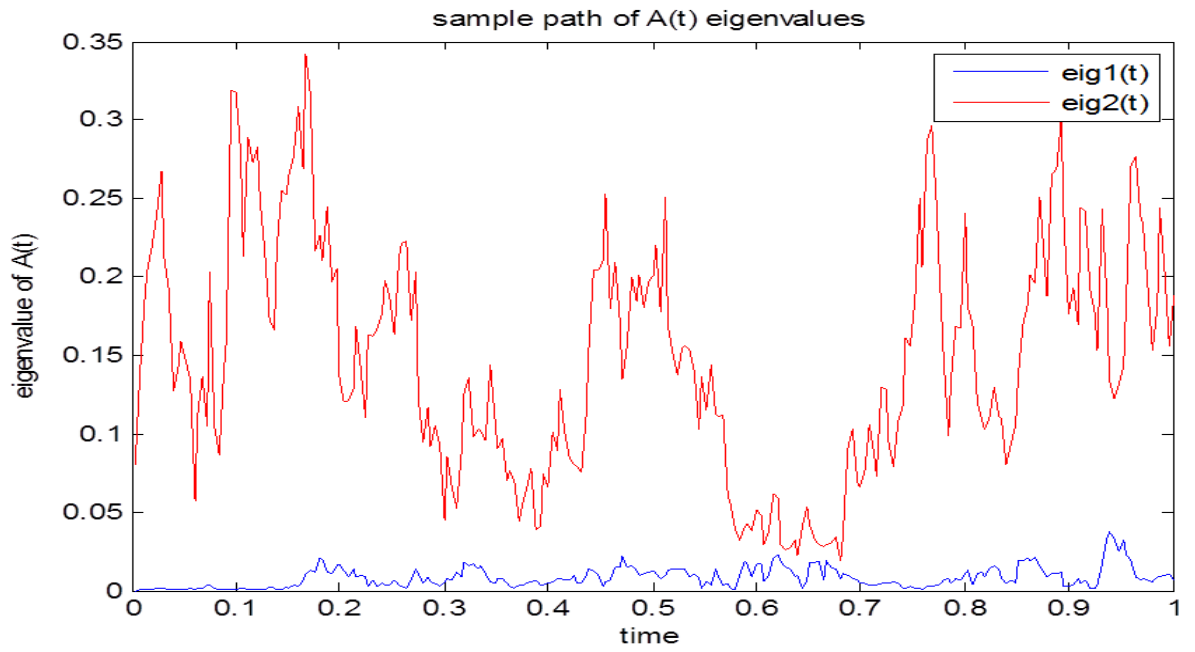
Figure 3.3: Eigenvalues for experiment 1

path represents larger volatility while lower path represents the smaller volatility. Volatility for asset 2 varies much more than asset 1. Moreover, we also note that the clustering pattern is not identical in both volatilities. The simulated path in Figure 3.2 of the correlation processes takes values between -1 and 1.

We also examine the eigenvalue series (Figure 3.3): The minimum eigenvalue is equal to the minimum of portfolio volatilities $\alpha^T A(t)\alpha$ with allocation standardized by $\alpha^T \alpha = 1$, while the maximum eigenvalue is equal to the maximum of portfolio volatilities computed for allocation standardized as before. These provide a measure of risk. The eigenvectors associated with the largest eigenvalue define the most risky portfolio allocation. In addition, when the smallest eigenvalue is close to zero, the associated eigenvector provides the arbitragist strategies.

$\boxed{\textbf{Experiment 2}}$ (Figure 3.4, 3.5, 3.6)

Simulation parameters for experiment 2:

$$M = \begin{pmatrix} -5 & -3 \\ -3 & -5 \end{pmatrix}, \quad Q = \begin{pmatrix} 0.113 & 0.033 \\ 0 & 0.0795 \end{pmatrix}, \quad \beta = 3.$$

In experiment 2, the off-diagonal elements in the volatility of volatility parameter Q are relatively small. This may explain the observations of lower correlation among two assets in Figure 3.5.
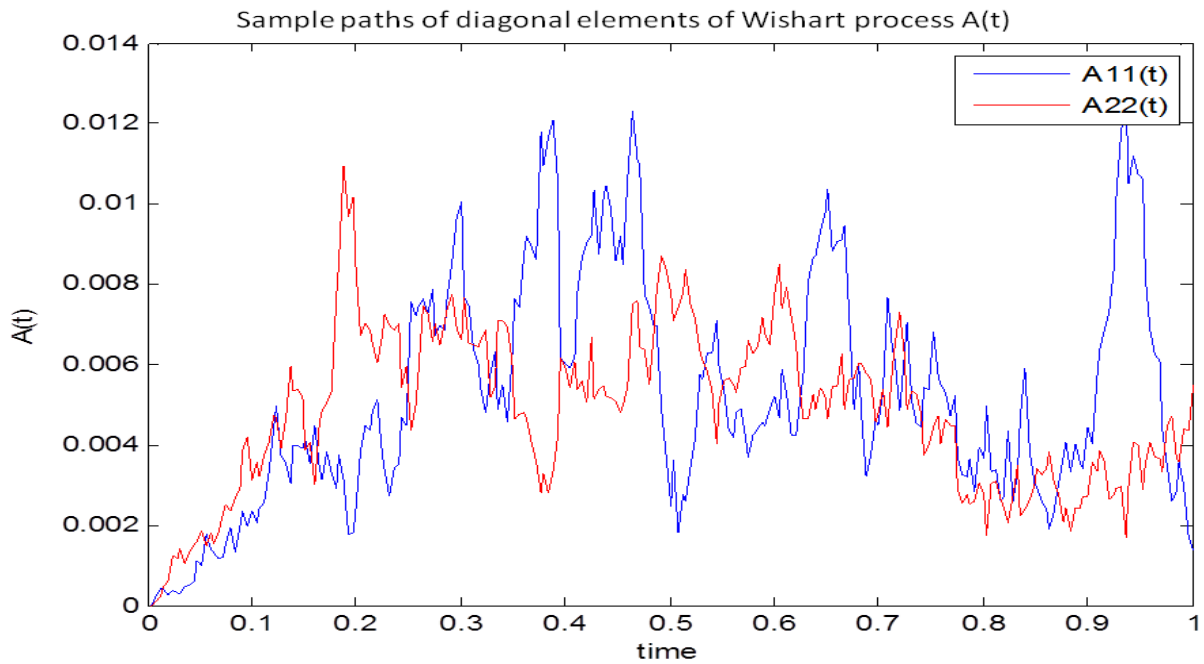
Figure 3.4: $A_{11}(t), A_{22}(t)$ evolution (Volatilities)for experiment 2
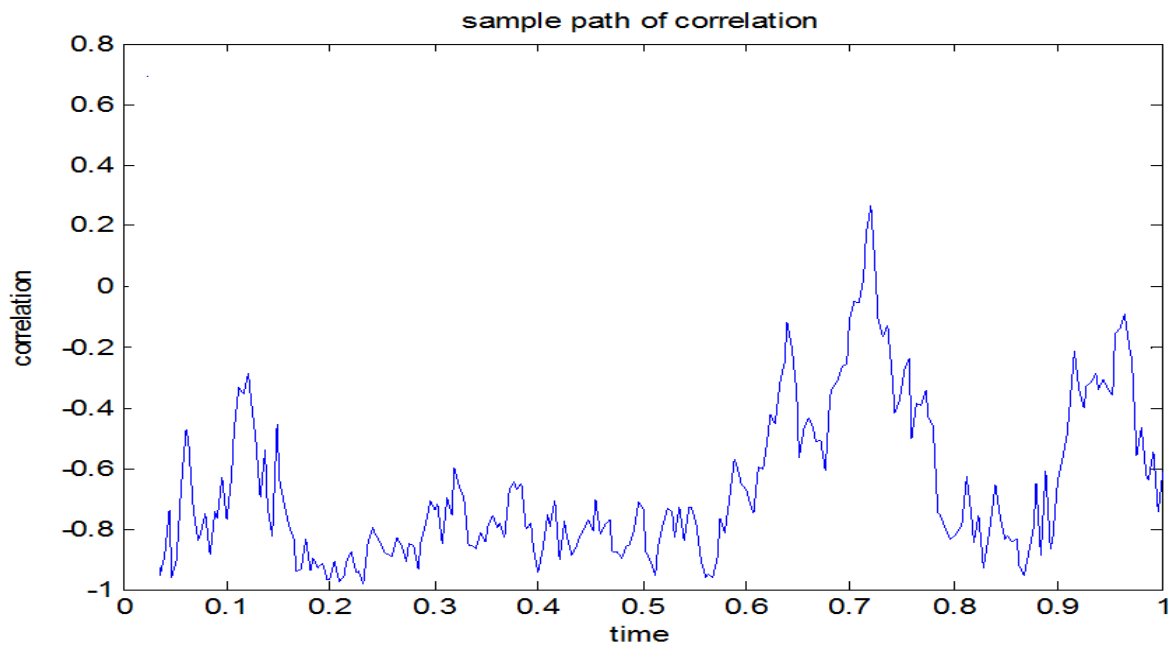

Figure 3.5: reflect covolatility evolution for experiment 2
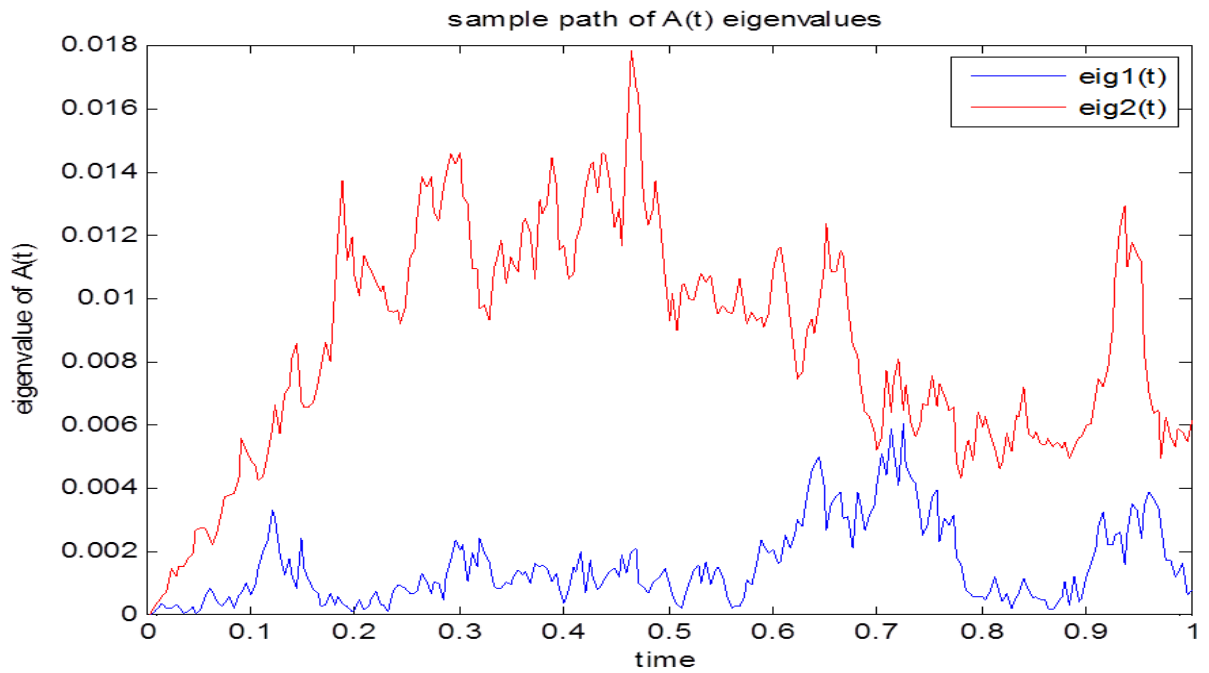
Figure 3.6: eigenvalues for experiment 2

Experiment 3 (Figure 3.7, 3.8, 3.9)

Simulation parameters for experiment 3:

$$M = \begin{pmatrix} -0.3420 & 0 \\ 0 & -0.1311 \end{pmatrix}, \quad Q = \begin{pmatrix} 0.243 & 0 \\ 0 & 0.243 \end{pmatrix}, \quad \beta = 3.$$

In this experiment 3, there are zero off-diagonal elements in parameters M and Q, and one can observe that correlation bounces freely between the values -1 to 1.
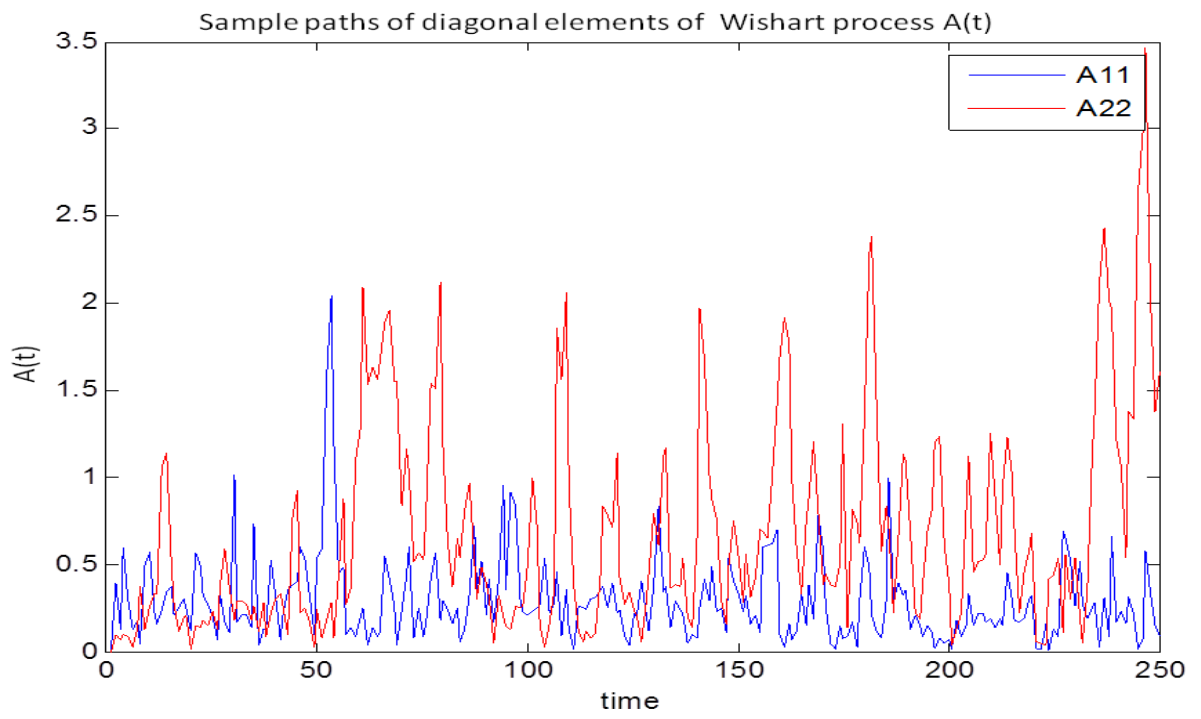
Figure 3.7: $A_{11}(t), A_{22}(t)$ evolution (Volatilities)for experiment 3
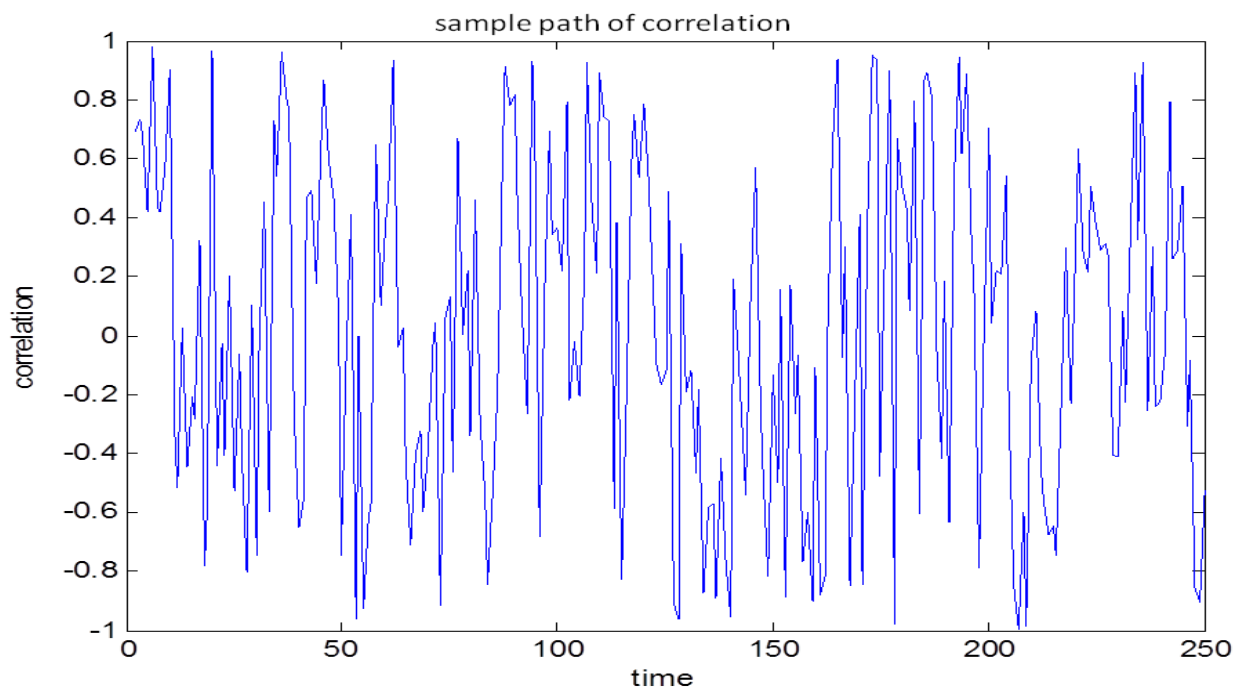
Figure 3.8: Reflect covolatility evolution for experiment 3
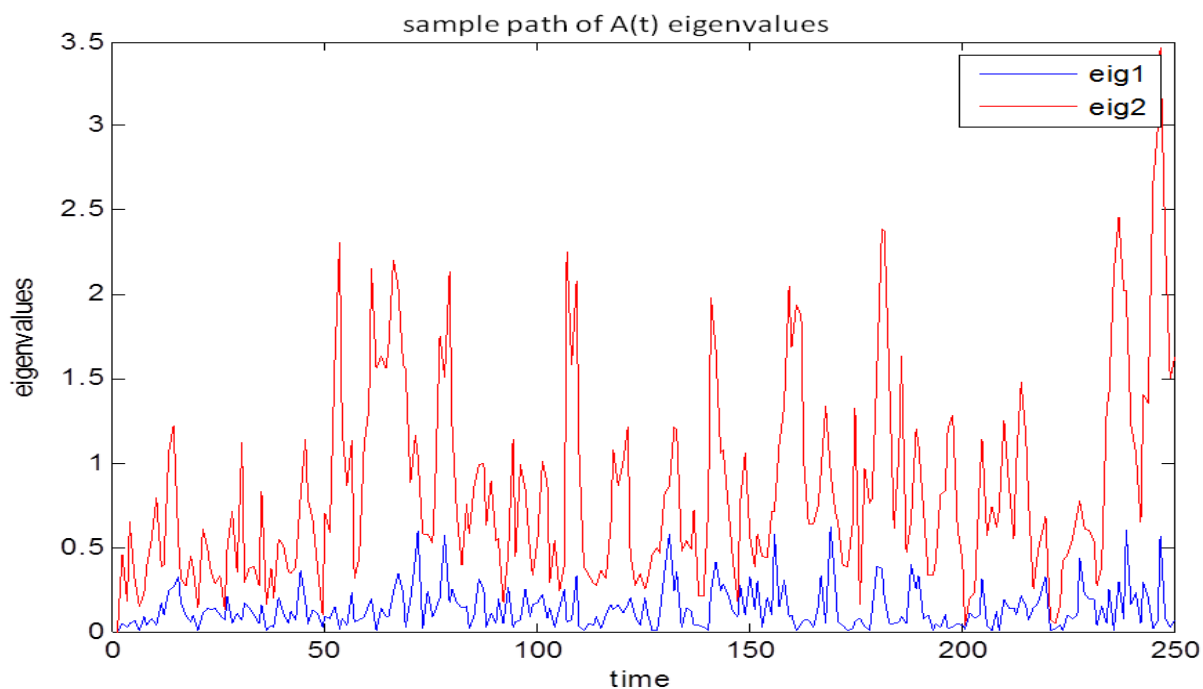
Figure 3.9: Eigenvalues for experiment 3

$X(t)$ **Sample Path Simulation**

Three simulated sample paths for asset return $X(t)$ are prensented. In order to see the effect of parameters M and Q clearly, we are using same parameter sets for the VG exponent in following three experiments ($\theta_1 = \theta_2 = 0.08, \sigma_1 = \sigma_2 = 1, \nu_1 = \nu_2 = 0.05$).

$\boxed{\textbf{Experiment 1 for } X(t)}$ (Figure 3.10)

$X(t)$ path simulation parameters for experiment 1:

$$M = \begin{pmatrix} -0.3420 & 0 \\ 0 & -0.1311 \end{pmatrix}, \quad Q = \begin{pmatrix} 0.243 & 0 \\ 0 & 0.243 \end{pmatrix}, \quad \beta = 3.$$

$X(t)$ path simulation parameters for experiment 2:

$$M = \begin{pmatrix} -0.03420 & 0.02 \\ 0.02 & -0.01311 \end{pmatrix}, \quad Q = \begin{pmatrix} 0.0243 & 0 \\ 0 & 0.0243 \end{pmatrix}, \quad \beta = 3.$$

Experiment 3 for $X(t)$ (Figure 3.12)

$X(t)$ path simulation parameters for experiment 3:

$$M = \begin{pmatrix} -0.3420 & 0.2 \\ 0.2 & -0.1311 \end{pmatrix}, \quad Q = \begin{pmatrix} 0.243 & 0 \\ 0 & -0.8 \end{pmatrix}, \quad \beta = 3.$$
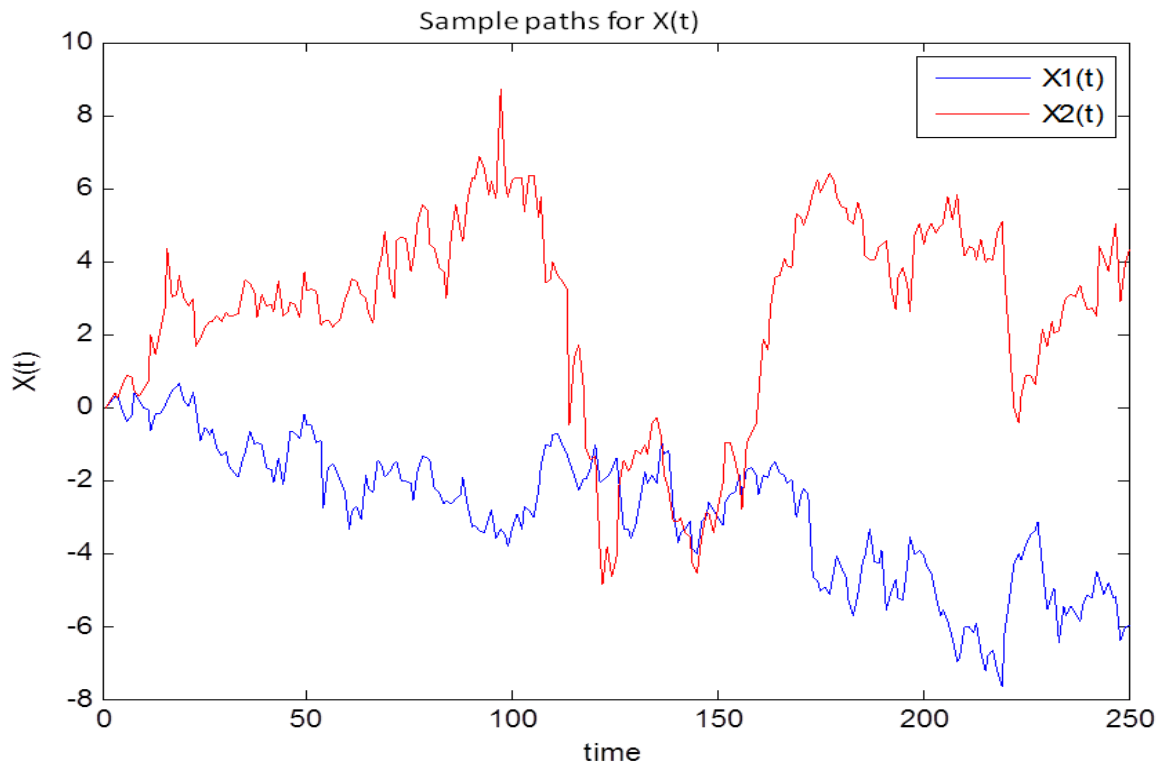

Figure 3.10: $X(t)$ sample path for experiment 1
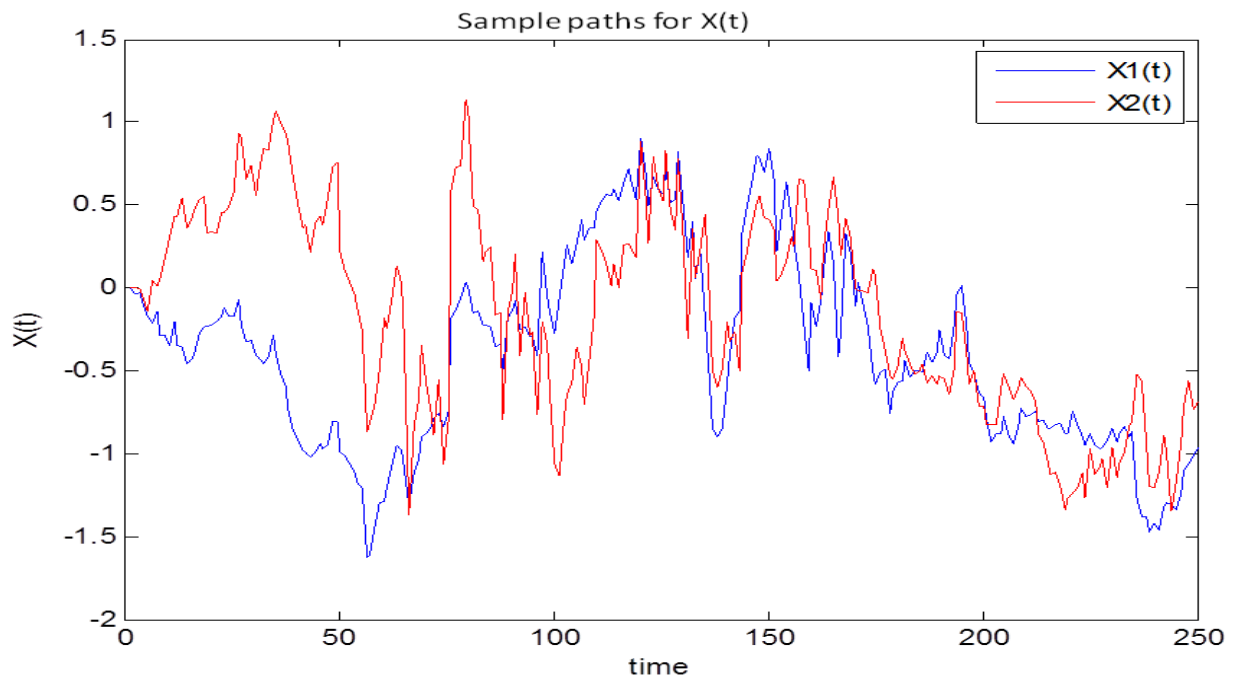
Figure 3.11: $X(t)$ sample path for experiment 2
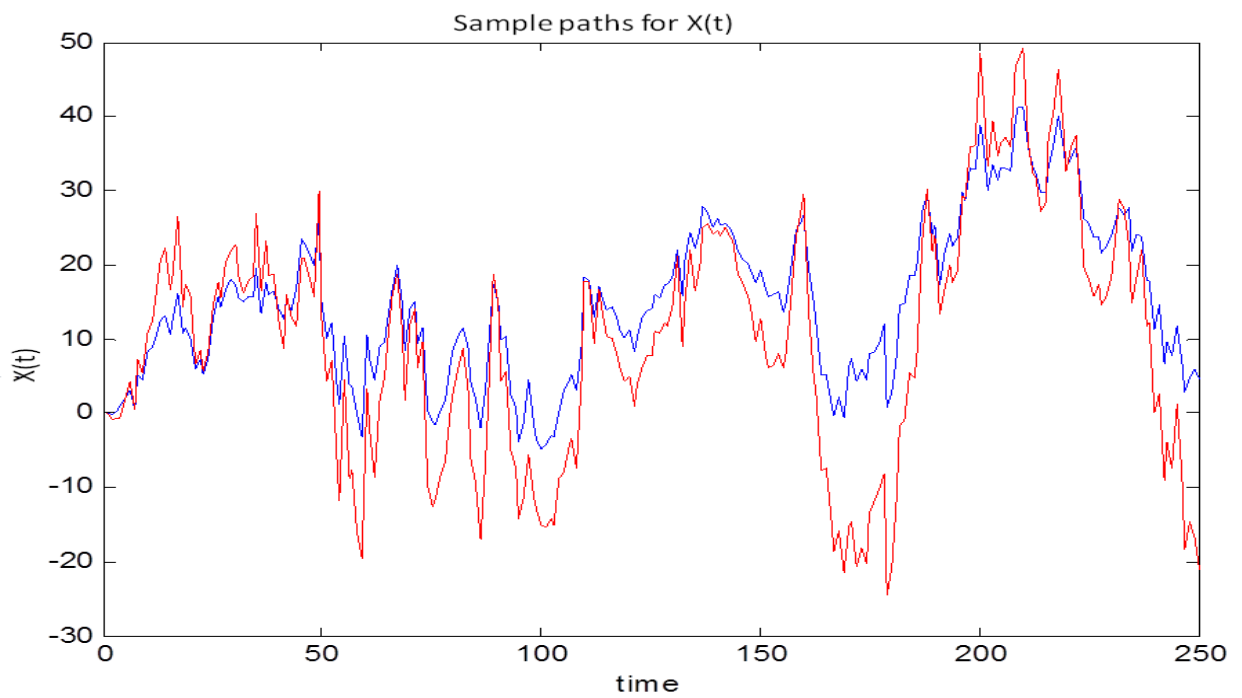
Figure 3.12: $X(t)$ sample path for experiment 3

3.4.2   Finding the Damping Factor α

In the FFT method introduced in Chapter 1.4, Carr and Madan [11] suggest choosing a damping factor α which satisfies:

$$E(S_T^{\alpha+1}) < \infty \tag{3.43}$$

FFT is efficient but it suffers from one drawback in application. The solutions produced depend on the choice of damping factor α. Moreover, in this new model the relationship between α and the parameters is not as trivial to identify as is done by Carr and Madan [11] for the VG model. We therefore test our model to find appropriate α that satisfies (3.43).
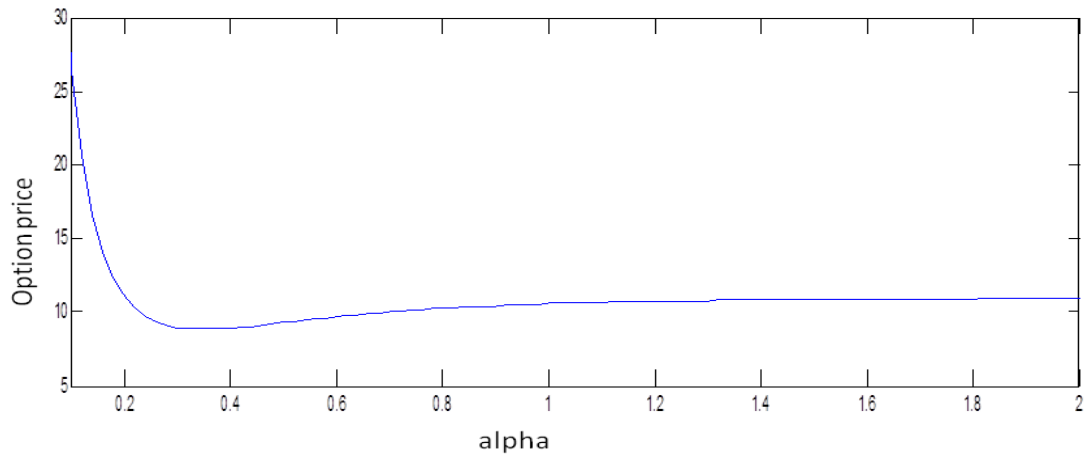
Figure 3.13: Damping factors for VG model

From Figure 3.13 and Figure 3.14 option prices decay as alpha increasing. Carr and Madan [11] suggest choosing $\alpha = 1.5$ for modified call price, and $\alpha = 1.1$ for modified time value. In Figure 3.14, option prices converge and become stable when α is greater than 1. We have tested different α values for the Lévy correlation
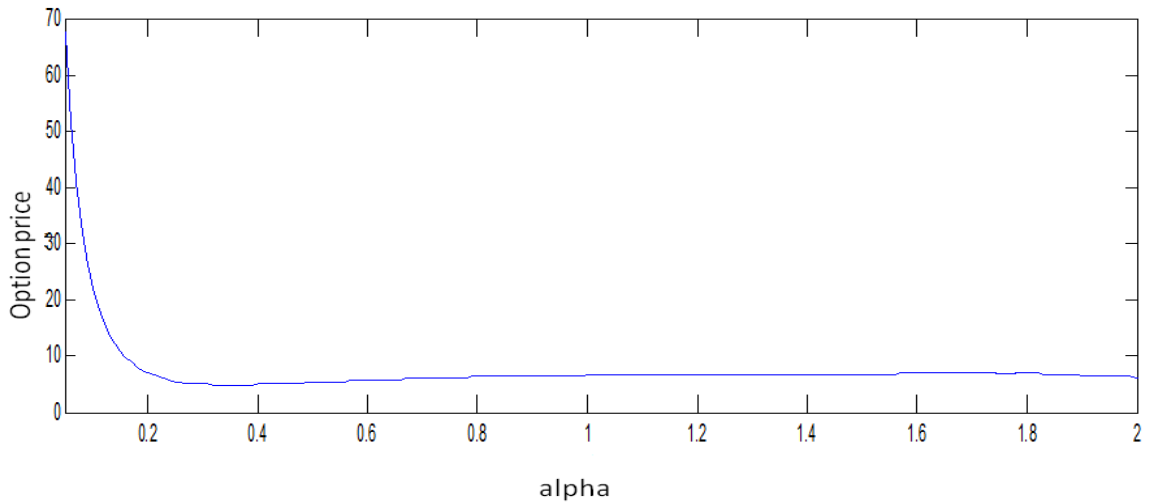
Figure 3.14: Damping factors for new correlation model

model resulting in choosing the damping factor α between 1 and 1.65. The model performs very well.

3.4.3 The Performance of Density Functions

In Proposition 3.6, the transition probability density function does not have a closed form. However, density functions can be recovered by applying the Fourier inversion theorem.

Theorem 3.16. *(Fourier Inversion Theorem)*

Let $X = (x_1, ..., x_p)^T$ be a $p \times 1$ random variable with cumulative density function(c.d.f.) F_X and consider $\forall \xi \in \mathbb{R}^p$, the characteristic function of X is the Fourier transform of F_X:

$$\Phi_X(\xi) = \int \dots \int_{\mathbb{R}^p} e^{-i\xi^T X} \, dF_X. \tag{3.44}$$

Now suppose that X has a density function f_X. If Φ_X is Lebesgue integrable ($\Phi_X \in$

$L^1(\mathbb{R}^p)$), then, by the inversion theorem:

$$f_X(X) = \frac{1}{(2\pi)^p} \int \cdots \int_{\mathbb{R}^p} e^{-i\xi^T X} \Phi_X(\xi)\, d\xi. \tag{3.45}$$

In Propositions 3.11 and 3.12, the conditional marginal characteristic function and joint characteristic function have been derived in explicit form. We therefore applied the Fourier Inversion Theorem on both characteristic functions to recover the density functions.

Histogram for Simulated Samples

To better visualize what the simulated data look like, we present a histogram. We simulated $10,000$ log returns for a single asset and present their histogram in Figure 3.15. The red solid line is the best normal fit to simulated data. The blue bars represent simulated log returns. We observed there is a skewness, which results the normal fitting inaccurately.
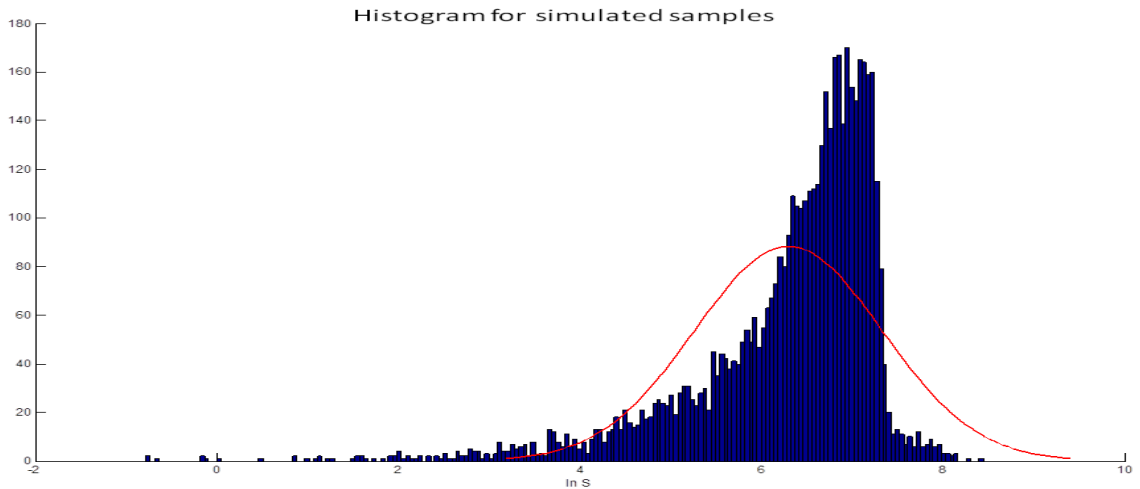
Figure 3.15: Simulated samples histogram with $Q = [0.05, 0.04; 0.03, 0.05]; M = [-15, -0.5; -0.5, -5]; \theta_1 = -1.5, \sigma_1 = 0.15, \nu_1 = 0.4344$.

Marginal PDF

We chose different sets of parameters to reveal the behavior of the marginal probability density function. Densities are displayed in Figures 3.16 – 3.19:
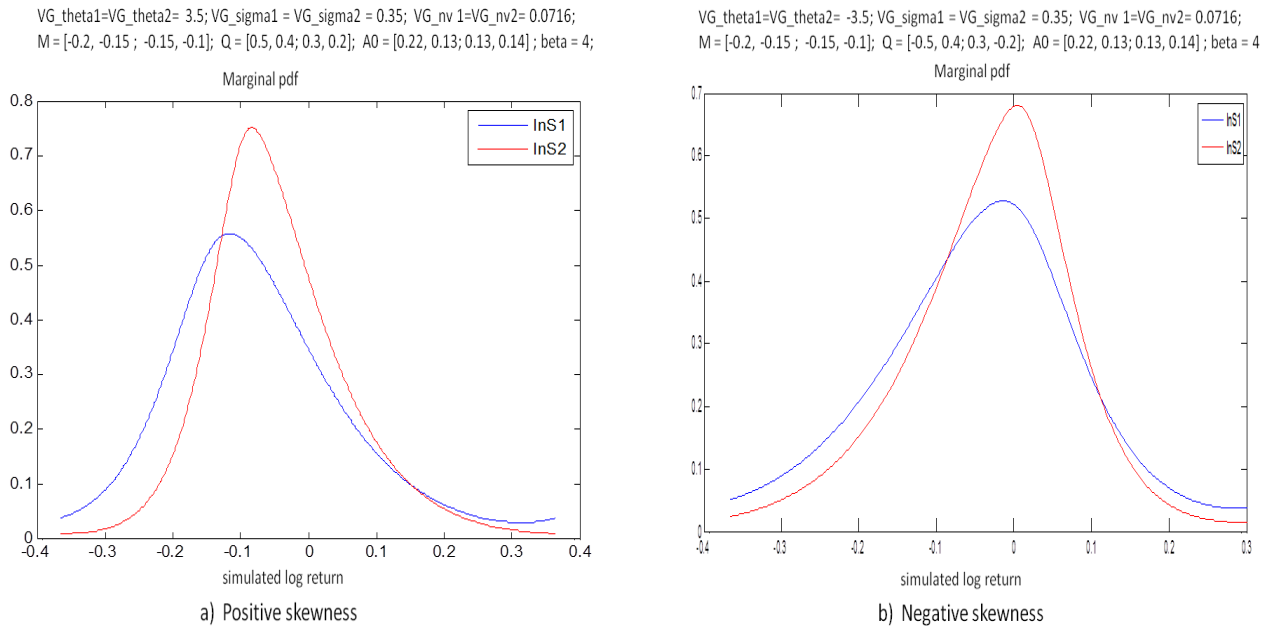
Figure 3.16: Marginal pdf of log returns I

As we know, market returns have a fat tail and skewness phenomena. From all these marginal pdf figures, we have seen that by choosing a broad range of parameters, the probability density function for log returns in our model has shown a wide range of skewness, kurtosis and rich dependent structures, which make this new model more flexible and a good candidate for market returns.

VG_theta1=VG_theta2= -2.5; VG_sigma1 = VG_sigma2 = 0.25; VG_nv 1=VG_nv2= 0.15;
A0 = [0.22, 0.13; 0.13, 0.14] ; M = [-15, -0.5 ; -0.5, - 5]; Q = [0.5, 0.4; 0.3, 0.2]; beta = 4;
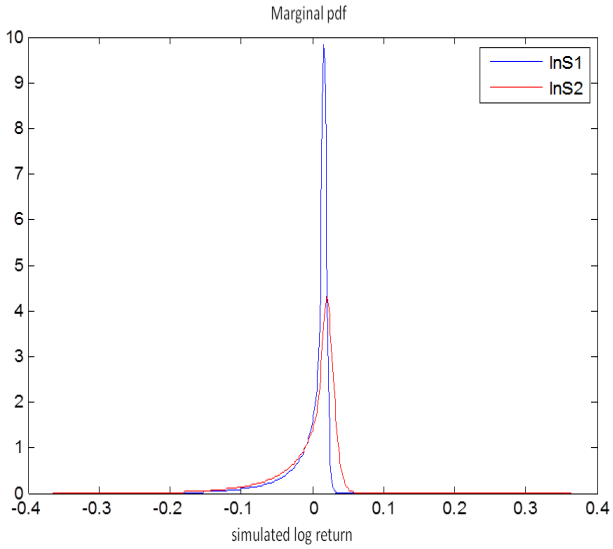
VG_theta1=VG_theta2= -2.5; VG_sigma1 = VG_sigma2 = 0.25; VG_nv 1=VG_nv2= 0.15;
A0 = [0.22, 0.13; 0.13, 0.14] ; M = [-0.2, -0.15; -0.15, -0.1]; Q = [0.0, 0.0; 0.0, 0.0]; beta = 4;
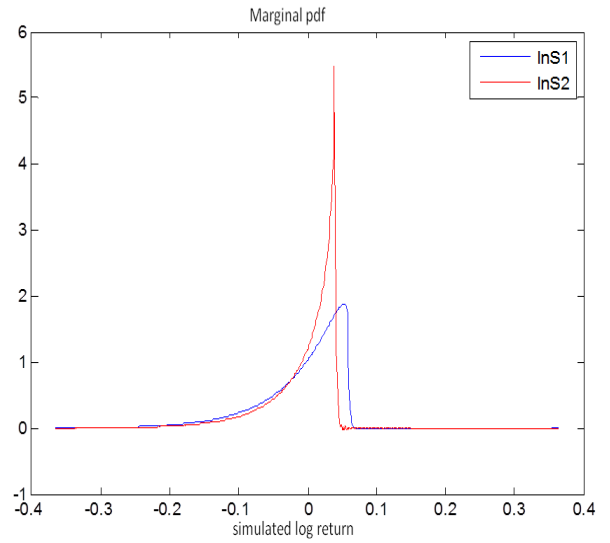
Figure 3.17: Marginal pdf of log returns II

VG_theta1=VG_theta2= -2.5; VG_sigma1 = VG_sigma2 = 0.25; VG_nv 1=VG_nv2= 0.15;
A0 = [0.22, 0.13; 0.13, 0.14] ; M = [-15, -0.5 ; -0.5, - 5]; Q = [0.5, 0.04; 0.03, 0.2]; beta = 4;
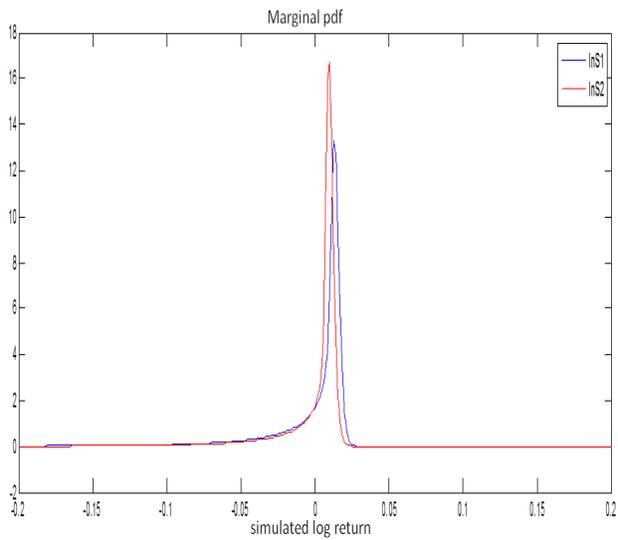
VG_theta1=VG_theta2= -3.5; VG_sigma1 = VG_sigma2 = 0.35; VG_nv 1=VG_nv2= 0.0716;
A0 = [0.22, 0.13; 0.13, 0.14] ; M = [-0.2, -0.15 ; -0.15, - 0.1]; Q = [0.0, 0.0; 0.0, 0.0]; beta = 4;
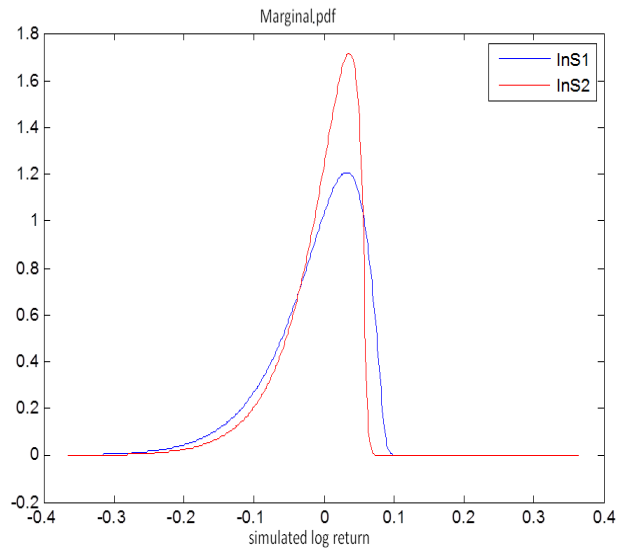
Figure 3.18: Marginal pdf of log returns III

Marginal pdf

simulated log return

g)

Marginal pdf

simulated log return

h)
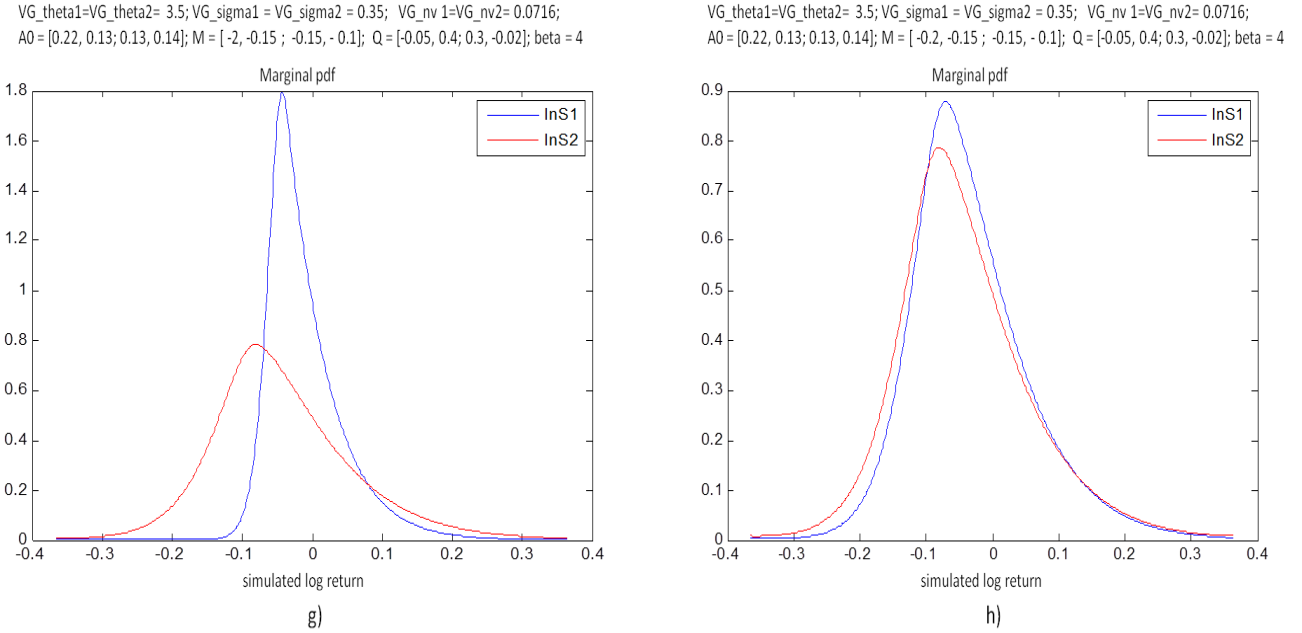
Figure 3.19: Marginal pdf of log returns IV

Joint PDF

Based on joint characteristic functions, the joint pdf can be obtained via Fourier inverse transformation theorem. Figures of joint density functions are provided for two experiments in Figure 3.20 and Figure 3.21. In order to see the effect of Wishart parameters better, we use the same VG parameters for two assets.

Experiment 1 for Joint PDF

(positive skewness)

parameters for experiment 1:

$$M = \begin{pmatrix} -0.2 & -0.15 \\ -0.15 & -0.1 \end{pmatrix}, \quad Q = \begin{pmatrix} 0.05 & 0.04 \\ 0.03 & 0.02 \end{pmatrix}, \quad \beta = 4.$$

$$\theta_1 = \theta_2 = 3.5, \quad \sigma_1 = \sigma_2 = 0.35, \quad \nu_1 = \nu_2 = 0.0716.$$

76
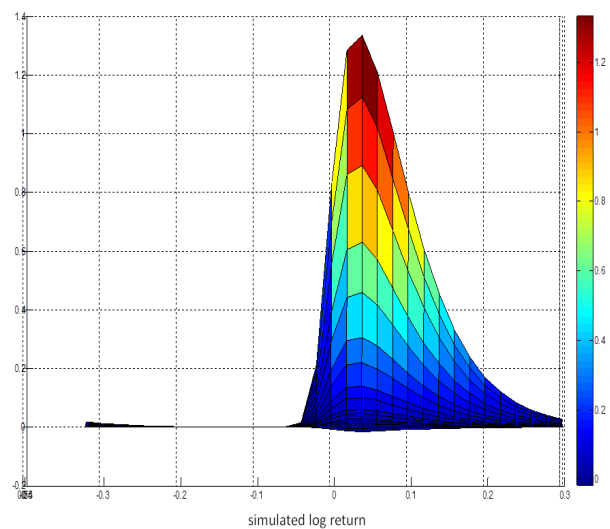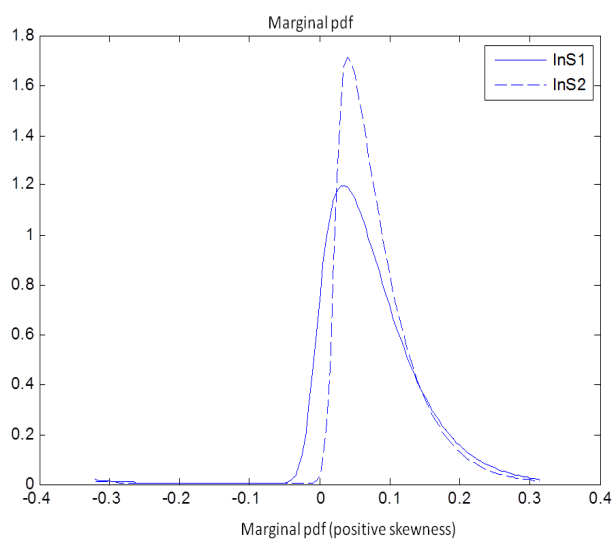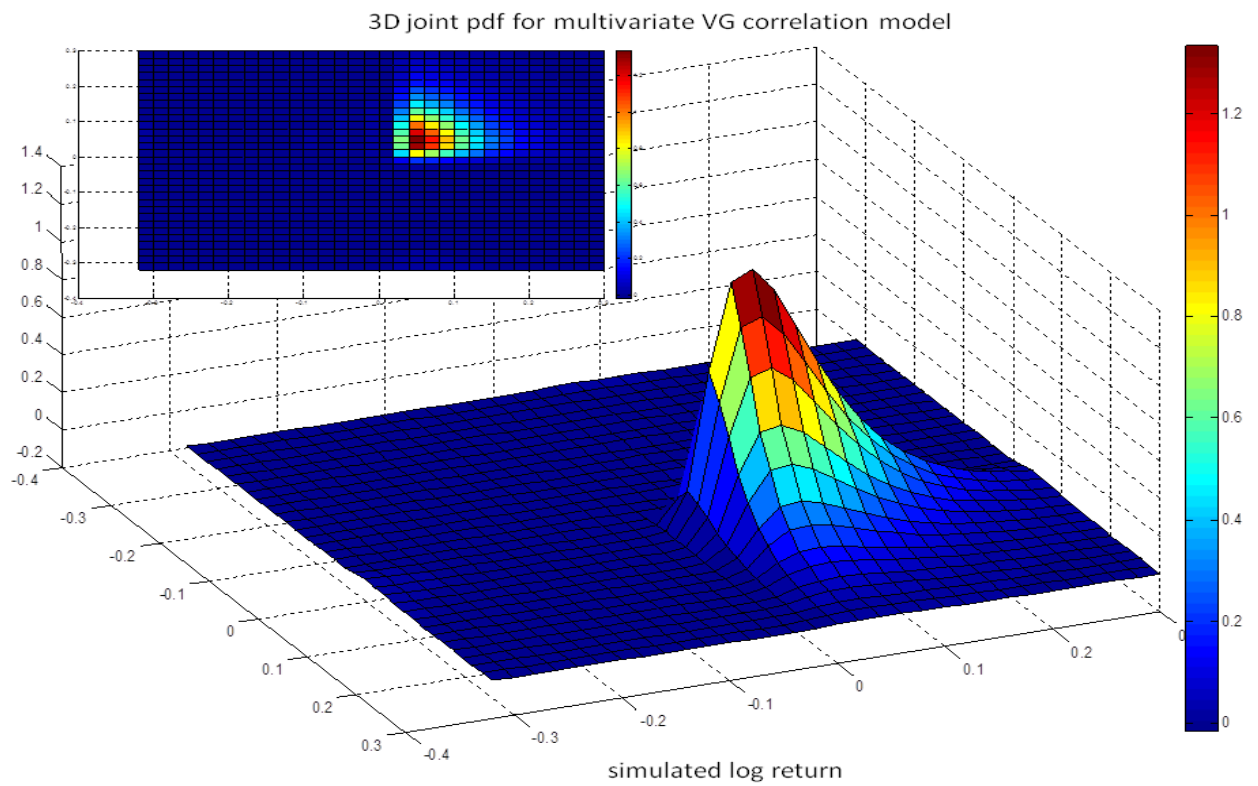
Figure 3.20: Joint pdf(with marginal pdf) of log returns for experiment 1

Experiment 2 for Joint PDF

(negative skewness)

parameters for experiment 2:

$$M = \begin{pmatrix} -0.2 & -0.15 \\ -0.15 & -0.1 \end{pmatrix}, \quad Q = \begin{pmatrix} 0.5 & 0.4 \\ 0.3 & 0.2 \end{pmatrix}, \quad \beta = 4.$$

$$\theta_1 = \theta_2 = -2.5, \quad \sigma_1 = \sigma_2 = 0.25, \quad \nu_1 = \nu_2 = 0.15.$$
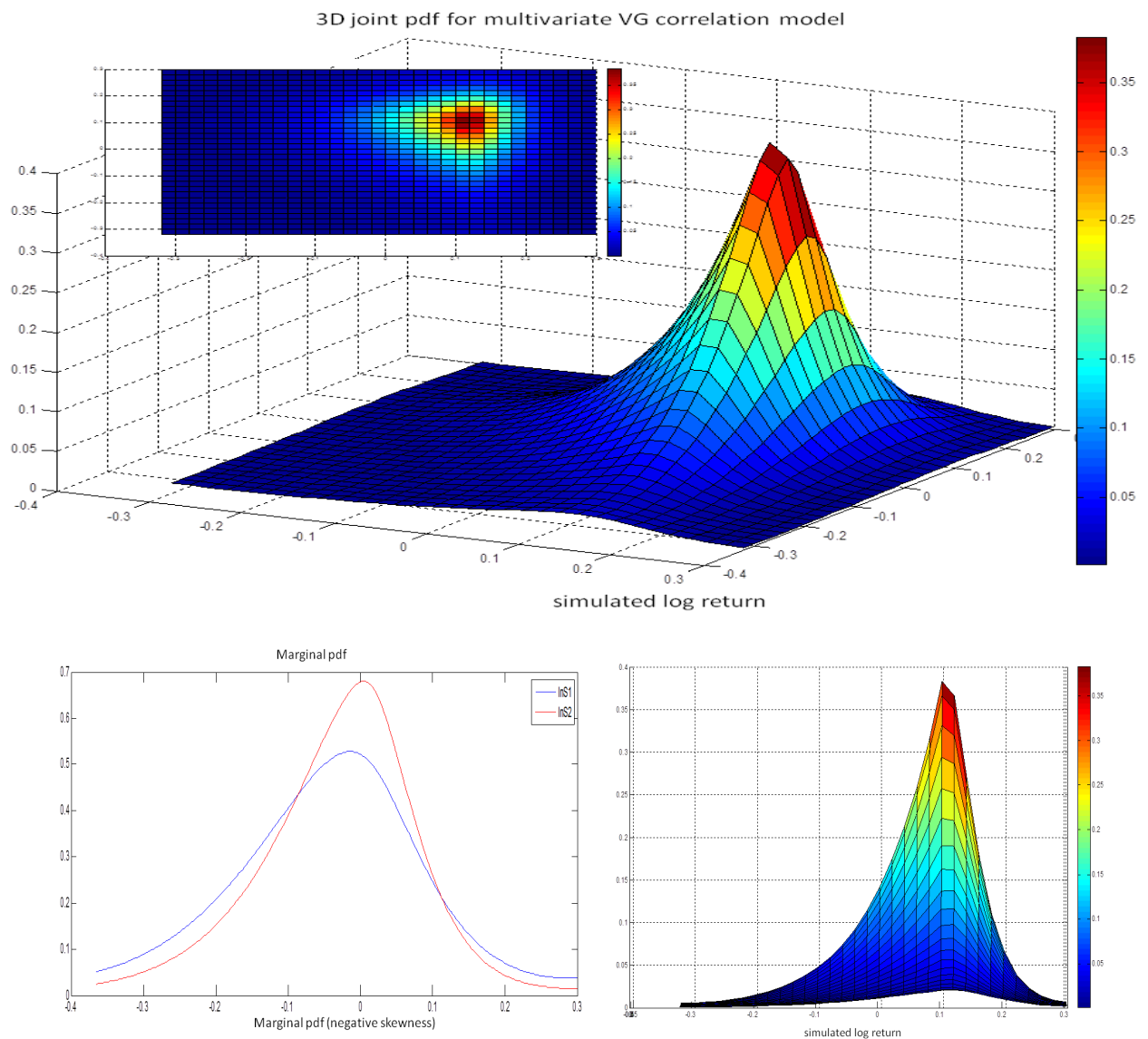
Figure 3.21: Joint pdf(with marginal pdf) of log returns for experiment 2

### 3.4.4 Is Lévy necessary?

Lévy processes are used as building blocks in our correlation model. As Brownian motion belongs to the Lévy family, we may wonder whether Lévy process is necessary in model fitting. Can we replace it with simple Brownian motion which is much easier to implement? We test our model by choosing the Lévy process $L(t)$ to be Brownian motion. Therefore the Lévy exponent becomes $\psi(u_j) = -u_j^2/2$. In order to visualize the difference between using VG exponent with standard Brownian motion exponent, we present probability density functions for simulated log returns, which were generated by using Brownian motion instead of VG process. Graphs are showing in Figure 3.22 and Figure 3.23.
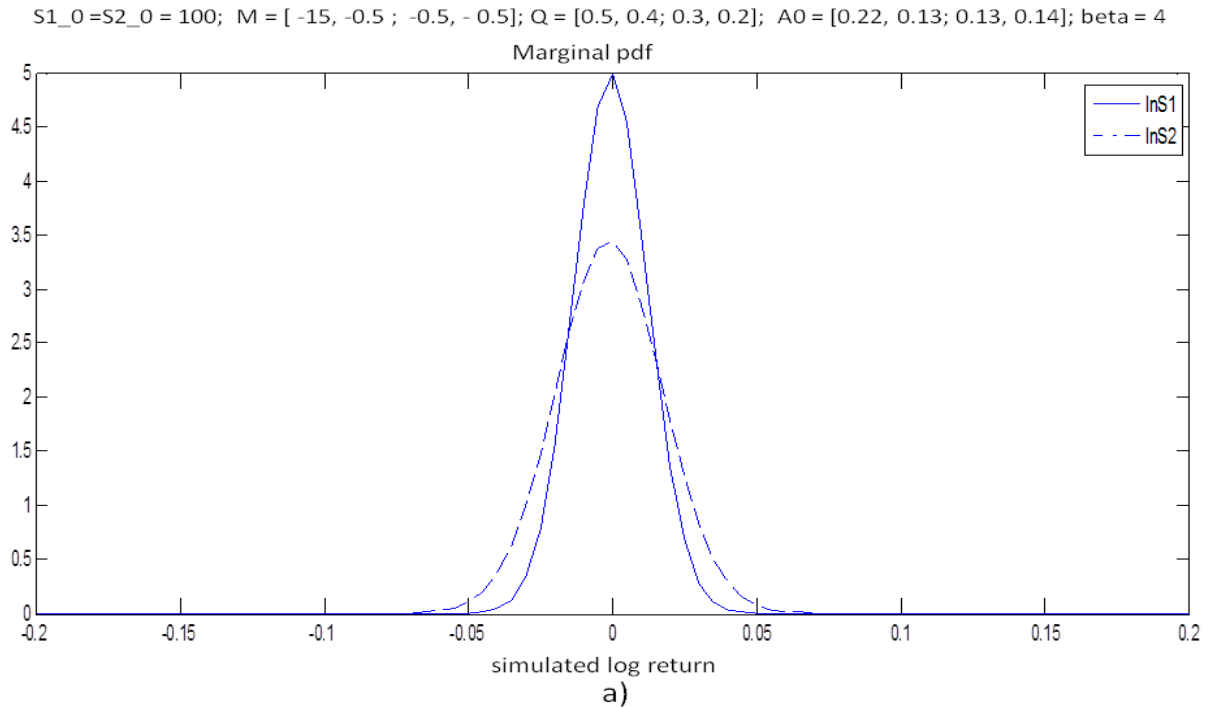
Figure 3.22: Brownian motion test I

S1_0 =S2_0 = 100; M = [-15, -0.5 ; -0.5, - 5]; Q = [0.5, 0.4; 0.3, 0.2]; A0 = [1, 0.2; 0.2, 1]; beta = 4

Marginal pdf

simulated log return

b)

S1_0 =S2_0 = 100; M = [-15, -0.5 ; -0.5, -0.5]; Q = [0.5, 0.4; 0.3, 0.2]; A0 = [1, 0.2; 0.2, 1]; beta = 4

Marginal pdf

simulated log return

c)
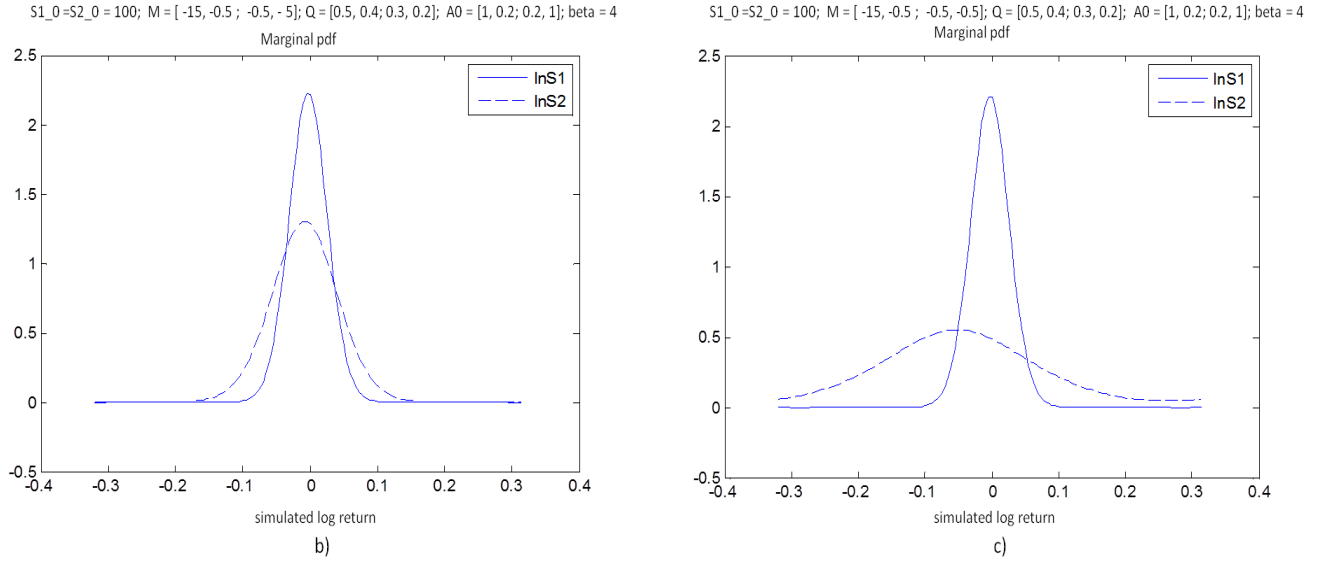
Figure 3.23: Brownian motion test II

In Figure 3.22 and Figure 3.23, it seems that the two marginal densities are still normal and no skewness effect has been observed. Even though Brownian motions are simple and easy, we can not use it as a substitute for all Lévy processes $L(t)$. Therefore, the general Lévy process setting in our model is indeed necessary and can capture skewness features as desired, which has been showed in Figure 3.16 to Figure 3.19.

3.4.5   Implied Volatility Surface

In financial mathematics, the implied volatility of an option contract is the volatility of the price of the underlying security that is implied by the market price of the option based on an option pricing model. In other words, implied volatility is the volatility that makes the model option price equal to the market option price. The implied volatility surface describes the relationship between the implied volatility of

the options, strike prices and maturities. For currency options, implied volatilities tend to be higher for in-the-money and out-of-money options than for at-the-money options. Thus, the implied volatility surface for currency options is usually described as a smile shape. In addition, for equity, volatility often decreases as the strike price increases, which known as a volatility skew.

The implied volatility surface for Black-Scholes model is flat, as its volatility is assumed to be constant over time. However, in reality, volatilities are neither constant nor deterministic. In fact, the volatility is a stochastic process itself. Our new multivariate Lévy correlation model assumes stochastic volatility, so the implied volatility surfaces showing in Figure 3.24, Figure 3.25 and Figure 3.26 display a desirable curved feature. The left figure is the implied volatility surface for asset one, and the right one is for asset two.
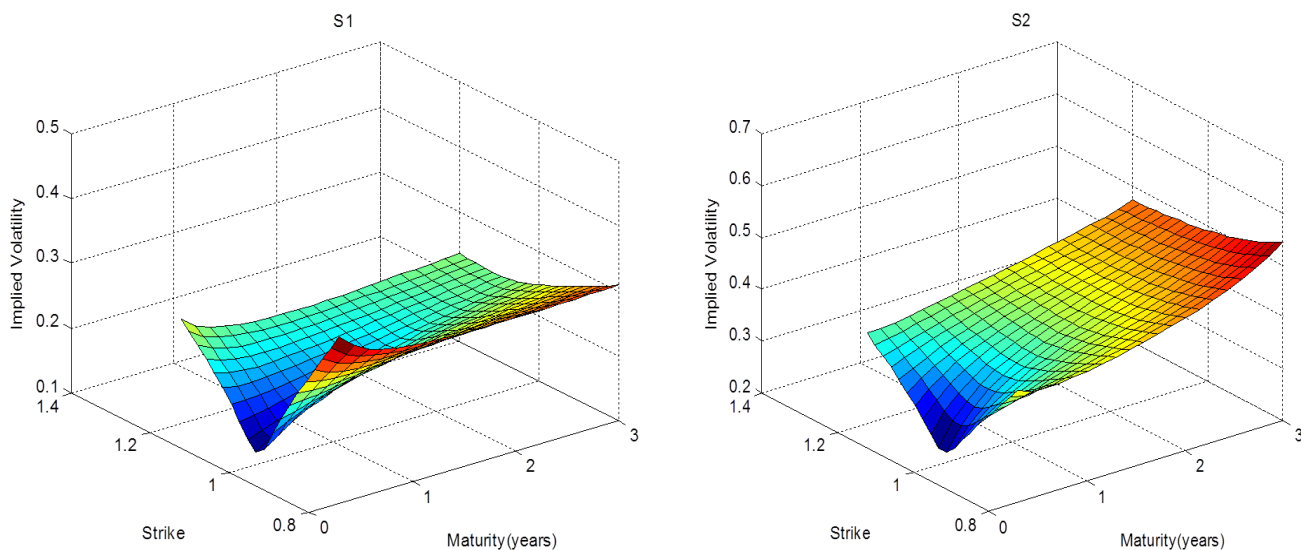
Figure 3.24: Implied Volatility Surface with $\theta_{VG1} = \theta_{VG2} = -0.15$; $\nu_{VG1} = \nu_{VG2} = 0.3$; $\sigma_{VG1} = \sigma_{VG2} = 0.9966$; $A_0 = [0.05, 0; 0, 0.05]$; $M = [-15, -0.5; -0.5, -5]$; $Q = [0.5, 0.4; 0.3, 0.5]$; $\beta = 4$
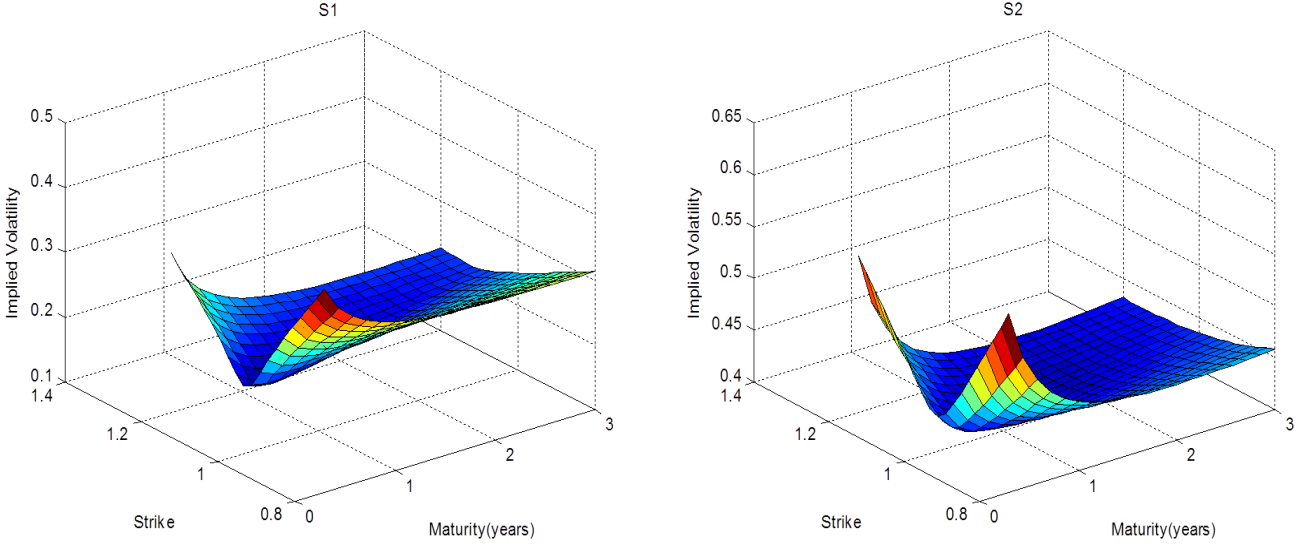
Figure 3.25: Implied Volatility Surface with $\theta_{VG1} = \theta_{VG2} = -0.35$; $\nu_{VG1} = \nu_{VG2} = 0.5$; $\sigma_{VG1} = \sigma_{VG2} = 0.9689$; $A_0 = [1, 0.8; 0.8, 1]$; $M = [-15, -0.5; -0.5, -5]$; $Q = [0.5, 0.4; 0.3, 0.5]$; $\beta = 4$
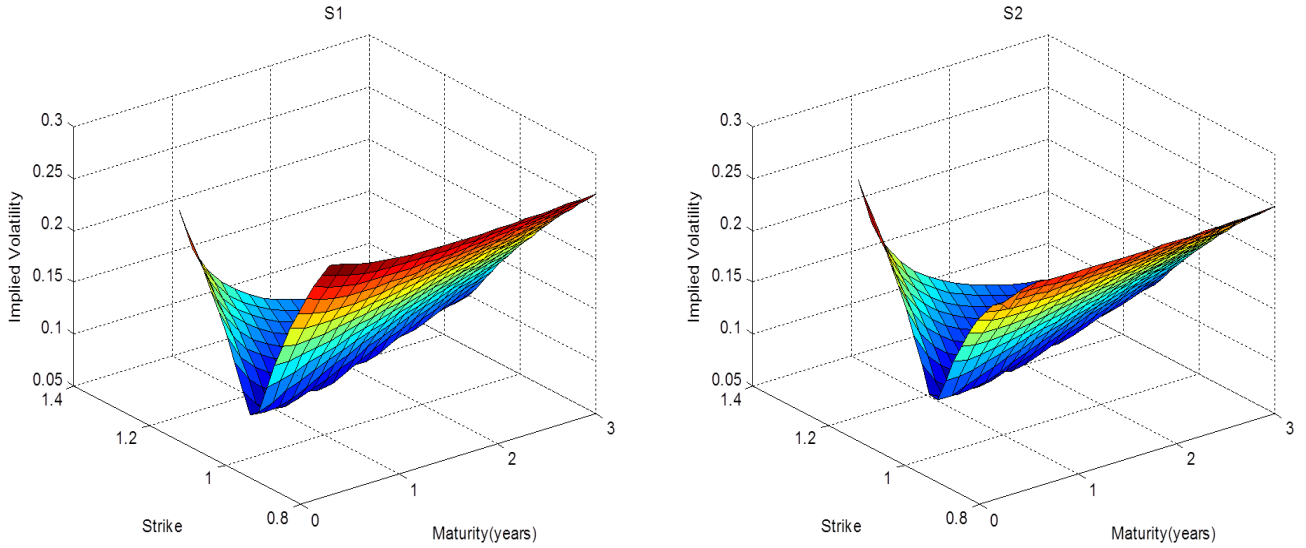

Figure 3.26: Implied Volatility Surface with $\theta_{VG1} = \theta_{VG2} = 0.05$; $\nu_{VG1} = \nu_{VG2} = 0.5$; $\sigma_{VG1} = \sigma_{VG2} = 0.9994$; $\beta = 4$ $M = [-15, -2.15; -2.15, -10]$; $Q = [0.15, 0.16; 0.18, 0.15]$; $A_0 = [0.4, 0.04; 0.04, 0.4]$;

3.4.6 Local Correlation

Pearson's correlation is known as linear correlation which effective represent co-movements between variables. However, for different sample values the co-movements of variables perform differently, so linear correlation may sometimes mislead if the marginal distributions are non-normal. We therefore provide the local correlation here to better investigate the local dependence structures of our multivariate Lévy correlation model.

In financial markets, asset prices tend to move together when market have big movements. One common drawback of multivariate Brownian motion and the Gaussian copula is that their joint dynamics was strongly rejected as a model for co-movement of two stock prices. Compared with those normal distributions, local correlation can used to determine the relative co-movement level of two variables.

Definition 3.17. *(Local Correlation)*

The local correlation $\rho_{local}(X_1, X_2)$ for the two dimensional distribution $(X_1, X_2) \in \mathbb{R}^2$ is defined as the correlation given that (X_1, X_2) has in the neighborhood $(x_1 \pm \varepsilon, x_2 \pm \varepsilon)$, where ε is small.

Proposition 3.18. *(Closed Form for Local Correlation)*

The closed form for $\rho_{local}(x_1, x_2)$ can be obtained by approximating the joint density $f(x_1, x_2)$ using the expansion of a joint Gaussian density:

$$g(x_1, x_2) := -2 \ln f(x_1, x_2) = c(g_{x_1 x_1} x_1^2 + 2 g_{x_1 x_2} x_1 x_2 + g_{x_2 x_2} x_2^2 + ...).$$

Then we have

$$\rho_{local} = \frac{\frac{\partial^2}{\partial x_1 \partial x_2}(-\ln(f))}{\sqrt{\frac{\partial^2}{\partial^2 x_1}(-\ln(f))\frac{\partial^2}{\partial^2 x_2}(-\ln(f))}}.$$

which can be represented as

$$\rho_{local} = \frac{f_{x_1 x_2} f - f_{x_1} f_{x_2}}{\sqrt{f_{x_1 x_1} f - f_{x_1}^2}\sqrt{f_{x_2 x_2} f - f_{x_2}^2}}. \tag{3.46}$$

where f_{x_1}, f_{x_2} denote the first derivatives of f with respect to x_1 and x_2 and $f_{x_1 x_1}, f_{x_1 x_2}, f_{x_2 x_2}$

denote the second derivatives of f with respect to the corresponding variables.

In equation 3.46, $f_{x_1}, f_{x_2}, f_{x_1 x_1}, f_{x_1 x_2}, f_{x_2 x_2}$ can be efficiently computed via FFT. Since there is no closed form for the two dimensional correlation Lévy model as we have discussed before, one needs to numerically invert the characteristic function by Fourier transform. We computed $f_{x_1}, f_{x_2}, f_{x_1 x_1}, f_{x_1 x_2}, f_{x_2 x_2}$ as follows:

$$f(x_1, x_2) = \frac{1}{(2\pi)^2} \int \int e^{-iu_1 x_1 - iu_2 x_2} \Phi(u_1, u_2) \, du_1 du_2$$

$$f_{x_1}(x_1, x_2) = \frac{1}{(2\pi)^2} \int \int e^{-iu_1 x_1 - iu_2 x_2} (-iu_1) \Phi(u_1, u_2) \, du_1 du_2$$

$$f_{x_2}(x_1, x_2) = \frac{1}{(2\pi)^2} \int \int e^{-iu_1 x_1 - iu_2 x_2} (-iu_2) \Phi(u_1, u_2) \, du_1 du_2$$

$$f_{x_1 x_1}(x_1, x_2) = \frac{1}{(2\pi)^2} \int \int e^{-iu_1 x_1 - iu_2 x_2} (-u_1^2) \Phi(u_1, u_2) \, du_1 du_2$$

$$f_{x_1 x_2}(x_1, x_2) = \frac{1}{(2\pi)^2} \int \int e^{-iu_1 x_1 - iu_2 x_2} (-u_1 u_2) \Phi(u_1, u_2) \, du_1 du_2$$

$$f_{x_2 x_2}(x_1, x_2) = \frac{1}{(2\pi)^2} \int \int e^{-iu_1 x_1 - iu_2 x_2} (-u_2^2) \Phi(u_1, u_2) \, du_1 du_2.$$

We have chosen different parameters to draw local correlation surfaces which are displayed in Figure 3.27, Figure 3.28, and Figure 3.29. These figures show that

the correlation surfaces of our new Lévy correlation model are non-flat, peaked at the corners of the first and third quadrants, and also went down to a very low level in the second and fourth quadrants, which are desirable features as we expected.

Experiment 1 for Local Correlation

The parameters for experiment 1 (Figure 3.27):

$$M = \begin{pmatrix} -0.2 & -0.15 \\ -0.15 & -0.1 \end{pmatrix}, \quad Q = \begin{pmatrix} 0.5 & 0.4 \\ 0.3 & 0.2 \end{pmatrix}, \quad A_0 = \begin{pmatrix} 0.22 & 0.13 \\ 0.13 & 0.14 \end{pmatrix},$$

$$\beta = 4, \quad \theta_1 = \theta_2 = 3.5, \quad \sigma_1 = \sigma_2 = 0.35, \quad \nu_1 = \nu_2 = 0.0716.$$
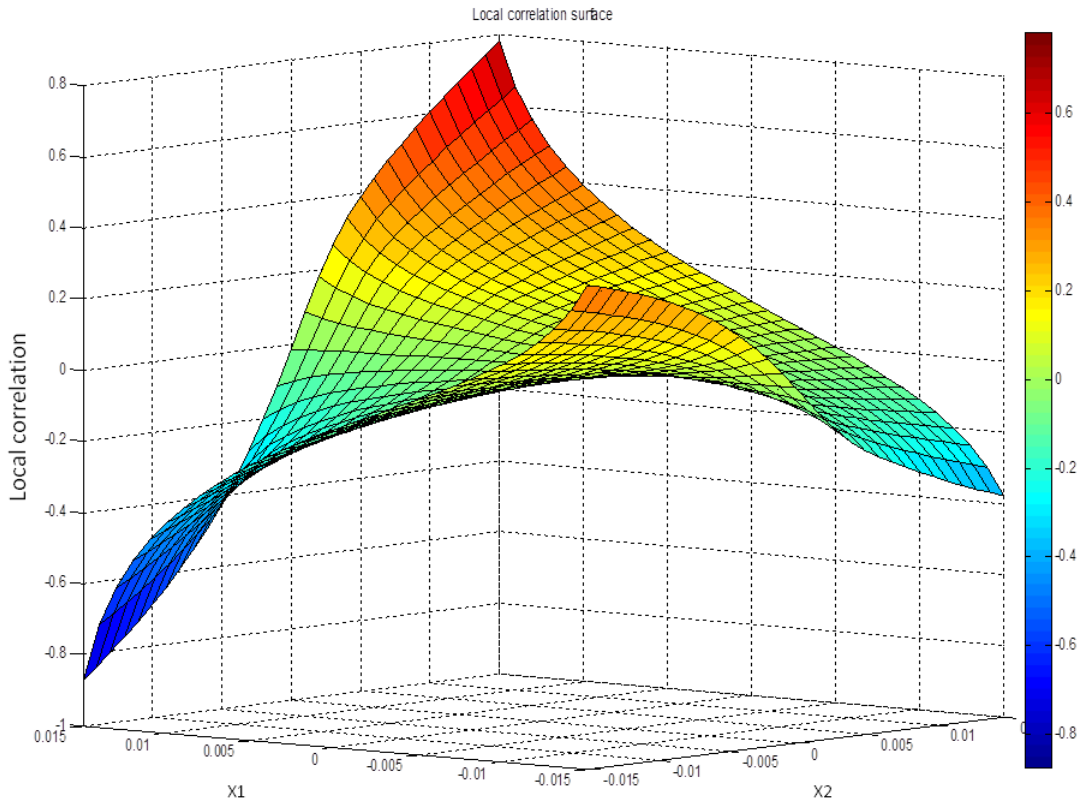
Figure 3.27: Local Correlation Surface I

Experiment 2 for Local Correlation

The parameters for experiment 2 (Figure 3.28):

$$M = \begin{pmatrix} -0.2 & -0.15 \\ -0.15 & -0.1 \end{pmatrix}, \quad Q = \begin{pmatrix} 0.5 & 0.4 \\ 0.3 & 0.2 \end{pmatrix}, \quad A_0 = \begin{pmatrix} 0.22 & 0.13 \\ 0.13 & 0.14 \end{pmatrix},$$
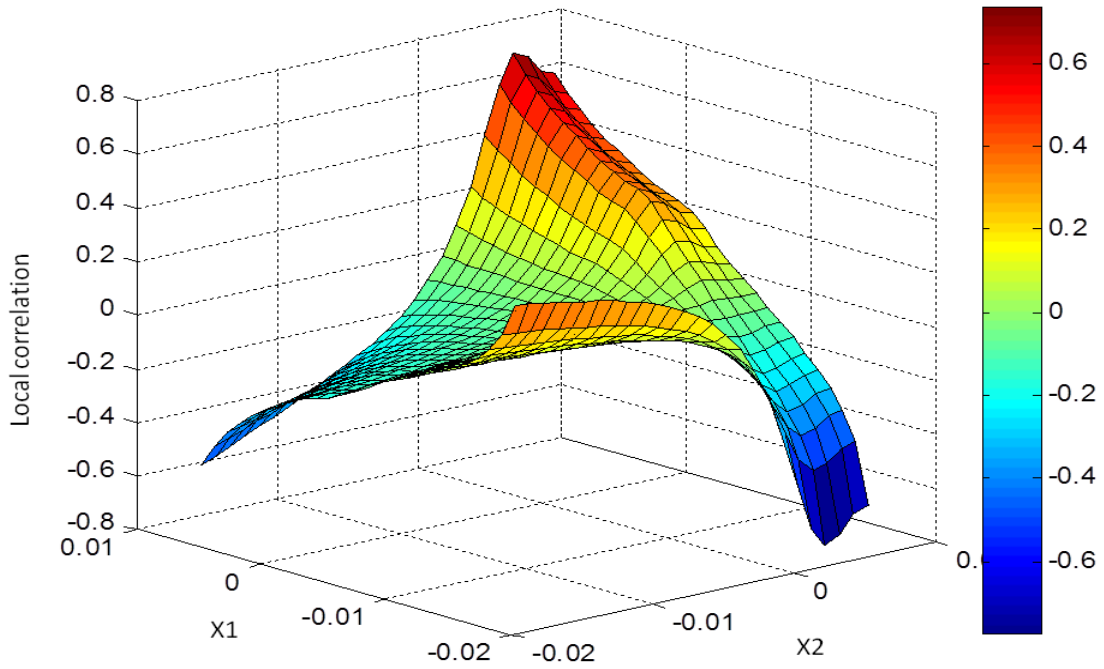
$$\beta = 4, \quad \theta_1 = \theta_2 = -2.5, \quad \sigma_1 = \sigma_2 = 0.25, \quad \nu_1 = \nu_2 = 0.15.$$

Figure 3.28: Local Correlation Surface II

Experiment 3 for Local Correlation

The parameters for experiment 3 (Figure 3.29):

$$M = \begin{pmatrix} -0.2 & -0.15 \\ -0.15 & -0.1 \end{pmatrix}, \quad Q = \begin{pmatrix} 0.5 & 0.04 \\ 0.03 & 0.2 \end{pmatrix}, \quad A_0 = \begin{pmatrix} 0.22 & 0.13 \\ 0.13 & 0.14 \end{pmatrix},$$

$$\beta = 4, \quad \theta_1 = \theta_2 = 2.5, \quad \sigma_1 = \sigma_2 = 0.25, \quad \nu_1 = \nu_2 = 0.15.$$
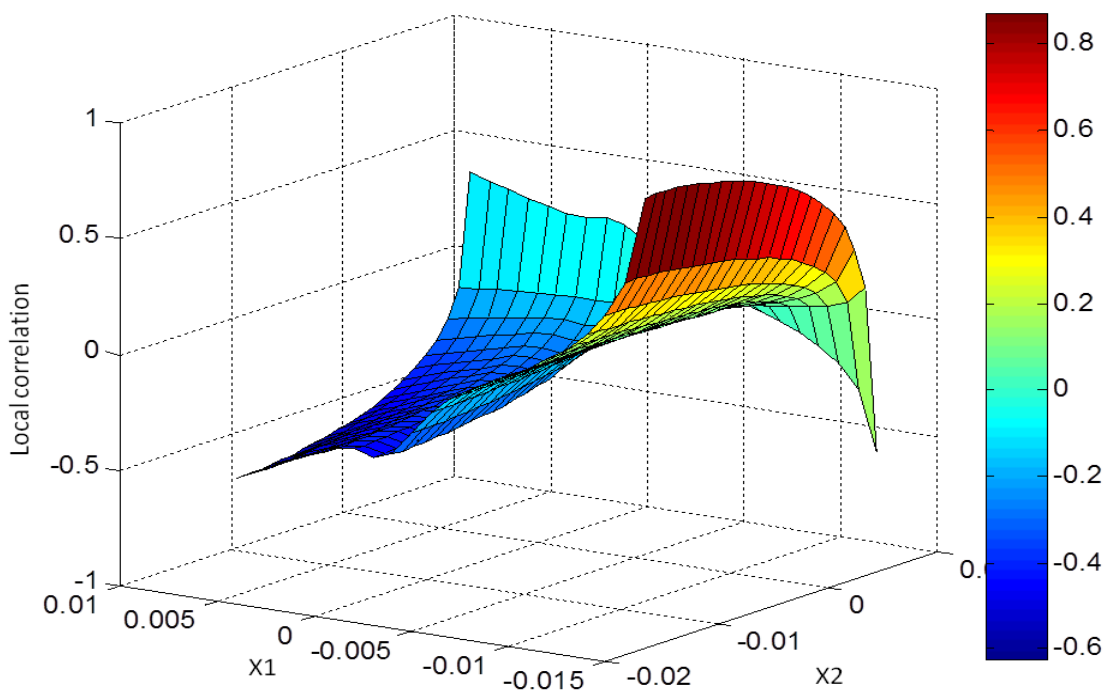
Figure 3.29: Local Correlation Surface III

Chapter 4

Application to Option Pricing and Calibration

4.1 Overview

In financial market, many derivatives are not only depend on single asset but also expose risks to more than one assets. While there is a wide variety of literature on pricing of single-asset options in equity market, the amount of literature considering the multi-asset case is rather limited. Since not only the individual assets but also their joint behavior has to be taken into account, a model under consideration should be reasonable and flexible to model the marginal as well as the joint dynamics of assets, and thus to price and hedge financial derivatives consistently.

In this chapter, we will discuss the pricing problem of applying our Lévy correlation model and show that this new model is able to obtain the prices of several different type of options, including options on single asset as well as options on multiple underlying assets. Meanwhile, the characteristic function can be computed in closed form, which makes option pricing and calibration feasible. In the last section of this chapter, FX option pairs are chosen as an illustrative example and we calibrate the bivariate Lévy correlation model with integrated Wishart time change to market price.

As we have described in Section 1.4, the Carr-Madan FFT method has become a popular and efficient tool in option pricing (for more details, refer to Section 1.4).

A closed form of the characteristic function is a key for evaluating option prices via FFT. Fortunately, marginal and joint characteristic functions for our Lévy correlation model have been derived in explicit form (See Section 3.3.2). In order to obtain option prices, analytic closed forms of characteristic functions for different styles of option will be derived later. Moreover, the FFT method has been applied to numerically compute the prices, and Monte Carlo simulation results are also provided for comparison. Although all pricing problems can be done by Monte Carlo simulation, the FFT method is more efficient and accurate than simulation.

We restrict our computation to the case of only two assets, due to the computational burden of the high-dimensional FFT algorithm. However, it is worth noting that those numerical methods can be applied to any multivariate model with closed form characteristic function. In particular, we choose the Lévy process to be Variance Gamma in all experiments, but other Lévy process such as NIG, CGMY, etc. can also be considered as feasible candidates. We only choose three different options, vanilla European option, forward start option, and exchange option, as typical examples for illustration. But one should notice that, this correlation model can be applied to other options with dependence structures as well, such as spread option, basket option, rainbow option, etc.

In our numerical illustrative examples, the two assets $S_1(t), S_2(t)$ follow the model

$$
\begin{aligned}
S_1(t) &= S_1(0)e^{(r-q_1)t}\frac{e^{X_1(0,t)}}{E(e^{X_1(0,t)})} \\
S_2(t) &= S_2(0)e^{(r-q_2)t}\frac{e^{X_2(0,t)}}{E(e^{X_2(0,t)})}
\end{aligned}
\tag{4.1}
$$

or more generally:

$$S_1(T) = S_1(t)e^{(r-q_1)(T-t)}\frac{e^{X_1(t,T-t)}}{E(e^{X_1(t,T-t)})}$$
$$S_2(T) = S_2(t)e^{(r-q_2)(T-t)}\frac{e^{X_2(t,T-t)}}{E(e^{X_2(t,T-t)})}$$

$$(4.2)$$

where X_1, X_2 are defined in **Definition 3.10**, and q_1, q_2 are dividend yields.

4.2 Single Asset Option Pricing

In this section we deal with the pricing problem of plain vanilla contingent claims, in particular the European call option. We are only using two assets in computation, but this Lévy correlation model can be applied to higher dimensional cases technically. The closed form of characteristic function is derived for the sake of applying FFT method, and Monte Carlo simulation result is also presented for comparison.

4.2.1 Vanilla European Option

One simple example for single asset option is vanilla European call option with payoff $(S_T - K)^+$. (The Option only depends on a single underlying asset.)

The two vanilla European call option prices are (put option prices can be obtained by put-call parity)

$$Callprice\,S_1 = e^{-(r-q_1)\tau}E^{\mathbb{Q}}(S_1 - K)^+$$
$$Callprice\,S_2 = e^{-(r-q_2)\tau}E^{\mathbb{Q}}(S_2 - K)^+$$

$$(4.3)$$

and the characteristic function for the log return is:

$$\phi_{lnS_1(T)}(u_1) = E(e^{iu_1(lnS_1(0)+(r-q_1)T)}\frac{\phi_{X_1;0,T}(u_1)}{[\phi_{X_1;0,T}(-i)]^{iu_1}}$$

$$\phi_{lnS_2(T)}(u_2) = E(e^{iu_2(lnS_2(0)+(r-q_2)T)}\frac{\phi_{X_2;0,T}(u_2)}{[\phi_{X_2;0,T}(-i)]^{iu_2}}$$

(4.4)

where closed-form for marginal characteristic functions $\phi_{X_1;0,T}(u_1)$ and $\phi_{X_2;0,T}(u_2)$ have been derived in **Proposition 3.11**.

The vanilla European option prices for S_1 and S_2 in (4.3) can now be easily computed by the Carr-Madan FFT method.

4.2.2   Numerical Results

In this subsection, to see the advantage of using the FFT method over Monte Carlo simulation, we compare their computational results for vanilla European option under the two-dimensional Lévy (VG) correlation model. In Monte Carlo simulation, we have run $100,000$ simulation paths each time to obtain an accurate estimation. The FFT algorithm and simulation were implemented in Matlab on the same machine. We observed that FFT is much faster compared with Monte Carlo simulation (FFT takes less than a second to get result while simulation usually takes over 1000 times longer than FFT). FFT is faster in a sense that it generates a matrix of prices with different strikes and is able to compute option prices across different strikes in one single run. Besides computation speed, Monte Carlo simulation converges very slowly without using variance reduction techniques.

We have performed the FFT method taking $N = 4096$ and ran $100,000$ sample paths for Monte Carlo simulation. The parameters we were using are as follows (for

Table 4.1)

$$M = \begin{pmatrix} -15 & -0.5 \\ -0.5 & -5 \end{pmatrix}, \quad Q = \begin{pmatrix} 0.5 & 0.4 \\ 0.3 & 0.5 \end{pmatrix}, \quad A_0 = \begin{pmatrix} 0.04 & 0.04 \\ 0.04 & 0.04 \end{pmatrix},$$

$$\beta = 4, \quad \theta_1 = \theta_2 = -0.15, \quad \sigma_1 = \sigma_2 = 0.9966, \quad \nu_1 = \nu_2 = 0.3, \quad T = 1$$

$$S_1(0) = S_2(0) = 100, \quad r = 0.05 \quad N = 4096, \quad \text{simulation numbers} = 100,000.$$

		FFT method	Simulation
$K = 80$	$C(S_1)$	24.7462	24.7309
	$C(S_2)$	27.6238	27.6117
$K = 90$	$C(S_1)$	15.9739	16.0023
	$C(S_2)$	20.3514	20.3391
$K = 100$	$C(S_1)$	7.8547	7.8345
	$C(S_2)$	14.5353	14.5188
$K = 110$	$C(S_1)$	4.0803	3.9782
	$C(S_2)$	11.9104	11.8920
$K = 120$	$C(S_1)$	2.9785	3.0244
	$C(S_2)$	9.1024	9.0769

Table 4.1: Computational Results for Vanilla European Option Prices

From Table 4.1, we can see that the two sets of computational results by using

FFT and Monte Carlo simulation separately are close, but FFT is much faster than

simulation. We also present the time change rate simulation paths for two assets and correlation path in Figure 4.1. We observe that the two assets are almost always positively correlated over time, and red line A_{22} dominate the blue line A_{11} for almost the entire time period. Since the instantaneous time change rate $A_{11}(t)$ path (blue line) reflects the dynamic evolution of volatility for asset $S_1(t)$, and the $A_{22}(t)$ path (red one) captures the stochastic volatility information for the second asset $S_2(t)$, the volatility for S_2 is more volatile than S_1 so that the second asset is more risky than asset one. This observation also explains the computation results showing in Table 4.1, in which call prices for S_2 is higher than S_1 at the same strike level. Intuitively, higher volatility result in higher call price.

4.3   Multi-asset Option Pricing

In this section we are going to show that our new Lévy correlation model is able to price multi-asset options. We deal with the pricing problem of one of the simplest multi-asset options: the exchange option. We are only using two assets in computation, but this Lévy correlation model can be applied to higher dimensional cases technically. The closed form of characteristic function is derived for the sake of applying FFT method, and Monte Carlo simulation result is also presented for comparison.
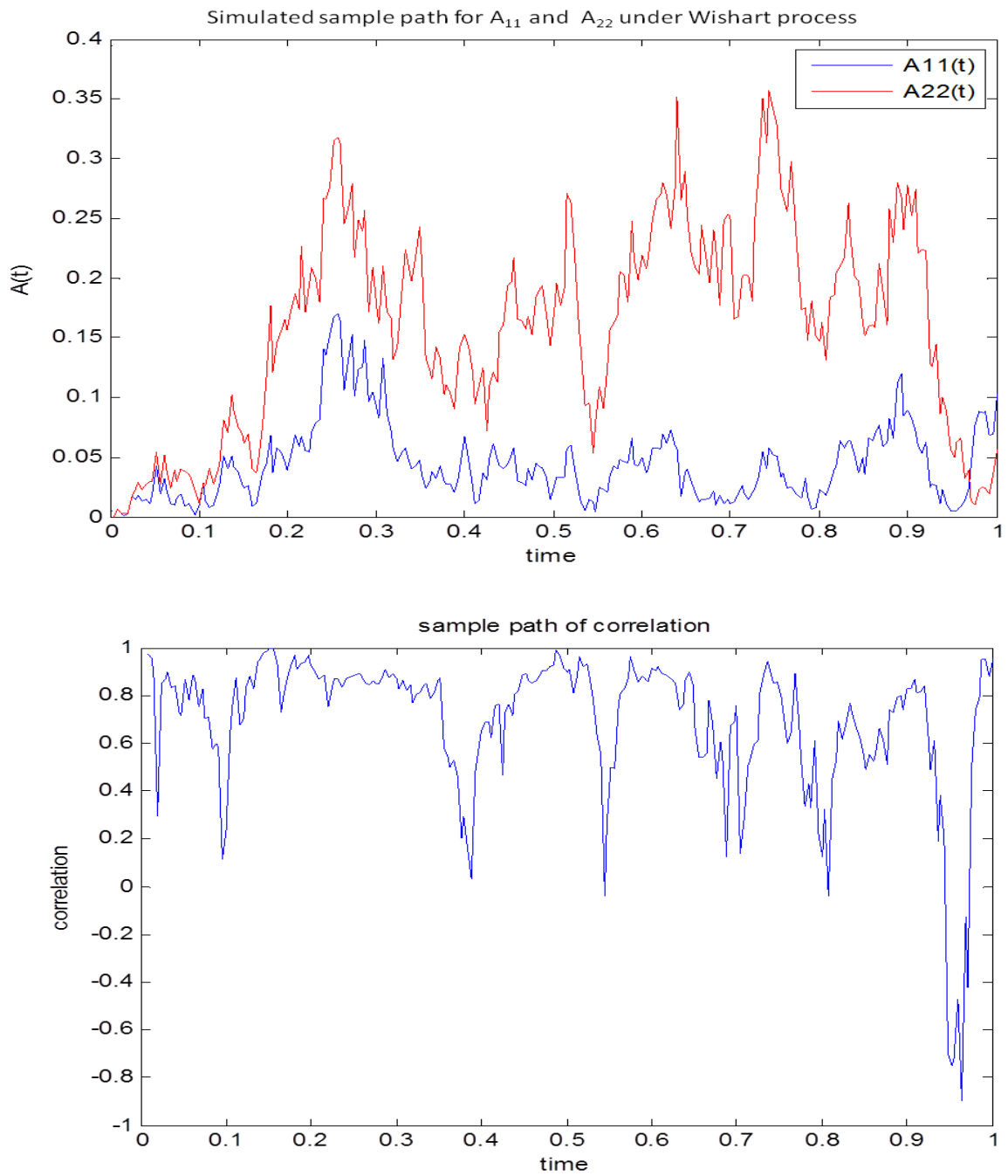
Figure 4.1: A_{11}, A_{22} and correlation evolution for S_1, S_2 (vanilla European option experiment)

4.3.1 Exchange Option

One simplest example for multi-asset option is Exchange option. Exchange Options were initially introduced by William "Dr. Risk" Margrabe in his seminal 1978 paper. These types of options allow the holder of the option to exchange one asset for another and are used commonly in foreign exchange markets, bond markets and stock markets, among others. The payoff of the exchange option depends on two correlated assets S_1 and S_2 with payoff $(S_1 - S_2)^+$. Exchange option can be seen as a special case of a spread option with zero strike.

We consider the exchange option pricing problem under the bivariate Lévy (VG) correlation model with integrated Wishat time change, where S_1 and S_2 are modeled as in Equation (4.1) or more generally as in Equation (4.2)

The exchange option price $EX\mathcal{OP}(S_1, S_2)$ with zero dividends at time 0 is:

$$EX\mathcal{OP}(S_1, S_2) = e^{-rT} E^{\mathbb{Q}}[S_1(T) - S_2(T)]^+ \tag{4.5}$$

By Theorem 1.8 introduced in Chapter One, we can simplify the calculation by change the measure from risk neutral $\mathbb{Q}$ to the new measure U_2 with numeraire S_2. Then the price for exchange option $EX\mathcal{OP}(S_1, S_2)$ becomes:

$$EX\mathcal{OP}(S_1, S_2) = S_2(0) E^{U_2} \left(\frac{S_1(T)}{S_2(T)} - 1 \right)^+ \tag{4.6}$$

where E^{U_2} is the expectation under measure U_2 with numeraire S_2. Therefore, the exchange option becomes vanilla European call option on $S_1(T)/S_2(T)$ under the new measure U_2 with strike $K = 1$.

In order to apply FFT method to get the price of the exchange option, the

characteristic function of $\ln[S_1(T)/S_2(T)]$ under the new measure U_2 is needed, and can be derived by change of numeraire technique.

Proposition 4.1. (***Characteristic function for*** $\ln[S_1(T)/S_2(T)]$)

The closed form of characteristic function for $\ln[S_1(T)/S_2(T)]$ *is:*

$$\phi_{\ln \frac{S_1}{S_2}}(u) = \exp\left[iu \ln \frac{S_1(0)}{S_2(0)} - iu \ln \phi_{X_1,X_2;0,T}(-i,0)\right.$$

$$\left. - (1-iu) \ln \phi_{X_1,X_2;0,T}(0,-i)\right] \cdot \phi_{X_1,X_2;0,T}(u,-i-u) \tag{4.7}$$

where the joint characteristic function $\phi_{X_1,X_2;0,T}$ *is derived in* ***proposition 3.12***.

Proof:

$$\phi_{\ln \frac{S_1}{S_2}}(u) = E^{U_2}\left[e^{iu \ln \frac{S_1(T)}{S_2(T)}}\right] = E^{\mathbb{Q}}\left[e^{iu \ln \frac{S_1(T)}{S_2(T)}} \frac{dU_2}{d\mathbb{Q}}\right]$$

$$= E^{\mathbb{Q}}\left[e^{iu \ln S_1(T) - iu \ln S_2(T)} \cdot e^{-rT + \ln S_2(T) - \ln S_2(0)}\right]$$

$$= E^{\mathbb{Q}}\left[e^{-rT + iu \ln S_1(T) + (1-iu) \ln S_2(T) - \ln S_2(0)}\right]$$

$$= E^{\mathbb{Q}}\left[e^{-rT + iu[\ln S_1(0) + rT + X_1(T) - \ln \phi_{X_1;0,T}(-i)] + (1-iu)[\ln S_2(0) + rT + X_2(T) - \ln \phi_{X_2;0,T}(-i)] - \ln S_2(0)}\right]$$

$$= E^{\mathbb{Q}}\left[e^{iu \ln \frac{S_1(0)}{S_2(0)} - iu \ln \phi_{X_1;0,T}(-i) - (1-iu) \ln \phi_{X_2;0,T}(-i)} \cdot e^{iuX_1(T) + (1-iu)X_2(T)}\right]$$

$$= e^{iu \ln \frac{S_1(0)}{S_2(0)} - iu \ln \phi_{X_1,X_2;0,T}(-i,0) - (1-iu) \ln \phi_{X_1,X_2;0,T}(0,-i)} \cdot \phi_{X_1,X_2;0,T}(u,-i-u)$$

$$\square$$

4.3.2 Numerical Results

We compare their computational results for exchange option under the two-dimensional Lévy (VG) correlation model. In Monte Carlo simulation, we have run $100,000$ simulation paths each time to obtain an accurate estimation. We have

perform FFT method for taking $N = 4096$ and run $100,000$ times for Monte Carlo simulation. The FFT algorithm and simulation were implemented in Matlab on the same machine.

The parameters we were using are as follows:(for Table 4.2)

$$
M = \begin{pmatrix} -15 & -0.5 \\ -0.5 & -5 \end{pmatrix}, \quad Q = \begin{pmatrix} 0.5 & 0.4 \\ 0.3 & 0.5 \end{pmatrix}, \quad A_0 = \begin{pmatrix} 0.04 & 0.04 \\ 0.04 & 0.04 \end{pmatrix},
$$

$$
\beta = 4, \quad \theta_1 = \theta_2 = -1.5, \quad \sigma_1 = \sigma_2 = 0.5701, \quad \nu_1 = \nu_2 = 0.3,
$$

$$
S_1(0) = 100, \ T = 1, \ r = 0.05, \ N = 4096, \text{ simulation numbers} = 100,000.
$$

	FFT method	Simulation
$S_2(0) = 80$	23.0125	23.0597
$S_2(0) = 90$	15.7805	15.7765
$S_2(0) = 100$	11.3444	11.3289
$S_2(0) = 110$	8.7915	8.8003
$S_2(0) = 120$	7.0667	7.0557

Table 4.2: Computational Results for Exchange Option Prices

4.4 Exotic Option Pricing

In finance, an exotic option is a derivative which has features making it more complex than commonly traded products (vanilla options). This product could

depend on more than one index and generally trades over the counter (OTC).

The payoff of an exotic option at maturity depends not just on the value of the underlying index at maturity, but at its value at several times during the contract's life. For example, one type of exotic option is known as a chooser option, which allows an investor to choose whether the options is a put or call at a certain point during the option's life. Because this type of option can change over the holding period, it is not be found on a regular exchange, which is why classified as an exotic option. Some other types of options include: barrier options, Asian options, digital options, mountain range options, etc. All belong to exotic option family.

In this section, we will show the Lévy correlation model is able to price exotic options. One type of exotic options, the forward-start call option is chosen as an implemented example. The closed form characteristic function is derived and numerical results via FFT and simulation are shown in the next section.

4.4.1   Forward Start Call Option

A forward start option is an advance purchase of a put or call option that will become active at some specified future time. It is essentially a forward on an option, only the premium is paid in advance. The asset price at the start of this option is not known, and the strike price is determined when the option becomes active. For instance, a forward start call option with payoff $(S_T/S_t - K)^+$ is an option that starts at some pre-specified time in the future (we call this strike date t), and has a maturity after that date. Forward start contracts can be used to give an investor

98

exposure to forward volatility, and represents the building block for both cliquet options[9] and variance swaps. All these contracts share the common feature of being pure variance contracts.

We can not know (today) the price of the underlying asset at the starting point, since the forward start option starts in the future, and for this reason it is standard to specify a strike price as a percentage of moneyness. For example, we can set the strike to be 100% of the price of the underlying at the strike date, so that the option starts at-the-money (ATM). Table 4.3 gives the position in which option start with different strikes for forward start calls.

	Call Option	Put Option
$K < 100\%$	starts $(1 - K)\%$ ITM	starts $(1 - K)\%$ OTM
$K > 100\%$	starts $(K - 1)\%$ OTM	starts $(K - 1)\%$ ITM
$K = 100\%$	starts ATM	starts ATM

Table 4.3: Strike for Forward Start Calls and the position in which the option starts.

We consider the forward start call option pricing problem under the bivariate Lévy (VG) correlation model with integrated Wishart time change, where two assets S_1 and S_2 are modeled as in Equation (4.1) or more generally as in Equation (4.2). The payoff of a forward-start call option at maturity T is $(S_T/S_t - K)^+$, where S_t is the stock price at a fixed time t, $0 \leq t \leq T$. Then by risk-neutral valuation, the

---

[9]A series of consecutive forward start options creates a cliquet option

initial price of options for S_1 and S_2 are given by:

$$\mathcal{FS}\,C_{S_1}(0) = e^{-rT}E^{\mathbb{Q}}\Big[\frac{S_1(T)}{S_1(t)} - K\Big]^+$$

$$\mathcal{FS}\,C_{S_2}(0) = e^{-rT}E^{\mathbb{Q}}\Big[\frac{S_2(T)}{S_2(t)} - K\Big]^+ \tag{4.8}$$

If we consider the forward log return: $\ln[S_T/S_t]$, the forward start call option prices

at time zero become:

$$\mathcal{FS}\,C_{S_1}(0) = e^{-rT}E^{\mathbb{Q}}\big[e^{\ln[S_1(T)/S_1(t)]} - e^{\ln K}\big]^+$$

$$\mathcal{FS}\,C_{S_2}(0) = e^{-rT}E^{\mathbb{Q}}\big[e^{\ln[S_2(T)/S_2(t)]} - e^{\ln K}\big]^+ \tag{4.9}$$

In order to price a forward-start call option via the FFT method, the forward

characteristic function of $\ln[S_T/S_t]$ is needed.[10] This will involve the computation

of the characteristic function of the Wishart process, which is given in following:

Proposition 4.2. (*The Conditional Characteristic Function of the Wishart*

***Process*)**

Given a real symmetric matrix D, the conditional characteristic function of

the Wishart process V_t is given by:

$$\phi_{D,t}^{V_t}(\tau) = E_t\,\exp(i\,Tr[DV_{t+\tau}]) = \exp\big(Tr[B(\tau)V_t] + C(\tau)\big) \tag{4.10}$$

where the deterministic complex-valued functions $B(\tau) \in M_n(\mathbb{C}^n)$, $C(\tau) \in \mathbb{C}$ are

given by:

$$B(\tau) = \big(iDB_{12}(\tau) + B_{22}(\tau)\big)^{-1}\big(iDB_{11}(\tau) + B_{21}(\tau)\big),$$

$$C(\tau) = Tr[\beta Q^T Q \int_0^\tau B(s)\,ds], \tag{4.11}$$

---

[10]The expectation in this section is under risk-neutral measure $\mathbb{Q}$ and we use E in stead of $E^{\mathbb{Q}}$

in all computations for simplicity.

with

$$
\begin{pmatrix}
B_{11}(\tau) & B_{12}(\tau) \\
B_{21}(\tau) & B_{22}(\tau)
\end{pmatrix}
= \exp \tau
\begin{pmatrix}
M & -2Q^T Q \\
0 & -M^T
\end{pmatrix}.
$$

Proof: See Appendix. $\square$

We now derive the forward characteristic function of the log returns:

$$
\phi_{\ln[S_T/S_t]}(u) = E\big[e^{iu \ln[S_T/S_t]}\big] = E\big[E_t(e^{iu(\ln S_T - \ln S_t)})\big]
$$

$$
= E\big[e^{-iu \ln S_t} \cdot E_t(e^{iu \ln S_T})\big]
$$

$$
= E\Big(e^{-iu \ln S_t} \cdot e^{iu \ln S_t + iu(r-q)(T-t)} \cdot \frac{\phi_{X;t,T}(u)}{[\phi_{X;t,T}(-i)]^{iu}}\Big)
$$

$$
= e^{iu(r-q)(T-t)} E\Big(\frac{e^{Tr[C(T-t,\Gamma)A_t]+b(T-t,\Gamma)}}{\big[e^{Tr[C(T-t,\Gamma(-i))]+b(T-t,\Gamma(-i))}\big]^{iu}}\Big)
$$

$$
= e^{iu(r-q)(T-t)+b(T-t,\Gamma)-iu\,b(T-t,\Gamma(-i))} E_0\big(e^{Tr\{[C(T-t,\Gamma)-iuC(T-t,\Gamma(-i))]A_t\}}\big)
$$

where $C(T-t,\Gamma)$, $b(T-t,\Gamma)$ are given in equation (3.31), A_t follows Wishart process, and $\Gamma(-i)$ represents similar to Γ but replacing all u elements$(u_1,...,u_n)$ with $-i$. If we denote $\tilde{C}(T-t) \triangleq C(T-t,\Gamma) - iuC(T-t,\Gamma(-i))$, then we have:

$$
\phi_{\ln[S_T/S_t]}(u) = e^{iu(r-q)(T-t)+b(T-t,\Gamma)-iu\,b(T-t,\Gamma(-i))} E_0\big(e^{Tr[\tilde{C}(T-t)A_t]}\big) \tag{4.12}
$$

Now we see that $E_0\big(e^{Tr[\tilde{C}(T-t)A_t]}\big)$ in equation (4.12) can be evaluated by using equation (4.10) with $iD = \tilde{C}(T-t)$, $V_{t+\tau} = A_t$, and $\tau = t$, $t = 0$. Then,

$$
E_0\big(e^{Tr[\tilde{C}(T-t)A_t]}\big) = e^{Tr[B(t)A_0]+C^*(t)} \tag{4.13}
$$

Therefore, the forward characteristic function will be:

$$
\phi_{\ln[S_T/S_t]}(u) = e^{iu(r-q)(T-t)+b(T-t,\Gamma)-iu\,b(T-t,\Gamma(-i))+Tr[B(t)A_0]+C^*(t)} \tag{4.14}
$$

with

$$B(t) = \left(\tilde{C}(T-t)B_{12}(t) + B_{22}(t)\right)^{-1}\left(\tilde{C}(T-t)B_{11}(t) + B_{21}(t)\right),$$

$$C^*(t) = Tr[\beta Q^T Q \int_0^t B(s)\, ds]. \tag{4.15}$$

Now the closed form of forward characteristic function is in hand, and we can apply FFT method to get the price of forward start option.

4.4.2 Numerical Results

We compare computational results for forward-start option under the two-dimensional Lévy(VG) correlation model. In Monte Carlo simulation, we have run $100,000$ simulation paths each time to obtain a considerable accurate estimation. We have perform FFT method for taking $N = 1024$ and run $100,000$ times for Monte Carlo simulation. The FFT algorithm and simulation were implemented in Matlab on the same machine. Results are showing in Table 4.4.

The parameters we were using are as follows:(for Table 4.4)

$$M = \begin{pmatrix} -15 & -0.5 \\ -0.5 & -5 \end{pmatrix}, \quad Q = \begin{pmatrix} 0.5 & 0.4 \\ 0.3 & 0.5 \end{pmatrix}, \quad A_0 = \begin{pmatrix} 0.04 & 0.04 \\ 0.04 & 0.04 \end{pmatrix},$$

$$\beta = 4, \quad \theta_1 = \theta_2 = -0.15, \quad \sigma_1 = \sigma_2 = 0.9966, \quad \nu_1 = \nu_2 = 0.3,$$

$$S_1(0) = S_2(0) = 100, \; r = 0.05, \; N = 1024, \; T = 1, \; t = 0.5.$$

		FFT method	Simulation
$K = 0.2$	$\mathcal{FS}\,C(S_1)$	0.7917	0.7932
	$\mathcal{FS}\,C(S_2)$	0.7967	0.8011
$K = 0.5$	$\mathcal{FS}\,C(S_1)$	0.5003	0.5005
	$\mathcal{FS}\,C(S_2)$	0.5047	0.5016
$K = 0.8$	$\mathcal{FS}\,C(S_1)$	0.2176	0.2185
	$\mathcal{FS}\,C(S_2)$	0.2277	0.2300
$K = 1$	$\mathcal{FS}\,C(S_1)$	0.0397	0.0388
	$\mathcal{FS}\,C(S_2)$	0.0786	0.0802
$K = 1.1$	$\mathcal{FS}\,C(S_1)$	0.0180	0.0178
	$\mathcal{FS}\,C(S_2)$	0.0557	0.0550
$K = 1.2$	$\mathcal{FS}\,C(S_1)$	0.0129	0.0133
	$\mathcal{FS}\,C(S_2)$	0.0429	0.0437

Table 4.4: Computational Results for Forward Start Call Option Prices

4.5 Calibration

The price to pay for more realistic models is the increased complexity of model calibration. Often, the estimation method becomes as crucial as the model itself [18].

Calibration consists in estimating the unknown parameters of the model which reproduce almost perfectly the market option prices. The main purpose of calibration is pricing OTC options, often exotic, which do not quote in any market and whose prices are therefore unknown.

The aim of this section is to show that the calibration of our Lévy integrated Wishart time change correlation model to market prices is feasible. To the best of our knowledge, no other multivariate stochastic volatility models with non-trivial dependence structure with Wishart process have been successfully calibrated to the real market. This is may due to the fact that the trade-off between flexibility and tractability is particularly delicate in a multivariate setting. Therefore, we think the content in this chapter is relatively new and can be considered as a good attempt. [11]

Though the closed form of characteristic function formula is given in the context for high dimensions, it is usually not numerically feasible in practice by FFT. Hence, we calibrate the model using two-asset options that incorporate pairwise dependencies. Moreover, it is difficult to obtain real price quotes of multi-asset options, since they are mostly traded over-the-counter. In order to circumvent this problem, we consider foreign exchange rates because of the special triangular relationship in FX market (more details will be provided in a later subsection) and use options on

---

[11]It may be considered as a first test rather than a finished product.

two liquid currency pairs to price options on the illiquid cross-currency pair. To my knowledge, the bivariate Lévy (VG) correlation model is the first model with stochastic volatility and correlation which can deal with this problem.

4.5.1 Estimation Methods: Non-Linear Least Squares

In the Lévy correlation model we developed earlier, the likelihood functions are not known in closed form, so using the maximum likelihood method [12] to estimate the statistical parameters is very difficult to implement. Frequently used methods for Lévy models include the generalized method-of-moments (GMM) developed by Hansen and Scheinkman [37], and the efficient method-of-moments (EMM) proposed by Gallant and Tauchen [31]. However, it is not convenient to employ these econometric tools in practice. An alternative and popular way is to use option prices to estimate the risk-neutral parameters directly.

Since calibration consists of estimating unknown parameters which produce the correct market prices of selected options, this is also considered as an *inverse* problem (as we solve for parameters indirectly through some implied structures). The most popular approach to solve such an inverse problem is to minimize the error or discrepancy between model prices and market prices. This usually turns out to be a *non-linear least squares* optimization problem. More specifically, the sum of squared differences between model option prices and market option prices is minimized over the parameter space.

The procedure is: we collect N options with different time to maturities and

---

[12]Please refer to some statistic books for Maximum Likelihood Estimation method for details

strike prices on the same stock in the same day. The parameter set Θ is then determined to find the minimum value of a sum of N squared residuals. We evaluate:

$$\hat{\Theta} = \arg\min_{\Theta} \sum_{i=1}^{N} \left[C_i^{Market}(K_i, T_i) - C_{i,\Theta}^{Model}(K_i, T_i) \right]^2 \qquad (4.16)$$

where $C_i^{Market}(K_i, T_i)$ and $C_{i,\Theta}^{Model}(K_i, T_i)$ are the ith option prices from the market and model respectively, with strike K_i and time to maturity T_i.

4.5.2 Empirical Application

We are using cross-currency options to implement the calibration, since one interesting problem in the FX market is using options on two liquid currency pairs to price options on illiquid cross-currency pairs. A currency pair is the quotation of the relative value of a currency unit against the unit of another currency in the foreign exchange market. We consider the options on illiquid FX pair j/k, which represents currency j against currency k. For example, the quotation EUR/USD 1.2500 means that one euro is exchanged for 1.2500 US dollars. The option price for this illiquid pair j/k may be computed from the prices of two options of liquid pairs k/i (currency k against currency i or alternatively currency k is quoted in units of currency i) and j/i. For instance, if we are interested in a vanilla option on GBP/EUR, we can use two liquid pairs GBP/USD and EUR/USD.

The risk-neutral processes for two spot FX rates $S_{j/i}(t)$ and $S_{k/i}(t)$ under measure Q^i, which represents the risk-neutral measure with numeraire i (a money market account invested in currency i), are defined as follows:

$$S_{j/i}(t) = S_{j/i}(0)e^{-(r_j-r_i)t}\frac{e^{X_1(t)}}{E^{Q^i}[e^{X_1(t)}]}$$

$$S_{k/i}(t) = S_{k/i}(0)e^{-(r_k-r_i)t}\frac{e^{X_2(t)}}{E^{Q^i}[e^{X_2(t)}]} \tag{4.17}$$

where r_i, r_j, r_k are assumed to be deterministic interest rates for three currencies and $X_1(t)$, $X_2(t)$ follows the Lévy correlation model we developed earlier. The characteristic functions for the log returns $\ln[S_{j/i}(t)/S_{j/i}(0)]$ and $\ln[S_{k/i}(t)/S_{k/i}(0)]$ are:

$$\phi_{\ln[S_{j/i}(t)/S_{j/i}(0)]}(u) = e^{-iu[(r_j-r_i)t - \ln(\phi_{X_1,X_2;0,t}(-i,0))]} \cdot \phi_{X1,X2;0,t}(u,0)$$

$$\phi_{\ln[S_{k/i}(t)/S_{k/i}(0)]}(u) = e^{-iu[(r_k-r_i)t - \ln(\phi_{X_1,X_2;0,t}(0,-i))]} \cdot \phi_{X1,X2;0,t}(0,u) \tag{4.18}$$

where ϕ_{X_1,X_2} is the joint characteristic function for X_1 and X_2.

The characteristic function of the log return $\ln[S_{j/k}(t)/S_{j/k}(0)]$ under measure Q^k can be derived by changing of measure:

$$\phi_{\ln\frac{S_{j/k}(t)}{S_{j/k}(0)}}(u) = E^{Q^k}[e^{iu\ln[S_{j/k}(t)/S_{j/k}(0)]}] = E^{Q^i}[e^{iu\ln[S_{j/k}(t)/S_{j/k}(0)]}\frac{dQ^k}{dQ^i}]$$

$$= E^{Q^i}[e^{iu\ln[S_{j/k}(t)/S_{j/k}(0)]} \cdot e^{(r_i-r_k)t+\ln[S_{k/i}(t)/S_{k/i}(0)]}$$

$$= E^{Q^i}[e^{iu\ln[S_{j/i}(t)/S_{j/i}(0)]\cdot e^{-(iu-1)\ln[S_{k/i}(t)/S_{k/i}(0)]-(r_i-r_k)t}}]$$

$$= E^{Q^i}[e^{i(u\ln[S_{j/i}(t)/S_{j/i}(0)]-(u+i)\ln[S_{k/i}(t)/S_{k/i}(0)])\cdot e^{-(r_i-r_k)t}}]$$

$$= \phi_{X_1,X_2;0,t}(u,-(u+i))e^{iu(r_k-r_j)t-iu\ln(\phi_{X_1,X_2;0,t}(-i,0))+i(i+u)\ln(\phi_{X_1,X_2;0,t}(0,-i))} \tag{4.19}$$

Now we have the closed form characteristic function of the log return for the interested currency pair j/k. The FFT method can be applied to price a European option written on cross FX rate $S_{j/k}(t)$.

In our calibration implement, we obtained two cross-currency option price data: EUU (ISE Spot EUR USD) and GBP (ISE Spot GBP USD) on June 17th, 2011 from OIC(The Options Industry Council) [13] [14]. We collected call option prices for 393 options (including ATM, ITM, OTM) in total, with 160 call options on the GBP/USD (symbol:GBP) exchange rate and 233 call options on the EUR/USD (symbol:EUU) exchange rate. Each of them had different strikes and four or five maturities, respectively (maturity days include: 29 days, 64 days, 92 days, 183 days, 274 days). The mid-value between bid and ask price is used as the option value. Table 4.5 shows the currency LIBOR rate we were using for exchange rate at that time.

Time to Maturity	USD LIBOR	EUR LIBOR	GBP LIBOR
29	0.18580%	1.27688%	0.62750%
64	0.24650%	1.45000%	0.82500%
92	0.28775%	1.52500%	0.89563%
183	0.56200%	1.91475%	1.35563%
274	0.72775%	2.11563%	1.57688%

Table 4.5: Libor rates on June 17th, 2011

[13]website: http://www.optionseducation.org

[14]The option chain data for EUU and GBP can also be obtained from MarketWatch: http://www.marketwatch.com

Our objective function for calibration is:

$$\hat{\Theta} = \arg\min_{\Theta} \sum_{alloptions} \left[C_i^{Market}(K_i, T_i) - C_{i,\Theta}^{Model}(K_i, T_i) \right]^2 \qquad (4.20)$$

4.5.3 Calibration Results

We calibrate two currency pairs for bivariate Lévy correlation model with integrated Wishart time change simultaneously and the parameter set Θ is: $M_{2\times2}, Q_{2\times2}, \beta,$ $A_{0\,(2\times2)}, \theta_1, \theta_2, \nu_1, \ \nu_2, \ \sigma_1, \sigma_2$ (19 parameters). Since M is required to be negative semi-definite, and A_0 should be positive semi-definite, M, A_0 have Cholesky decompositions

$$M = -L_M L_M^T, \qquad A_0 = L_{A_0} L_{A_0}^T$$

with

$$L_M = \begin{pmatrix} m_{11} & 0 \\ m_{21} & m_{22} \end{pmatrix}, \qquad L_{A_0} = \begin{pmatrix} l_{11} & 0 \\ l_{21} & l_{22} \end{pmatrix},$$

Then the parameter set need to be estimated has be reduced to 15 parameters: $l_{11}, l_{21}, l_{22}, m_{11}, m_{21}, m_{22}, q_{11}, q_{12}, q_{21}, q_{22}, \beta, \theta_1, \theta_2, \nu_1, \nu_2, \sigma_1, \sigma_2$. where Q is denoted as:

$$Q = \begin{pmatrix} q_{11} & q_{12} \\ q_{21} & q_{22} \end{pmatrix},$$

and $\beta > n - 1$ (n is the number of underlying assets; for the bivariate case $n = 2$). The parameter σ_1 and σ_2 can be evaluated by $\theta^2 \nu + \sigma^2 = 1$, since centered independent Lévy (VG) processes with unit variance were chosen in model setting.

We totally have 15 parameters to be estimated. For such a large parameter set, Genetic Algorithm performs better in selecting solutions to minimize the objective function. We therefore use Genetic Algorithm (GA) to find optimization parameters. The calibration result can be found in Table 4.6.

Calibration Parameters	l_{11}	l_{21}	l_{22}	m_{11}	m_{21}	m_{22}
Results	0.2146	-0.2201	0.2071	4.3564	-2.8998	3.5063
Calibration Parameters	q_{11}	q_{12}	q_{21}	q_{22}	β	θ_1
Results	0.0706	0.1780	0.2574	0.6145	1.4341	-3.5349
Calibration Parameters	θ_2	ν_1	ν_2			
Results	0.0070	-2.6561	0.0177			

Table 4.6: Calibrated parameters for options on GBP/USD and EUR/USD on June 17th, 2011

	Overall	GBP/USD	EUR/USD
RMSE	0.1334	0.1118	0.1462
APE	0.0199	0.0194	0.0203

Table 4.7: RMSE and APE Results for Calibration

Table 4.7 shows error results: The overall root mean squared error (RMSE) is 0.1334, and absolute percent error (APE) is 0.0199. The RMSE for only considering

GBP/USD is 0.1118 and APE is 0.0194; the RMSE for only considering EUR/USD is 0.1462 and APE is 0.0203. To depict the good fit visually we provide Figure 4.2, where market and model prices are compared for a sample of different strikes and maturities(marker 'o' represents market prices, and marker '+' represents model prices). We also tested the sensitivity of the calibration with respect to the initial values of the optimization and found that the calibration parameters could be re-covered quite well from a broad range of initial values. From Figure 4.2, we can see that model prices for two options fit the market prices for various maturities and strikes very well with the calibration parameters. Figures 4.3 and 4.4 show fitting results for different maturities separately.

4.5.4 Discussion-Volatilities:EUR/USD over GBP/USD?

The previous subsection shows the calibration parameters for two currency options: GBP/USD and EUR/USD. With the calibration parameter results shown in Table 4.6, we could simulate instantaneous time change rate sample paths, which capture the dynamics of volatilities for two options, and also correlation sample paths. Two figures are shown in Figure 4.5 (a) and (b).

In Figure 4.5 (a), $A_{11}(t)$ (Blue line) reflects the volatility variation for option on GBP/USD, while $A_{22}(t)$(Red line) reflects the volatility variation for option on EUR/USD. We observed that EUR/USD is more volatile and risky than GBP/USD in these days (around June 2011), as the red line is over blue line for almost en-tire time period. And from Figure 4.5 (b), it is obvious that EUR/USD is highly
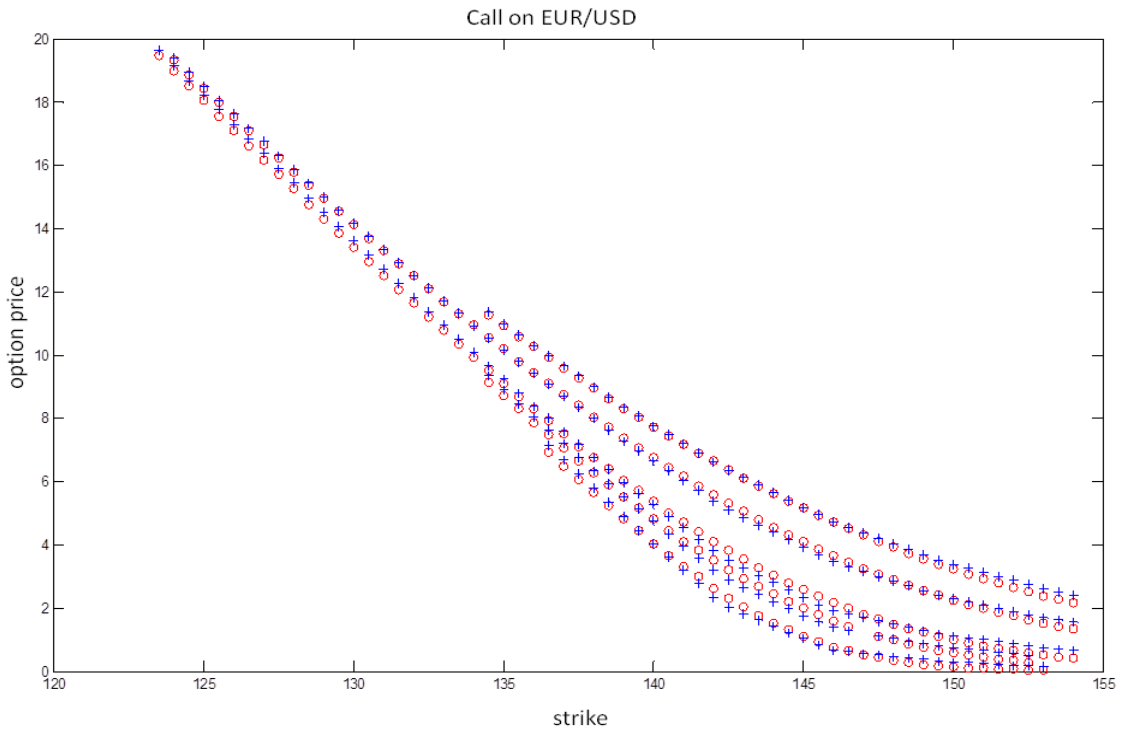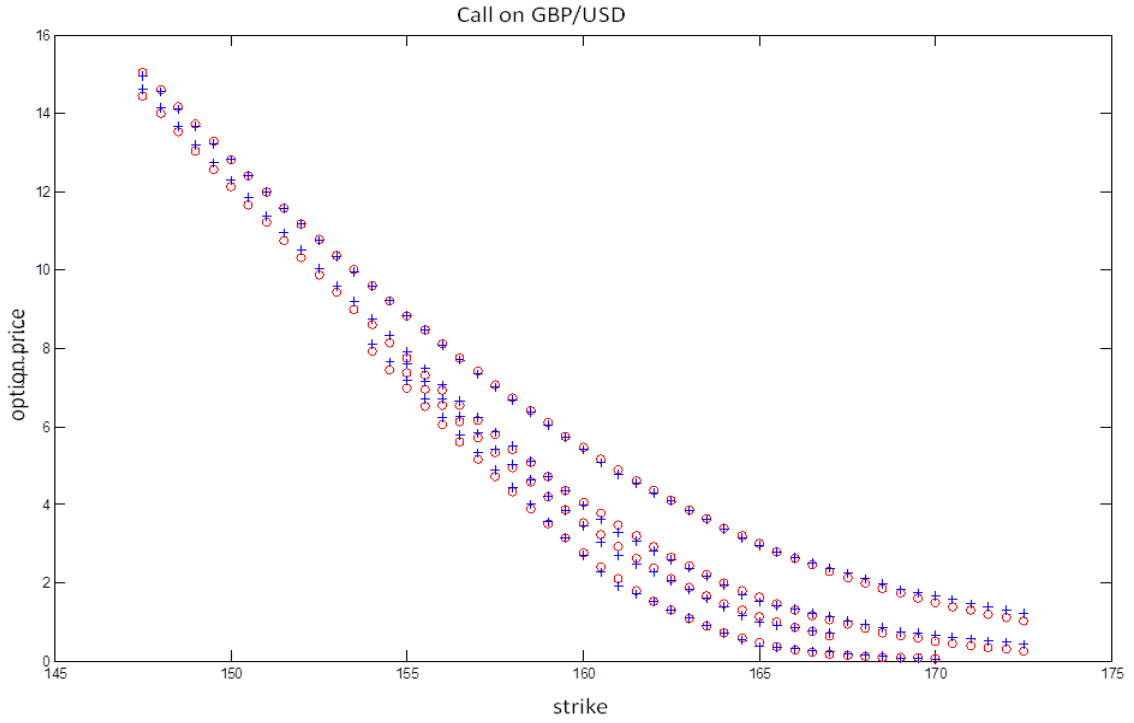
Figure 4.2: Calibration results for bivariate Lévy(VG) correlation model with integrated Wishart time change: market prices (circle) against model prices (plus).
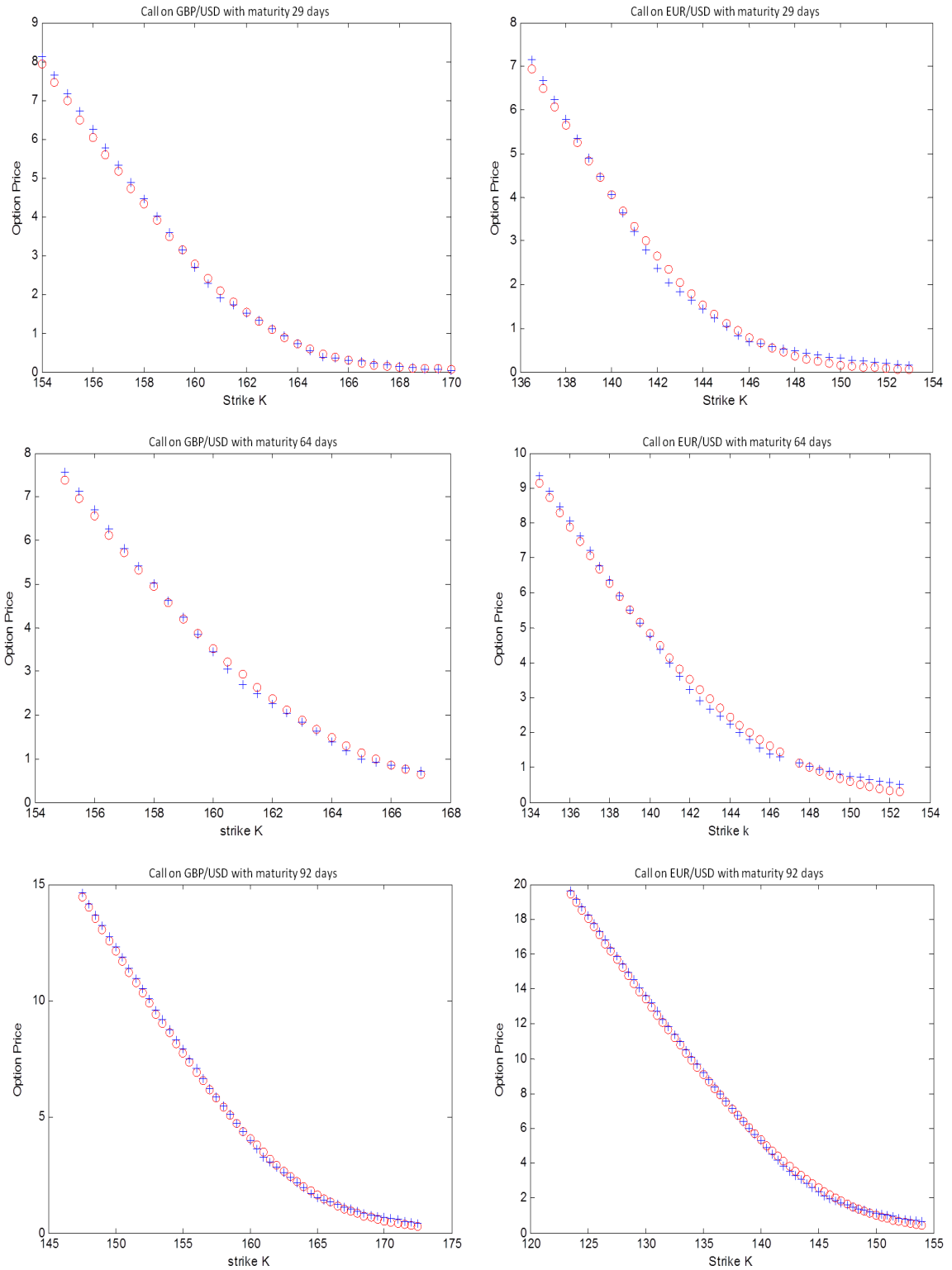
Figure 4.3: Calibration results with different maturities 29 days, 64 days, 92 days: market prices (circle) against model prices (plus).
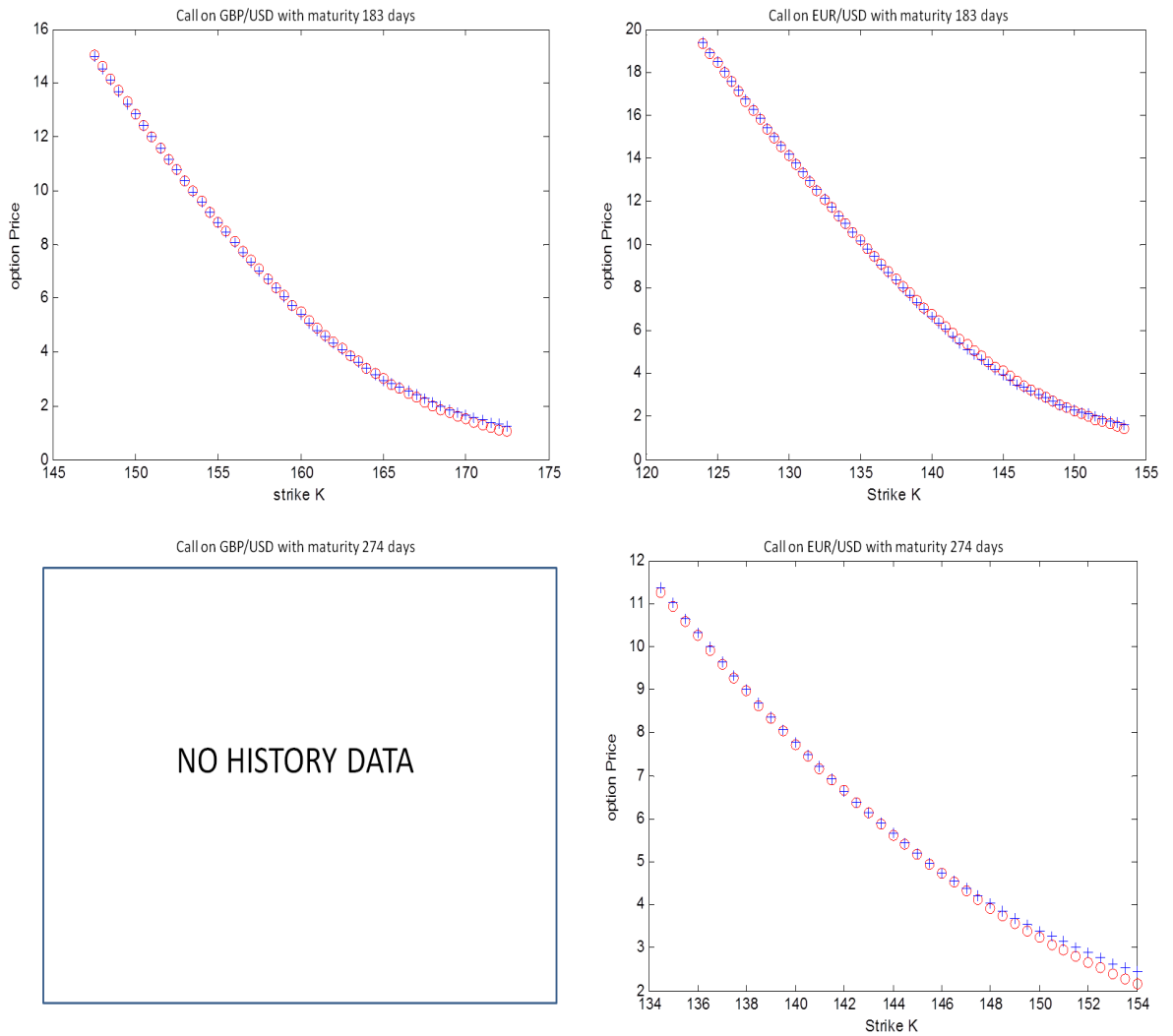
Figure 4.4: Calibration results with different maturities 183 days, 274 days: market prices (circle) against model prices (plus).
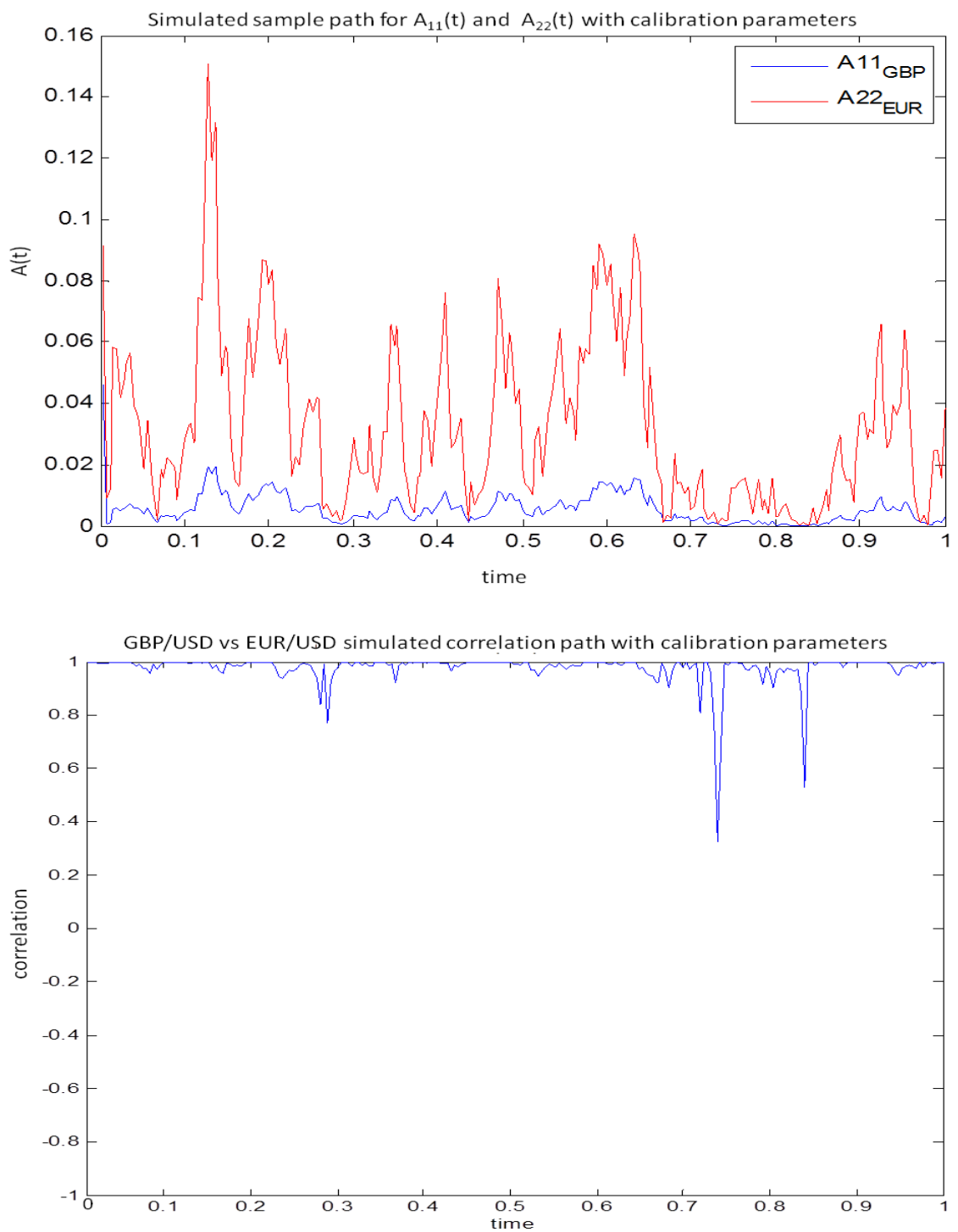
Figure 4.5: $A_{11}(t)$, $A_{22}(t)$ and correlation simulated paths from calibration parameters

correlated with GBP/USD. However, GBP/USD is usually more volatile than EUR/USD (GBP/USD usually has higher volatility and lower liquidity in the market than EUR/USD).

Why have we seen this shift? Is EUR/USD over GBP/USD these days? Let us refer to an article on June 27th, 2011, named "$EURUSD vs $GBPUSD - Volatility Favors EU over GU these days?" [59]

Volatility Favors: $EURUSD over $GBPUSD these days?

"There was a time when the daily volatility (measured in pip range) of the GBPUSD was always above that of the EURUSD. Combine the higher volatility and the lower liquidity of GU versus EU, and I could understand how the bid offer spread on GU was typically a bit wider than on the EU. But these days, the daily ranges show that EU is giving us more volatility than the GU (i.e., more pip potential in any potential move). When you combine that with the lower pip spread it looks like you are getting a bit better bang for your buck whenever you trade the EU compared to when you trade the GU." [59]

Daily history volatilities for EUR/USD and GBP/USD are shown in Figure 4.6 and Figure 4.7

Figure 4.6 shows from (Forex Ticker)www.mataf.net the daily pip (shorten for in points) range over the last couple of years on EUR/USD. Notice how during much of 2010 the daily average was less than 150 pips but now are routinely seeing daily average ranges exceeding 150 pips.

Figure 4.7 shows the daily pip range over the last couple of years on GBP/USD.
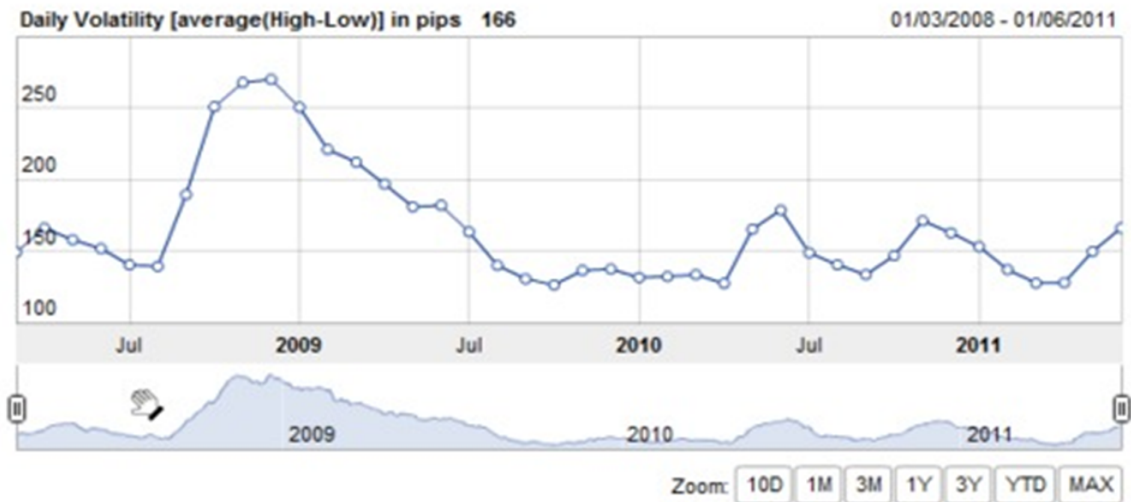
Figure 4.6: Daily History Volatilities for EUR/USD from $03/2008 - -06/2011$

Notice how during much of 2010 the range was above 150 pips and during early 2010 it was even close to 170 or 180 pips average. What is quite surprising now is to see that the pip range is sub-150 pips on many days.


Figure 4.7: Daily History Volatilities for GBP/USD from $03/2008 - -06/2011$

From two charts, we could see the history volatilities result show the similar trend as our simulated sample path for time change A_{11}, A_{22}, and our model sim-

ulation results draw the same conclusion as the history results—the volatility for EUR/USD is above GBP/USD in those days around June 2011. We may wonder why this happened? It may due the Greek Debt Crisis and ECB rate hikes around those days [15].

---

[15]low interest rates, no apparent near term prospects for rate hikes, not directly implicated in the Greek crisis although you can never rule it out 100% [59]

Chapter 5

Conclusion and Future Work

In conclusion, we explored how to extend stochastic volatility for Lévy process to multivariate level and study the properties of this new model in this thesis. Our model is a multidimensional Lévy process with stochastic mean, stochastic volatility, stochastic skewness as well as stochastic correlation of cross-sectional of asset returns. Compared with the existing models, our Lévy correlation model has a very flexible dependence structure without sacrificing tractability. It allows each asset to have its own business clock as well the co-movements of business clocks of multiple assets, and also allows flexible correlation dynamics with independent variation. Meanwhile, we derived the marginal and joint characteristic functions in closed form, and we also derived pricing methods for different types of options, including single asset option and muti-asset options, by using Monte Carlo simulation and Fast Fourier transformation methods. Moreover, we have shown the skewness for our new model varies stochastically over time, which therefore can deal with stochastic skewness effects introduced by Carr and Wu [14]. Finally, we calibrated this model to the options on FX currency pairs and remarkable consistence has been observed. We compared model prices with market prices by drawing calibration figures and show that this model can simultaneously fit the cross-rate option market prices surface across different maturities and strikes very closely.

Our model can be widely used in many fields, such as some other OTC derivative pricing(for instance, variance swap, volatility swap, or other relative derivatives), credit risk management, optimal portfolio choice, etc. My future work will devote on applying this model to those fields.

Appendix A

Relative Proofs and Concepts

A.1 One Dimensional Riccati Equation

A univariate Riccati equation:

$$\frac{da(h)}{dh} = b[a(h) - c_0][a(h) - c_1].$$

(A.1)

can be written as:

$$da(h)\left[\frac{1}{a(h) - c_0} - \frac{1}{a(h) - c_1}\right] = b(c_0 - c_1)dh.$$

(A.2)

By taking integral we will get:

$$a(h) = c_1 + \frac{[a(0) - c_1](c_0 - c_1)}{a(0) - c_1 - [a(0) - c_0]exp[b(c_0 - c_1)h}$$

(A.3)

A.2 Proof of Proposition 2.7

Proof: In equation (2.9), the conditional Laplace transform of the CIR process y_t has an exponential affine form as:

$$\psi_{t,h}(u) = E_t[exp(-uy_{t+h})] = exp[-a(h, u)y_t - b(h, u)]$$

(A.4)

By iterated expectation theorem we get:

$$\psi_{t,h}(u) = E_t E_{t+dt}[exp(-uy_{t+h})] = E_t[\psi_{t+dt,h-dt}(u)]$$

$$= E_t exp[-a(h - dt, u)y_{t+dt} - b(h - dt, u)]$$

$$= E_t exp[-a(h - dt, u)y_{t+dt}[y_t - k(y_t - \theta)dt + (\eta^2 y_t)^{1/2} dW_t] - b(h - dt, u)]$$

$$\sim exp[-a(h - dt, u)y_t + a(h - dt, u)k(y_t - \theta)dt - b(h - dt, u)]$$

$$E_t exp[-a(h - dt, u)(\eta^2 y_t)^{1/2} dW_t]$$

$$\sim exp[-a(h - dt, u)y_t + a(h, u)k(y_t - \theta)dt - b(h - dt, u) + \frac{1}{2}a^2(h, u)\eta^2 y_t dt].$$

By identifying with the assumed expression in equation (A.4), we obtain:

$$\begin{cases} a(h, u) \sim a(h - dt, u) - ka(h, u)dt - \frac{1}{2}\eta^2 a^2(h, u)dt, \\ \\ b(h, u) \sim b(h - dt, u) + k\theta a(h, u)dt. \end{cases}$$

If we take $dt \to 0$, two functions are solutions of the following differential system:

$$\begin{cases} \dfrac{\partial a(h, u)}{\partial h} = -ka(h, u) - \dfrac{1}{2}\eta^2 a^2(h, u), \\ \\ \dfrac{\partial b(h, u)}{\partial h} = k\theta a(h, u). \end{cases} \tag{A.5}$$

with initial conditions:(since $E_t exp(-uy_t) = exp(-uy_t)$

$$a(0, u) = u, \quad b(0, u) = 0.$$

From equations (A.5), we note that the function $a(h, u)$ satisfies a Riccati equation

in (A.1) with: $b = \frac{-\eta^2}{2}$, $c_1 = 0$, $c_0 = -\frac{2k}{\eta^2}$, and initial condition $a(0, u) = u$.

Then by applying formula (A.3), we derived that:

$$a(h, u) = \frac{-\frac{2k}{\eta^2}u}{u - [u + \frac{2k}{\eta^2}]e^{kh}} = \frac{ue^{kh}}{1 + \frac{\eta^2 u}{2k}[1 - e^{-kh}]}.$$

By integrating the second equation in (A.5), we get:

$$b(h, u) = \frac{2k\theta}{\eta^2} log \left[1 + u \frac{\eta^2}{2k}(1 - e^{-kh}) \right].$$

$\square$

A.3   Proof of Proposition 3.4

Proof: Since $E_t(dW_t) = 0$, the drift of Wishart process V_t is easily obtained:

$$E_t dV_t = (\beta QQ^T + V_t M^T + M^T V_t)dt$$

and the covariance:

$$Cov_t(\alpha^T dV_t \alpha, \beta^T dV_t \beta)$$

$$= Cov_t(\alpha^T V_t^{1/2} dW_t Q\alpha + \alpha^T Q^T dW_t Y_t^{1/2}\alpha, \ \beta^T Q^T dW_t^T Y_t^{1/2}\beta)$$

$$= E_t[(\alpha^T V_t^{1/2} dW_t Q\alpha + \alpha^T Q^T dW_t Y_t^{1/2}\alpha)(\beta^T Q^T dW_t^T Y_t^{1/2}\beta)].$$

we note that for any vectors $u, v \in \mathbb{R}^n$:

$$E_t(dW_t uv^T dW_t^T) = E_t(dW_t^T uv^T dW_t) = v^T uI dt,$$

$$E_t(dW_t uv^T dW_t) = E_t(dW_t^T uv^T dW_t^T) = vu^T dt,$$

then we deduce that:

$$Cov_t(\alpha^T dV_t \alpha, \beta^T dV_t \beta) = (4\alpha^T dV_t \beta \alpha^T Q^T Q\beta)dt.$$

$\square$

A.4 Proof of Proposition 3.5

Proof: Given $V_{t+h} = x_{t+h}x_{t+h}^T$, where x_t is an OU process: $dx_t = Mx_t dt + Q^T dW_t$, with the distribution of $x_{t+1}|x_t \sim \mathcal{N}\left(\tilde{M}(h)x_t, \Sigma(h)\right)$. Then the conditional Laplace transform of V_{t+h} is:

$$E_t e^{Tr(\Gamma V_{t+h})} = E_t e^{x_{t+h}^T \Gamma x_{t+h}}$$

$$= \int_{\mathbb{R}^n} exp\, x^T \left(\Gamma - \frac{\Sigma(h)^{-1}}{2}\right) x + x^T \Sigma(h)^{-1}\tilde{M}(h)x_t \, dx$$

$$\frac{1}{(2\pi)^{n/2}} \frac{1}{(det\Sigma(h))^{1/2}} exp\left(-\frac{1}{2}x_t^T \tilde{M}(h)^T \Sigma(h)^{-1}\tilde{M}(h)x_t\right).$$

In order to simplify the above result, we apply the following lemma:

Lemma A.1. *For any symmetric positive semi-definite matrix Ω, and $\mu \in \mathbb{R}^n$, we obtain:*

$$\int_{\mathbb{R}^n} exp(-x^T\Omega x + \mu^T x)dx = \frac{\pi^{n/2}}{(det\Omega)^{1/2}} exp(\frac{1}{4}\mu^T\Omega^{-1}\mu). \qquad (A.6)$$

Thus, we get:

$$E_t e^{Tr(\Gamma V_{t+h})} = \frac{1}{det(Id - 2\Sigma(h)\Gamma)^{1/2}}$$

$$exp-\frac{1}{2}x_t^T\tilde{M}(h)^T\Sigma(h)^{-1}\tilde{M}(h)x_t + \frac{1}{2}x_t^T\tilde{M}(h)^T\Sigma(h)^{-1}(\Sigma(h)^{-1} - 2\Gamma)^{-1}\Sigma(h)^{-1}\tilde{M}(h)x_t$$

$$= \frac{exp\,Tr[\Gamma(Id - 2\Sigma(h)\Gamma)^{-1}\tilde{M}(h)V_t\tilde{M}(h)^T]}{(det[Id - 2\Sigma(h)\Gamma])^{1/2}}.$$

This is the result for $\beta = 1$ of Proposition 3.5. The general case is immediately deduced. $\qquad \square$

A.5 Proof of Proposition 3.7

Proof: Let $f : S_n(\mathbb{R}) \to \mathbb{R}$ be a two times differentiable function. By applying Itô's lemma, we first have:

$$df(V_t) = \sum_{i,j=1}^{n} \frac{\partial f}{\partial V_t^{ij}} V_t \, dV_t^{ij} + \frac{1}{2} \sum_{i,j,k,l=1}^{n} \frac{\partial^2 f}{\partial V_t^{ij} \partial V_t^{kl}} V_t \, d\langle V^{ij}, V^{kl} \rangle_t. \qquad (A.7)$$

Then from (3.4), we will get:

$$dV_t^{ij} = (\beta Q^T Q + M V_t + V_t M^T)^{ij} dt + \sum_{p,q=1}^{n} (\sqrt{V_t})^i p (dW_t)^{pq} Q_{qj} + Q^{qi}(dW_t)^{pq}(\sqrt{V_t})^{jp}$$

Thus,

$$d\langle V^{ij}, V^{kl} \rangle_t = \sum_{p,q=1}^{n} \left[(\sqrt{V_t})^{ip} Q^{qj} + Q^{qi}(\sqrt{V_t})^{jp} \right] \left[(\sqrt{V_t})^{kp} Q^{ql} + Q^{qk}(\sqrt{V_t})^{lp} \right]$$

$$= 4 \sum_{p,q=1}^{n} (\sqrt{V_t})^{ip} Q^{qj} (\sqrt{V_t})^{kp} Q^{ql} = 4 V_t^{ik}(Q^T Q)^{jl}. \qquad (A.8)$$

If replacing those quantities in the equation (A.7), we can easily get the matrix formulation in (3.9). $\qquad \square$

A.6 Proof of Proposition 3.9

Proof:

$$\psi_{t,h+dt}^*(\Gamma) = E_t \exp[Tr\left(\int_t^{t+dt} \Gamma V_\tau \, d\tau \right)] \psi_{t+dt,h}^*(\Gamma)$$

$$\simeq \exp Tr(\Gamma V_t) dt + b^*(h,\Gamma) E_t \exp Tr(M^*(h,\Gamma) V_{t+dt})$$

$$\simeq \exp\{Tr(\Gamma V_t) dt + b^*(h,\Gamma) + E_t Tr(M^*(h,\Gamma) V_{t+dt}) + \frac{1}{2} V_t Tr(M^*(h,\Gamma) v_{t+dt})\}$$

$$= \exp\{Tr(\Gamma V_t) dt + b^*(h,\Gamma) + Tr[M^*(h,\Gamma) V_t + (\beta Q Q^T + V_t M^T + M V_t) dt]\}$$

$$+ 2Tr[M^*(h,\Gamma) V_t M^*(h,\Gamma) Q^T Q] dt.$$

$$(A.9)$$

Let $t \to 0$, and by identifying both expressions of the Laplace transform, we will get the result. Now, let us consider a matrical Riccati differential system:

$$\frac{dA(h)}{dh} = B^T A(h) + A(h)B + 2A(h) \wedge A(h) + C, \tag{A.10}$$

where $A(h), \wedge, C$ are symmetric $n \times n$ matrices and B is a square $n \times n$ matrix. The solution of the multidimensional equation (A.10) is [35]:

$$A(h) = A^* + exp[(B + 2 \wedge A^*)h]^T$$

$$\{(A(0) - A^*)^{-1} + 2 \int_0^h exp[(B + 2 \wedge A^*)u] \wedge exp[(B + 2 \wedge A^*)u]^T du\}$$

$$exp[(B + 2 \wedge A^*)h],$$

where A^* satisfies:

$$B^T A^* + A^* B + 2A^* B A^* + C = 0.$$

In order to get the result in proposition 3.9, we directly apply the above result to the multi-dimensional partial Riccati equation. $\qquad\square$

A.7 Proof of Proposition 4.2

Proof: The complex-valued non-symmetric Matrix Riccati ODE satisfied by $B(\tau)$ becomes:

$$\frac{d}{d\tau}B(\tau) = B(\tau)M + M^T B(\tau) + 2B(\tau)Q^T QB(\tau),$$
$$B(0) = iD, \tag{A.11}$$

while

$$C(\tau) = Tr[\beta Q^T Q \int_0^\tau B(s)ds].$$

Applying the linearization procedure, we obtain the explicit solution for $B(\tau) = F(\tau)^{-1}G(\tau)$, with

$$\begin{bmatrix} G(\tau) & F(\tau) \end{bmatrix} = \begin{bmatrix} G(0) & F(0) \end{bmatrix} exp \left[\tau \begin{pmatrix} M & -2Q^T Q \\ 0 & -M^T \end{pmatrix} \right]$$

$$= \begin{bmatrix} B(0) & I_n \end{bmatrix} exp \left[\tau \begin{pmatrix} M & -2Q^T Q \\ 0 & -M^T \end{pmatrix} \right]$$

$$= \begin{bmatrix} iDB_{11}(\tau) + B_{21}(\tau) & iDB_{12}(\tau) + B_{22}(\tau) \end{bmatrix}$$

which completes the proof. □

Bibliography

[1] Anderson, T.W. and M.,Girshick.(1944) Some Extensions of the Wishart Distribution. *Annals of Mathematical Statistics*,15,345-357.

[2] Barndorff-Nielsen, O.E., (1997) Normal Inverse Guassian Distributions And Stochastic Volatility Modeling. *Scandinavian Journal of Statistics* 24, 1-13

[3] Barndorff-Nielsen, O.E., (1998) Processes of normal inverse Gaussian type. *Finance and Stochastics* 2, 41-68. A

[4] Barndorff-Nielsen and N.Shephard(1999) Non-Gaussian OU based models and some of their uses in financial economics, *working paper* no. 37, Center for Analytical Finance, University of Aarhus.

[5] Bates, D. (1996) Jumps and Stochastic Volatility: Exchange Rate Processes Implicit in Deutschemark Options. *Review of Financial Studies*, 9, 69-108

[6] Bates, D. (2000) Post-'87 Crash fears in S&P 500 Futures Options. *Journal of Econometrics*, 94, 181-238

[7] Benabid, A., Bensusan, H., and El Karoui, N. (2010) Wishart Stochastic Volatility: Asymptotic Smile and Numerical Framework, *Preprint*

[8] Black, F. and M.Scholes (1973) The Pricing of Options and Corporate Liabilities. *Journal of Computational Finance*, 2, 61-73

[9] Bru, M.F.,(1991) Wishart Processes. *J. Theor. Probab.*, 4, 725-743

[10] Buraschi, A., Porchia, P., and Trojani, F.,(2010) Correlation Risk and Optimal Portfolio Choice. *The Journal of Finance.* Vol. LXV, No.1, 393-420

[11] Carr,P., Madan,B.D.,(1998) Option pricing using the fast Fourier transform. *Journal of Computational Finance* 2, 63-72

[12] Carr, P., Geman, H., Madan, D. B., Yor, M., (2001) Stochastic Volatility for Lévy Processes, *Mathematical Finance.*

[13] Carr, P., Geman, H., Madan, D. B., Yor, M. (2002) The Fine Structure of Asset Returns: An Empirical Investigation. *Journal of Business*, April 2002, 75 2, 305-32

[14] Carr, P. and Wu, L.,(2004) Stochastic skew in currency options.

[15] Carr, P. Liu, W.,(2004) Time changed Lévy Process and Option Pricing. *Journal of Financial Economics* 71 (2004) 113-141

[16] Clark, P. K.,(1973), A Subordinated Stochastic Process with Finite Variance for Speculative Prices,*Econometrica*, Vol. 41, pp. 135-155.

[17] Cont, R. and Tankov, P. (2004) Financial Modeling with Jump Processes. *Chapman& Hall/CRC*, Boca Raton.

[18] Cont,R. (2005) Recovering volatility from option prices by evolutionary optimisation. *Research Paper Series.*

[19] Cox, J. C., Ingersoll, J. E., and Ross, S. A., (1985) A Theory of the Term Structure of Interest Rates. *Econometrica 53*: 385C407

[20] Cox, J. C., Ingersoll, J. E., and Ross, S. A. (1985) An intertemporal general equilibrium model of asset prices, *Econometrica* 53, 363C384

[21] Da Fonseca, J., Grasselli, M., Ielpo, F.,(2007) Estimating the Wishart Affine Stochastic Correlation Model using the Empirical Characteristic Function. *Preprint*

[22] Da Fonseca, J., Grasselli, M. and Tebaldi, C. (2007) Option pricing when correlations are stochastic: an analytical framework, *Review of Derivatives Research* 10: 151-180

[23] Da Fonseca,J., Grasselli, M., and Tebald, C.,(2008) A multifactor volatility Heston model. *Quantitative Finance*, Vol 8, No. 6, 591-604

[24] Dimitroff, G., Lorenz, S. and Szimayer, A. (2009) A parsimonious multi-asset Heston model: Calibration and derivative pricing. *Preprint*

[25] Duffie, D., and R.,Kan,(1996) A Yield Factor Model of Interest Rates. *Mathematical Finance*,6,379-406

[26] Dufresne, D.(2001) The integrated square-root process. *Working paper, University of Montréal.*

[27] Eberlein, E., and Madan, D. B. (2008) On Correlating Lévy Processes. *Working paper*

[28] Engle, R.(1982) Autoregressive Conditional Heteroskedasticity with Estimates of the Variance of U.K. Inflation. *Econometrica*, 50, 987-1008

[29] Engle, R., and K.,Sheppard. (2001) Theoretical and Empirical Properties of Dynamic Conditional Correlation Multivariate GARCH. *NBER Working Paper* 8554

[30] Freiling,G.,(2002) A survey of nonsymmetric Riccati equations. *Linear Algebra and Its Applications,* 351(2):243-270

[31] Gallant, A. R., and Tauchen, G. (1996), Which Moments to Match? *Econometric Theory*, 12, 657C681.

[32] Gauthier,P., and Possamai, D. (2009) Efficient Simulation of the Wishart model. *Working Paper.*

[33] Gourieroux, C., and Sufana, R. (2004) Derivative pricing with multivariate stochastic volatility: application to credit risk. *Working parper, CREST.*

[34] Gourieroux, Christian (2006) Continuous Time Wishart Process for Stochastic Risk

[35] Gourieroux,C., Jasiak, J., and Sufana, R. (2009) The Wishart Autoregressive Process of Multivariate Stochastic Volatility. *Journal of Econometrics*, 150,167-181

[36] Grasselli, M. and Tebaldi, C. (2008) Soluable affine term structure models. *Math. Finan.,* 18,135-153.

[37] Hansen, L. P., and Scheinkman, J. (1995), Back to the Future: Generating Moment Implications for Continuous-Time Markov Processes. *Econometrica*, 63, 767C804.

[38] Heston, S. (1993) Closed form solution for options with stochastic volatility, with application to bond and currency options. *Review of Financial Studies* 6, 327-343

[39] Ho,T., and S.,Lee (2004) A Multifactor Binomial Interest Rate Model with State Time Dependent Volatilites. DP, Hanyang Univ.

[40] Hubalek, F. and Nicolato, E. (2005) On multivariate extensions of Lévy driven Ornstein-Uhlenbeck type stochastic volatility models and multi-asset options. *Preprint.*

[41] Hull J, and A. White. (1988) The Pricing of Options on Assets with Stochastic Volatility. *Journal of Finance*, Jun., 281-300

[42] Jacod,J.,Shiryaev,A.(2003) Limit Theorems for Stochastic Processes, *Springer-Verlag*, Berlin.

[43] James, A.(1968) Calculation of Zonal Polynomial Coefficients by Use of the Laplace Beltrami Operator. *Ann. Math. Stat.,* 39, 1711-1718.

[44] Kallsen,J., and Tankov, P., (2006) Characterization of dependence of multidimensional Lévy processes using Lévy copulas.*Journal of Multivariate Analysis Vol.* 97, 1551-1572

[45] Kou, S. (2002) A jump-diffusion model for option pricing, *Management Science*, 48, 1086-1101

[46] Lord,R., Koekkoek,R., and Van Dijk, D.,(2008) A Comparison of Biased Simulation Schemes for Stochastic Volatility Models. *Tinbergen Institute Discussion Paper No.* 06-046/4

[47] Luciano, E. and Schoutens, W. (2006) A multivariate jump-driven financial asset model. *Quantitative Finance* 6: 385-402

[48] Madan, D. B. and Seneta, E. (1990) The variance gamma model for share market returns. *Journal of Business* 63, 511-524

[49] Madan, D.B., Carr, P.P., Chang, E.C. (1998) The variance gamma process and option pricing, *European Finance Review*, 2, 79-105.

[50] Mandelbrot, B.,(1963) The Variation of Certain Speculative Prices. *Journal of Business*,Vol. 36, 394

[51] Merton, R.C. (1973) Theory of Rational Option Pricing. *Bell Journal of Economics and Management Science*, 4, 141-183

[52] Muirhead, R. (1982) Aspects of Multivariate Statistical Theory. *Wiley.*

[53] Prause, K. (1999) The Generalized Hyperbolic Model: Estimation, Financial Derivatives, and Risk Measures, *Dissertation University at Freiburg.*

[54] Saporta G. (2006) Probability, data analysis and statistics, *Editions Technip.*

[55] Sato, K.,(1999) Lévy processes and infinitely divisible distribution, *Cambridge Press*.

[56] Schoutens, W. (2003) Lévy processes in Finance: Pricing Financial Derivatives, *Wiley*, New York.

[57] Tankov, P., (2003) Dependence structure of spectrally positive multidimensional Lévy processes. *Preprint*.

[58] Vasicek, Oldrich.(1977) An equilibrium characterization of the term structure. *Journal of Financial Economics 5*, no.2(November):177-188

[59] $EURUSD vs $GBPUSD - Volatility Favors EU over GU these days? *http://fxdibs4pips.posterous.com/eurusd-vs-gbpusd-volatility-favors-eu-over-gu*